

APPLICATION OF THE U.S. GEOLOGICAL SURVEY'S  
PRECIPITATION-RUNOFF MODELING SYSTEM TO THE  
PRAIRIE DOG CREEK BASIN, SOUTHEASTERN MONTANA  
by Lawrence E. Cary

---

U.S. GEOLOGICAL SURVEY

Water-Resources Investigations Report 84-4178

Prepared in cooperation with the  
U.S. BUREAU OF LAND MANAGEMENT



Helena, Montana  
December 1984

UNITED STATES DEPARTMENT OF THE INTERIOR

WILLIAM P. CLARK, Secretary

GEOLOGICAL SURVEY

Dallas L. Peck, Director

---

For additional information  
write to:

District Chief  
U.S. Geological Survey  
428 Federal Building  
301 South Park, Drawer 10076  
Helena, MT 59626

Copies of this report can be  
purchased from:

Open-File Services Section  
Western Distribution Branch  
U.S. Geological Survey  
Box 25425, Federal Center  
Denver, CO 80225

# CONTENTS

	Page
Abstract . . . . .	1
Introduction . . . . .	1
Study area . . . . .	3
General features . . . . .	3
Climate and streamflow . . . . .	4
Model description and operation . . . . .	7
System operation . . . . .	7
Model components . . . . .	8
Continuous simulation . . . . .	9
Storm simulation . . . . .	12
Optimization and sensitivity analyses . . . . .	13
Watershed partitioning . . . . .	13
Daily simulation . . . . .	13
Storm simulation . . . . .	15
Parameter estimation . . . . .	20
Daily simulation . . . . .	21
Climatic parameters . . . . .	21
Land phase parameters . . . . .	28
Storm simulation . . . . .	32
Model test . . . . .	35
Optimization and sensitivity analyses . . . . .	35
Objective function . . . . .	37
Hydrologic response units . . . . .	37
Model components . . . . .	37
Results . . . . .	39
Daily simulation . . . . .	39
Results of initial sensitivity analysis . . . . .	39
Results of daily optimization . . . . .	40
Results of final sensitivity analysis . . . . .	44
Mean daily streamflow . . . . .	47
Snow accumulation and melt . . . . .	49
Soil moisture . . . . .	53
Evapotranspiration . . . . .	54
Subsurface and ground-water reservoirs . . . . .	58
Annual water balance . . . . .	60
Storm simulation . . . . .	60
Interfacing with daily simulation . . . . .	60
Rainfall excess and storm runoff . . . . .	62
Precipitation variability . . . . .	74
Routing of storm runoff . . . . .	77
Improvement of simulation results . . . . .	78
Summary . . . . .	80
References cited . . . . .	83
Supplemental information . . . . .	87
Subroutine BASFL1 . . . . .	87
Introduction . . . . .	87
Model development . . . . .	87
Application . . . . .	88
Dictionary of new and revised variables in BASFL1 . . . . .	91

## ILLUSTRATIONS

	Page
Figure 1. Map showing location of study area . . . . .	2
2. Hydrograph of mean daily streamflow, Prairie Dog Creek, 1979 water year . . . . .	8
3. Hydrograph of mean daily streamflow, Prairie Dog Creek, 1980 water year . . . . .	10
4-6. Maps showing:	
4. Hydrologic response units under alternative A. . . . .	16
5. Hydrologic response units under alternative B. . . . .	18
6. Hydrologic response units under alternative C and associated surface runoff planes . . . . .	22
7-14. Hydrographs of:	
7. Observed and simulated mean daily streamflow, Prairie Dog Creek, 1979 water year . . . . .	48
8. Observed and simulated mean daily streamflow, Prairie Dog Creek, 1980 water year . . . . .	50
9. Observed and simulated snowpack water equivalent, Prairie Dog Creek basin, November 1978 through April 1979. . . . .	52
10. Observed and simulated snowpack water equivalent, Prairie Dog Creek basin, November 1979 through April 1980. . . . .	52
11. Observed and simulated soil moisture, Prairie Dog Creek basin, 1979 water year. . . . .	54
12. Observed and simulated soil moisture, Prairie Dog Creek basin, 1980 water year. . . . .	56
13. Simulated evapotranspiration, Prairie Dog Creek basin, 1979 water year . . . . .	58
14. Simulated evapotranspiration, Prairie Dog Creek basin, 1980 water year . . . . .	59
15. Graph showing reduction in objective function during optimization of four storm simulation parameters and 17 storms . . . . .	64
16. Graph showing reduction in objective function with number of optimization cycles. . . . .	68

## TABLES

Table 1. Mean monthly and annual precipitation at Prairie Dog Creek for water years 1979-81 and at Birney 2SW for the period 1954-81 and for water years 1979-81. . . . .	5
2. Average maximum, minimum, and mean monthly air temperatures at Birney 2SW and Prairie Dog Creek. . . . .	6
3. Total monthly solar radiation, in calories per square centimeter, at the Prairie Dog Creek meteorological station . . . . .	7
4. Hydrologic response unit alternative A for the Prairie Dog Creek basin. . . . .	14
5. Hydrologic response unit alternative B for the Prairie Dog Creek basin. . . . .	15
6. Hydrologic response unit alternative C, modified for the storm mode with associated runoff planes. . . . .	21
7. Precipitation-runoff modeling system parameters for the daily simulation mode. . . . .	24

TABLES--Continued

	Page
Table 8. Estimates of RCB (R) in Glover's (1966) equation. . . . .	31
9. Precipitation-runoff modeling system parameters for the storm simulation mode . . . . .	32
10. Consolidation of hydrologic response units (HRU's) alternatives A and B . . . . .	38
11. Mean squared runoff prediction error resulting from a 20-percent parameter error, hydrologic response unit (HRU) alternatives A and B . . . . .	40
12. Results of optimization on average parameter values, hydrologic response unit (HRU) alternative A . . . . .	41
13. Results of optimization on average parameter values, hydrologic response unit (HRU) alternative B . . . . .	41
14. Simulated mean monthly streamflow before and after optimization for hydrologic response unit (HRU) alternative A . . . . .	43
15. Simulated mean monthly streamflow before and after optimization for hydrologic response unit (HRU) alternative B . . . . .	44
16. Effects of a 20-percent error in parameter value upon mean squared prediction error, hydrologic response unit (HRU) alternatives A and B . . . . .	45
17. Parameter coefficients of variation (percent), hydrologic response unit (HRU) alternatives A and B . . . . .	45
18. Correlation coefficients greater than 0.75 in absolute value under various levels of basin partitioning, hydrologic response unit (HRU) alternatives A and B . . . . .	45
19. Annual water balance of the model simulations in inches . . . . .	61
20. Average values of parameters before and after optimization for hydrologic response unit alternatives A and C . . . . .	62
21. Simulated and observed storm-runoff volumes and values of the hat matrix following optimization of the sums of squares of the loga- rithms of flows . . . . .	63
22. Initial and final parameter values following optimization using 17 storms and the sum of squares objective function. . . . .	65
23. Optimization of the parameter pair KSAT-RGF, using 17 storms. . . . .	67
24. Optimization of the parameter pair PSP-RGF, using 17 storms . . . . .	67
25. Observed and simulated storm runoff for 17 storms . . . . .	69
26. Diagonal elements of the hat matrices for four sensitivity analyses of storm runoff . . . . .	70
27. Hydraulic conductivity at the wetting front (KSAT) by soil texture class . . . . .	71
28. Values of the product of matric suction at the wetting front and moisture deficit at field capacity (calculated as soil moisture at saturation minus soil moisture at one-third bar suction), PSP. . . . .	72
29. Characteristics of storms used in model testing . . . . .	75
30. A summary of the results of routing rainfall excess to the basin outlet. . . . .	77

## CONVERSION FACTORS

The following factors can be used to convert inch-pound units in this report to the International System of units (SI).

<u>Multiply inch-pound unit</u>	<u>By</u>	<u>To obtain SI unit</u>
	<u>Length</u>	
foot (ft)	0.3048	meter
inch (in.)	25.40	millimeter
	2.540	centimeter (cm)
mile (mi)	1.609	kilometer
	<u>Area</u>	
square mile (mi <sup>2</sup> )	2.590	square kilometer
	<u>Volume</u>	
acre-foot	1233	cubic meter
	<u>Flow</u>	
cubic foot per second (ft <sup>3</sup> /s)	0.02832	cubic meter per second
	<u>Transmissivity</u>	
foot squared per day (ft <sup>2</sup> /d)	0.09290	meter squared per day
	<u>Pressure</u>	
bar	100	kilopascal
	<u>Rate</u>	
inch per hour (in./hr)	25.40	millimeter per hour
inch per day (in./d)	25.40	millimeter per day

Temperature can be converted to degrees Celsius (°C) or degrees Fahrenheit (°F) by the equations:

$$^{\circ}\text{C} = 5/9 (^{\circ}\text{F} - 32)$$

$$^{\circ}\text{F} = 9/5 (^{\circ}\text{C}) + 32$$

National Geodetic Vertical Datum of 1929 (NGVD of 1929): A geodetic datum derived from a general adjustment of the first-order level nets of both the United States and Canada, formerly called mean sea level. NGVD of 1929 is referred to as sea level in this report.

APPLICATION OF THE U.S. GEOLOGICAL SURVEY'S PRECIPITATION-RUNOFF MODELING  
SYSTEM TO THE PRAIRIE DOG CREEK BASIN, SOUTHEASTERN MONTANA

by

Lawrence E. Cary

---

ABSTRACT

The U.S. Geological Survey's precipitation-runoff modeling system was tested using 2 water years of daily data for the daily simulation mode and 17 storms for the storm simulation mode from a small basin in southeastern Montana. Two hydrologic response unit delineations were studied. The more complex delineation did not provide clearly superior results. In this application, the optimum numbers of hydrologic response units were 16 and 18 for the two alternatives. The first alternative with 16 units was modified to facilitate interfacing with the storm mode.

A seven-parameter subset was defined for the daily mode using sensitivity analysis. Following optimization, the simulated hydrographs approximated the observed hydrograph during the first year, a year of greater than average snowfall. Simulated runoff was larger than occurred the second year. Rainfall-runoff events were not simulated well by the daily mode. Correspondence between the observed snowpack and the simulated snowpack was reasonable the first snow season but poor the second. More soil moisture was withdrawn than was indicated by soil moisture observations.

Optimization of parameters in the storm mode resulted in much larger values than originally estimated, commonly larger than published values of the Green and Ampt parameters. Following optimization, variable results were obtained when storm runoff volumes and peak flows were simulated. The errors are probably related to inadequate representation of basin infiltration characteristics and to precipitation variability.

Future studies probably could benefit from inclusion of parameter estimation techniques and delineation of hydrologic response units. The model results might improve if the model were tested with longer data sets and on other basins.

INTRODUCTION

A precipitation-runoff modeling study was begun in 1978 by the U.S. Geological Survey in cooperation with the U.S. Bureau of Land Management. The purpose of the study was to develop, calibrate, and verify a watershed model that could be used to simulate hydrologic processes on small basins where data are lacking. Basins for study were selected and instrumented in several coal-producing States. The purpose of this report is to describe application of the model to the Prairie Dog Creek basin near Birney (fig. 1), which was the area selected in Montana.

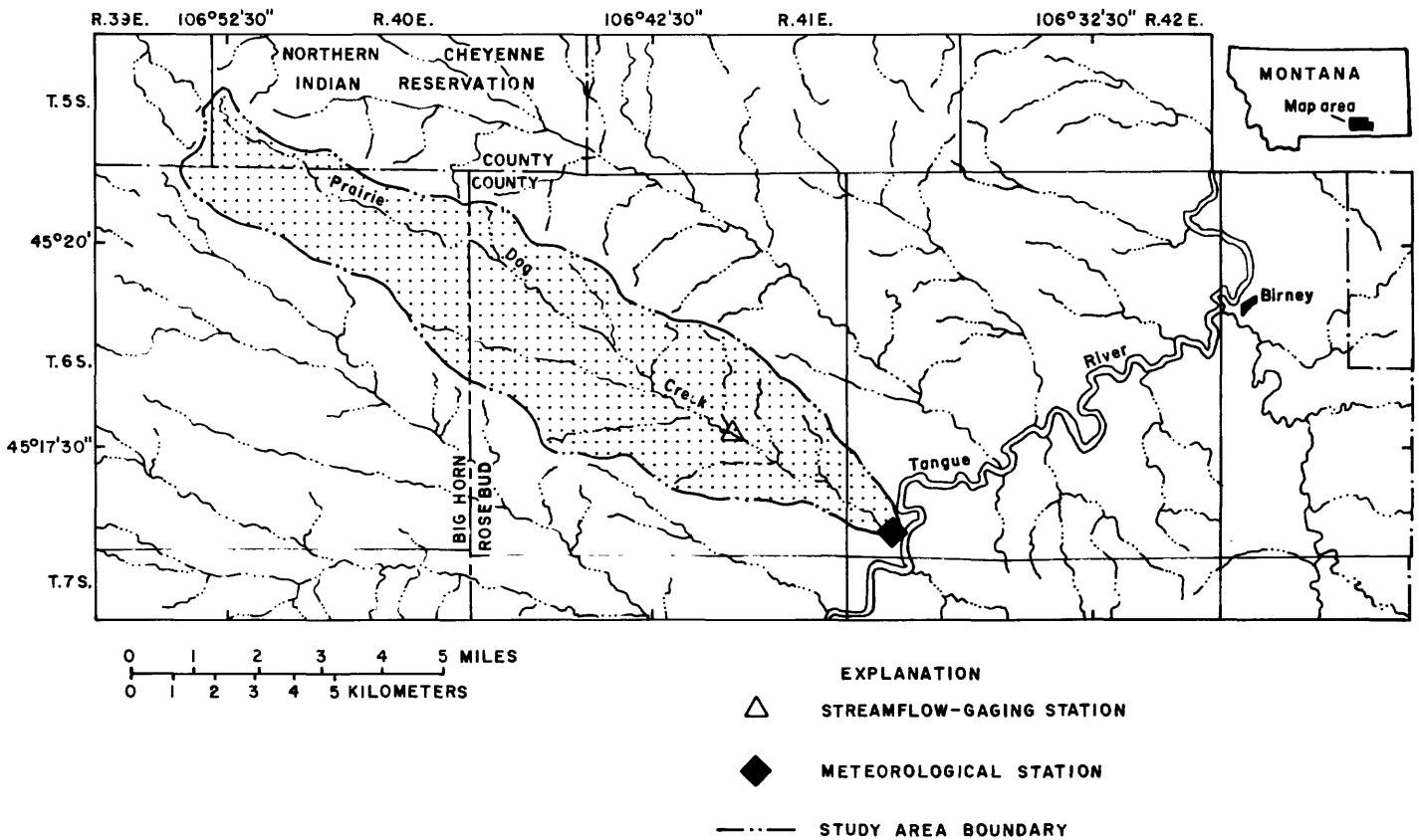


Figure 1.--Location of study area.

This study used the Geological Survey's precipitation-runoff modeling system. The modeling system was developed by Leavesley and others (1984) by combining a continuous snowmelt model (Leavesley, 1973) with a storm-runoff model (Dawdy and others, 1972 and 1978). The modeling system is a continuous simulation, distributed-parameter model having an optional storm mode that includes erosion and sediment-transport components.

Use of the model required several types of data. Hydrologic response units<sup>1</sup> were defined, basin characteristics were determined, and model parameters for the Prairie Dog Creek basin were estimated. Three years of data were available for use in testing the model. However, the second and third years were similar in that both were dry periods with small amounts of streamflow resulting from runoff over frozen ground or convective thundershowers. Therefore, only data from the first and second years were used in testing the daily simulation mode. Because the third year contained several periods of runoff from rainfall, data from all 3 years were used in the test of the combined daily and storm simulation modes.

<sup>1</sup> A subdivision of a watershed based on physical characteristics; the subdivision is a collection of irregular, but hydrologically similar, areas.

Two methods for delineating hydrologic response units for the daily simulation mode were compared. Sensitivity analysis was used to study model sensitivity to the parameters and to define a subset of parameters to be used in optimization. The daily simulation results using the optimized parameter subset were compared with 2 years of data.

One method of hydrologic response unit delineation was modified to provide a direct correlation between the response units and the surface runoff planes used in the storm mode, and to facilitate the definition of channel segments used in channel routing. Sensitivity and optimization analyses were used in the evaluation of the storm mode.

The Prairie Dog Creek basin was the subject of a small area reclamation study, part of the U.S. Bureau of Land Management's Energy Minerals Rehabilitation Inventory and Analysis (EMRIA) program. As part of this study, McClymonds (1982) discussed the hydrology of the basin. The coal resources and potential for reclamation are provided in a report of the U.S. Department of the Interior (1983). The basin instrumentation and data collection that are ongoing as part of this concurrent modeling study were presented by Cary and Johnson (1981).

Data collection for this study began in October 1978 with the activation of the meteorological station near the mouth of Prairie Dog Creek. Precipitation, air temperature, relative humidity, wind speed and direction, soil temperature, and incident solar radiation were continuously monitored. Snowpack and soil moisture were periodically measured.

The stream-gaging station was activated in November. Three additional precipitation gages were installed during this month. In December, six additional snow courses and one additional soil moisture station were established.

Severe weather precluded any further installations until spring. During late spring and early summer 10 additional soil-moisture stations, 3 precipitation gages, and 3 snow courses were added to the data-collection network.

## STUDY AREA

### General features

The study area is located within the Tongue River drainage in southeastern Montana (fig. 1). Prairie Dog Creek originates on the south end of the Northern Cheyenne Indian Reservation in Big Horn County and joins the Tongue River about 7 mi southwest of Birney, in Rosebud County. The area of the basin is about 25 mi<sup>2</sup>. The principal streamflow-gaging station was located about 3 mi from the mouth, upstream from a livestock reservoir, yielding an effective study area of about 19 mi<sup>2</sup>.

The basin is long and narrow, with a topographic relief of about 1,400 ft. The altitude at the mouth of Prairie Dog Creek is 3,185 ft above sea level. The terrain is relatively steep and dissected, especially on the north side of Prairie Dog Creek. Near the headwaters and along the flanks of the watershed, the terrain consists of nearly level, plateau-like erosional remnants. Three terraces in the Prairie Dog Creek valley are evidence of water erosion during at least three major climatic cycles (McClymonds, 1982).

The surficial geology of the basin is the Tongue River Member of the Paleocene Fort Union Formation. According to McClymonds (1982), the Tongue River Member in this area is a series of lenticular layers of sandstone, siltstone, mudstone, claystone, carbonaceous shale, and coal. Additional description of the geology in the Prairie Dog Creek basin, and the relationship of the geology to the hydrology, is given by McClymonds (1982).

Low- to medium-intensity soil surveys have recently been completed by the U.S. Soil Conservation Service in the upstream part of the basin in Bighorn County (Meshnick and others, 1977; U.S. Department of Agriculture, 1978) and are in progress in Rosebud County. Soil depths ranged from thick profiles on the main valley floors and on terraces to shallow, rocky soils on steep hillsides. More soils had a loam texture than any other texture class, and ranged from fine sandy loam to clay loam.

Several vegetation types are present in the basin. In general, these are sagebrush steppe, sagebrush grassland, mid and short grass, ponderosa pine, riparian grassland, and mixed ponderosa pine and Rocky Mountain juniper. Eleven vegetation types in the basin were identified and mapped by F. A. Branson (U.S. Geological Survey, written commun., 1979).

Current land use is livestock grazing. In the past, the basin was divided between several homesteads. Some farmers practiced limited flood irrigation in the valley of the main stem of Prairie Dog Creek. Numerous reservoirs in the basin are used for livestock watering. Several water wells are completed in the alluvium and used for livestock water.

#### Climate and streamflow

The climate of the area is semiarid, continental steppe, which is characteristic of the northern Great Plains. The mean annual precipitation is about 13 inches, with almost 60 percent occurring from April to July. During the first part of this period, cyclonic storms are common; however, during the summer months convective storms are predominant. About 30 to 40 percent of the annual precipitation occurs as snow. Nearly all precipitation from November through March is in the form of snow, and late spring snowstorms are not uncommon. The seasonal temperature ranges widely, with cold winters and hot summers. Mean January temperature is 17°F and mean July temperature is 71°F.

Precipitation records in the region indicate that the years 1971-78 were wetter than normal (McClymonds, 1982). Precipitation data for Prairie Dog Creek collected during this study and precipitation records from Birney 2SW, a National Weather Service station located about 5 mi northeast of the mouth of Prairie Dog Creek, are summarized by month in table 1.

Precipitation at the primary meteorological station during the 1979 water year was less than the 1954-81 average at Birney 2SW in October, January, March, and May through September. It was greater than average in November, December, and February. Greater than average precipitation fell during December, February, and March of the 1980 water year. Precipitation during November, January, and May was nearly average, but less than average during the remaining months of the water year. In 1981 near average precipitation fell during December, March, and July. Precipitation during May was double the 1954-81 average at Birney 2SW. The remaining months were less than average. Annual total precipitation was less than the 1954-81 average at Birney 2SW in 1979 and 1980, but near average in 1981.

Table 1.--Mean monthly and annual precipitation at Prairie Dog Creek for water years 1979-81 and at Birney 2SW for the period 1954-81 and for water years 1979-81

Station and water year	Precipitation, in inches, for indicated period												Annual
	Oct.	Nov.	Dec.	Jan.	Feb.	Mar.	Apr.	May	June	July	Aug.	Sept.	
Birney 2SW 1954-81	1.00	0.70	0.51	0.49	0.48	0.46	1.44	2.19	2.77	1.06	0.92	1.05	13.07
Birney 2SW 1979	.20	1.86	.98	.26	.90	.24	1.39	1.71	.60	1.26	.40	.33	10.13
Birney 2SW 1980	.83	.61	.29	.36	.76	.91	.48	2.12	3.19	.13	1.53	.52	11.73
Birney 2SW 1981	1.09	.36	.60	.31	.34	.48	.14	3.18	2.07	2.32	.76	.67	12.32
Prairie Dog Cr. <sup>1</sup> 1979 primary gage	.2	1.7	1.3	.3	1.1	.3	1.6	1.6	1.3	.9	.5	.4	11.2
Prairie Dog Cr. 1980 primary gage	.7	.6	1.4	.4	1.0	.9	.4	2.3	1.9	.2	.8	.4	11.0
Prairie Dog Cr. 1981 primary gage	.8	.4	.5	.3	.4	.5	.2	4.3	1.6	1.1	.3	.8	11.2
Prairie Dog Cr. <sup>2</sup> 1979 gage average	<sup>1</sup> .2	<sup>1</sup> 1.7	1.52	.46	1.07	.30	1.92	1.38	.69	.84	.30	.53	10.9
Prairie Dog Cr. 1980, 7-gage average	.68	.77	.62	.52	1.06	1.18	.67	2.12	2.03	.29	.88	.65	11.47
Prairie Dog Cr. 1981, 7-gage average	1.08	.49	.73	.34	.43	.73	.23	4.12	1.99	2.15	.26	.72	13.27

<sup>1</sup> Precipitation gage at the meteorological station is accurate only to one-tenth of an inch.

<sup>2</sup> One gage Oct. and Nov.; four gages Dec. through Mar.; five gages Apr. through June; seven gages July through Sept.

The last three rows in table 1 are average values of monthly precipitation for the basin. The precipitation measured at Birney 2SW and the meteorological station in the Prairie Dog Creek basin are more nearly comparable because of their close proximity to the valley of the Tongue River and their separation by about 5 mi. However, the average of all gages provides a more accurate estimate of the basin precipitation. The basin total annual precipitation was less than the average at Birney 2SW the first 2 years, and nearly the same during the third. A comparison of monthly totals between the meteorological station and the seven-gage average shows considerable variation during the summer. The variation is a reflection of the greater spatial variation in summer thundershowers.

Monthly average maximum, minimum, and mean temperatures at Birney 2SW and at the Prairie Dog Creek meteorological station are given in table 2. The consistently lower temperatures at the Prairie Dog Creek station are primarily due to difference in location and elevation.

Monthly temperatures during the 1979 water year were lower than the 1954-81 average, particularly during the period November through February. The low temperatures during this period resulted in the average annual temperature being much lower than the long-term average. Winter temperatures were generally higher in 1980 and 1981 than in 1979. Although higher than in 1979, 1980 temperatures were lower than average during 8 months, particularly November, January, March, and August. The mean annual temperature was slightly lower than the 1954-81 average at Birney 2SW. In 1981, temperatures were near or slightly higher than the 1954-81 average, except January, which was much warmer than the average.

Table 2.--Average maximum, minimum, and mean monthly air temperatures at Birney 2SW and Prairie Dog Creek

Station and water year		Temperature, in degrees Fahrenheit, for indicated period												
		Oct.	Nov.	Dec.	Jan.	Feb.	Mar.	Apr.	May	June	July	Aug.	Sept.	Annual
Birney 2SW (1954-81)	Maximum	64.6	44.8	36.2	31.2	38.8	47.8	60.4	70.7	80.0	89.7	87.8	75.8	60.7
	Minimum	29.8	16.7	8.6	2.4	10.1	18.6	29.4	39.4	48.0	52.6	49.7	39.5	28.7
	Mean	47.2	30.4	22.4	16.8	24.5	33.3	44.9	55.1	64.0	71.2	68.8	57.7	44.7
Birney 2SW (1979)	Maximum	64.6	37.6	25.1	18.1	32.2	48.7	59.3	69.5	82.6	88.6	84.0	81.0	57.6
	Minimum	28.4	11.0	- 1.2	-11.5	- .1	19.3	28.6	38.1	47.2	54.6	53.2	41.5	25.8
	Mean	46.5	24.3	12.0	3.3	16.1	34.0	44.0	53.8	64.9	71.6	68.6	61.3	41.7
Birney 2SW (1980)	Maximum	65.3	42.6	42.9	30.1	40.5	45.9	68.3	74.9	82.9	91.1	81.7	76.4	61.9
	Minimum	33.9	18.8	11.7	2.6	13.9	17.9	32.3	41.6	50.2	54.7	50.3	42.3	30.9
	Mean	49.6	30.7	27.3	16.4	27.2	31.9	50.3	58.3	66.6	72.9	66.0	59.4	46.8
Birney 2SW (1981)	Maximum	64.6	49.3	37.0	44.6	42.1	57.0	67.2	69.5	77.9	88.5	86.2	78.9	63.6
	Minimum	30.5	22.0	13.7	17.7	13.4	23.9	32.1	42.7	48.6	55.5	52.0	42.7	32.9
	Mean	47.6	35.7	25.4	31.1	27.8	40.5	49.7	56.1	63.3	72.0	69.1	60.8	45.4
Prairie Dog Cr. (1979)	Maximum	63.4	35.3	24.0	16.3	30.3	45.8	54.4	64.3	79.6	87.4	83.3	81.8	55.5
	Minimum	24.6	7.6	- 6.6	-16.5	- 5.2	16.1	25.9	34.6	44.1	52.6	52.2	38.4	22.3
	Mean	44.0	21.5	8.7	- 0.1	12.6	30.9	40.1	49.5	61.8	70.0	67.8	60.1	38.9
Prairie Dog Cr. (1980)	Maximum	63.3	40.3	43.4	27.3	36.6	43.0	63.8	71.2	81.0	91.1	79.5	76.0	59.7
	Minimum	29.1	13.5	7.7	- 1.7	9.2	15.0	28.5	38.1	48.3	52.1	47.6	37.6	27.1
	Mean	46.2	26.9	24.0	12.8	22.9	29.0	46.2	54.7	64.6	71.6	63.5	56.8	43.3
Prairie Dog Cr. (1981)	Maximum	61.4	47.5	35.6	43.5	39.9	53.8	61.7	65.3	74.5	86.5	87.6	79.0	61.4
	Minimum	27.7	18.5	8.8	14.0	9.0	20.1	28.2	39.6	46.2	53.4	50.4	40.3	29.7
	Mean	44.5	32.0	21.9	26.6	24.8	36.5	46.4	52.7	61.7	70.7	69.8	59.9	45.6

There were no long-term solar radiation records with which to compare incoming solar radiation at the Prairie Dog Creek meteorological station. Total incoming solar radiation was about 1 percent less in 1979 than in 1980 or 1981 (table 3). A major difference between years occurred between December of 1979 and 1980. Incoming solar radiation was 27 percent less in December 1979 than in December 1980.

The greater precipitation during November and December of the 1979 water year and the low temperatures during November through February resulted in the formation of an above average snowpack. The snowpack persisted throughout the season with no noticeable periods of melt until late February. The continued buildup of the snowpack was aided by the low solar radiation in January.

Even though the total amounts of precipitation received in 1979 (4.7 inches) and 1980 (4.3 inches) during November through March were similar, snow did not accumulate and remain on the ground in 1980. Warmer temperatures resulted in more rain in 1980. The fraction of precipitation that was snow formed snowpacks, which melted in a short time.

Precipitation during the same period in 1981 (2.72 inches) was near the 27-year average at Birney 2SW (2.64 inches). Decreased precipitation and temperatures that were higher than the 27-year average at Birney 2SW resulted in a higher percentage of rain and melting of the snow that did fall.

Table 3.--Total monthly solar radiation, in calories per square centimeter, at the Prairie Dog Creek meteorological station

Solar radiation, in calories per square centimeter, for indicated period												
Water year	Oct.	Nov.	Dec.	Jan.	Feb.	Mar.	Apr.	May	June	July	Aug.	Sept.
1979	8,724	4,961	3,192	4,644	6,525	10,303	12,031	15,449	17,244	18,516	13,937	12,918
1980	7,680	4,687	4,344	4,722	5,146	9,925	14,185	15,846	18,383	18,616	14,940	11,558
1981	8,417	4,600	3,217	5,244	6,298	11,014	14,402	13,293	17,090	17,648	16,057	12,869

During years of average or greater than average precipitation, Prairie Dog Creek is an intermittent stream in the downstream reaches. It has a small perennial flow for short distances from springs in the upstream reaches.

Prairie Dog Creek flowed from the onset of snowmelt until the December freezeup in 1978. Flow began again at the main gaging station early in April 1979 and continued through mid-September. During the winter of 1980 there were instances of flow from snowmelt over frozen ground. These were for only a few days duration. The greatest peak flows occurred during spring and summer in response to convective thundershowers in the basin. Streamflow during the 1981 water year was similar to that of the 1980 water year. Hydrographs of mean daily streamflow for the 1979 and 1980 water years are shown in figures 2 and 3.

The prolonged base flow during 1979 was due primarily to melting of the greater than average snowpack and percolation of the water to water tables that were already relatively high because of several preceding years of increased precipitation. As indicated above, this above average snowfall during the winter was accompanied by a cold winter. A similar amount of precipitation fell during the winter of 1980. However, warmer temperatures in December, January, and February resulted in greater melting and evaporation of the snowpack. The near average precipitation during 1981 and the probable greater evaporation loss resulted in no snowmelt runoff other than occasional runoff over frozen ground.

#### MODEL DESCRIPTION AND OPERATION

A complete description of the precipitation-runoff modeling system is given in Leavesley and others (1983). A brief description of the modeling system components used in the preparation of this report is provided here.

#### System operation

The daily hydrologic and climatic data were retrieved from the National Water Data Storage and Retrieval System (WATSTORE) of the U.S. Geological Survey (1975). The data were converted to card-image format, with all values of mean daily discharge and daily climatic data (including data from seven recording precipitation gages) stored on one card image. These data were stored in an online file. The basin characteristics data were entered directly and also stored in an online file.

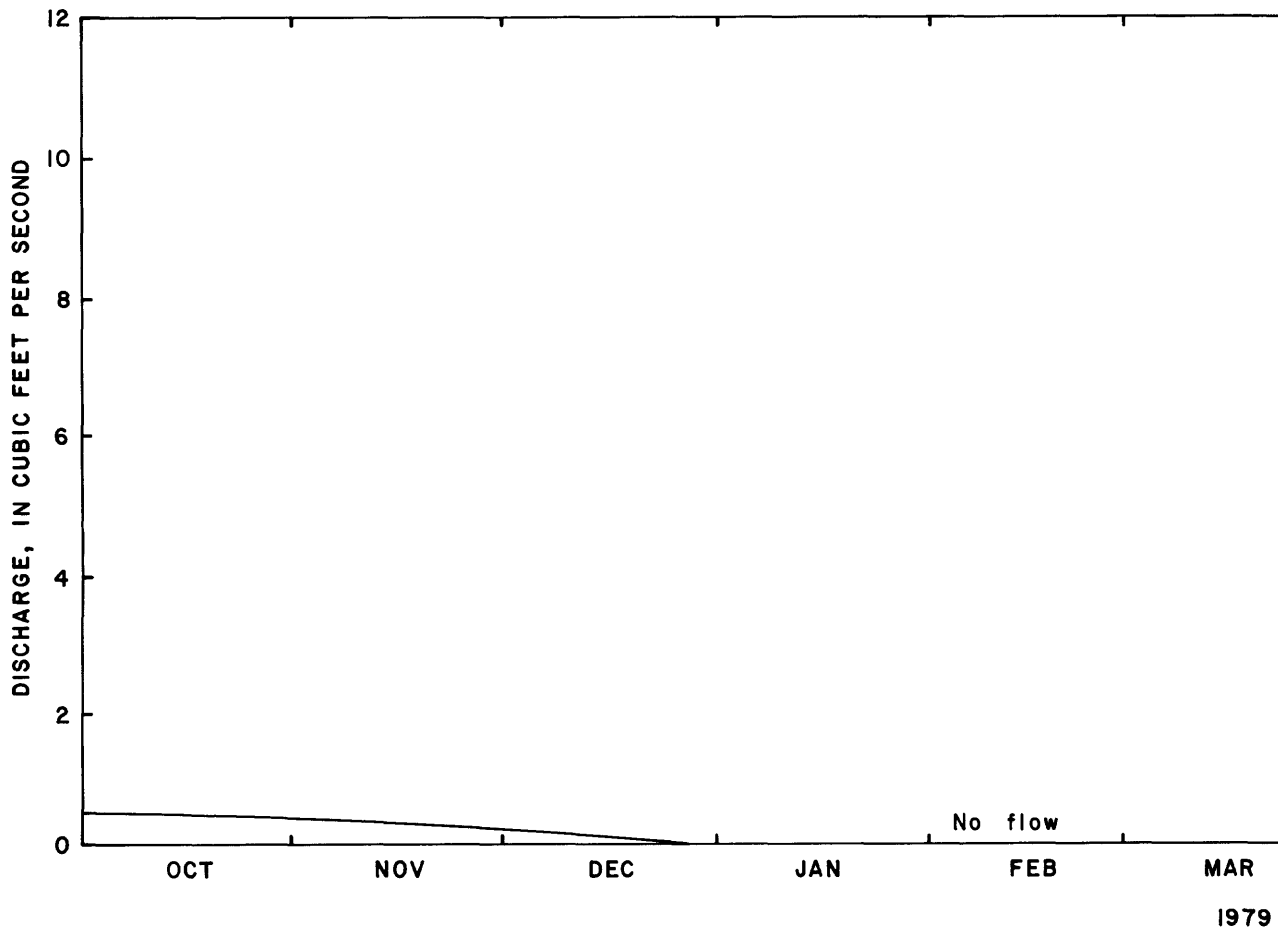
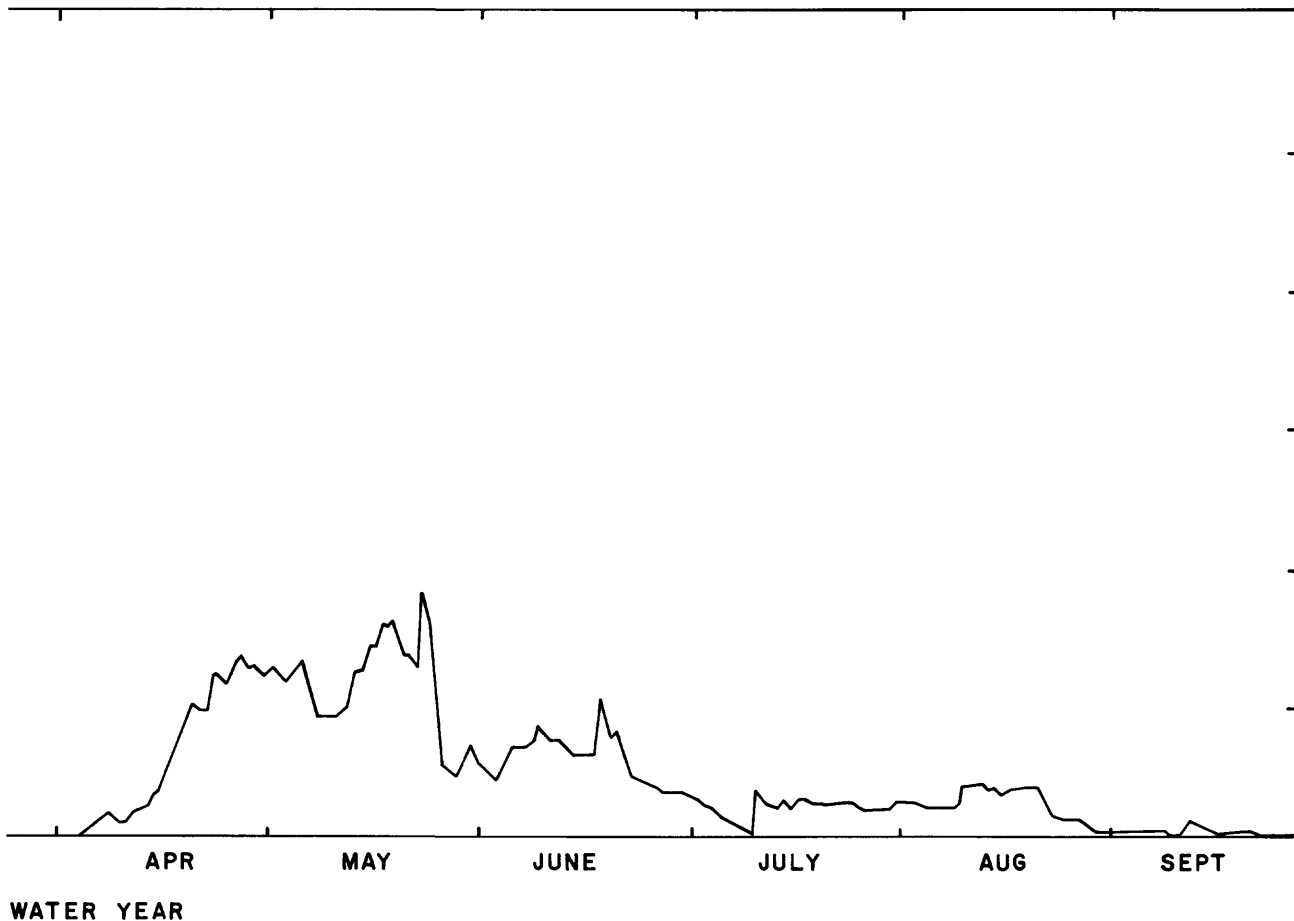


Figure 2.--Hydrograph of mean daily streamflow,

Rainfall and storm-discharge data for the storm mode were also stored in an online file. Rainfall and discharge data at 15-minute intervals were used during operation of the model in the storm mode. Files for basin characteristics and storm-period identification information, as well as hydraulic routing parameters, were developed.

#### Model components

The model uses a modular approach in which each component of the hydrologic cycle is represented by separate subroutines. This approach facilitates component modification in that, usually, only single subroutines need be changed. All major subroutines are called from the main program. Other subroutines which perform specialized functions or which are not required for every day of model operation are called, when needed, from the major subroutines. The continuous simulation mode can be operated without optimization or sensitivity analysis by setting the appropriate switches.



Prairie Dog Creek, 1979 water year.

#### Continuous simulation

The precipitation-runoff modeling system is a model of the hydrologic cycle of small watersheds. The continuous, or daily, mode simulates components of the cycle important on such watersheds. The components include infiltration, evapotranspiration, interception, soil moisture, snow accumulation and ablation, surface flow, subsurface flow, base flow, and seepage to ground water.

Potential evapotranspiration is computed in one of three ways. If daily evaporation pan data are used, potential evapotranspiration is computed using these data and monthly pan coefficients. If air temperature and solar radiation data are available, the Jensen-Haise equation is used to compute potential evapotranspiration (Jensen and Haise, 1963). This equation is a simplified energy budget using solar radiation and air temperature. The third method uses air temperature and sunshine data (Hamon, 1961). The Jensen-Haise method was used in the application.

On days when precipitation occurs, the form (rain, snow, or mixed) is computed based upon the daily maximum, daily minimum, and a base temperature. The precipitation form can also be specified for certain periods of the year. Net precipitation is computed as total precipitation minus that intercepted by vegetation.

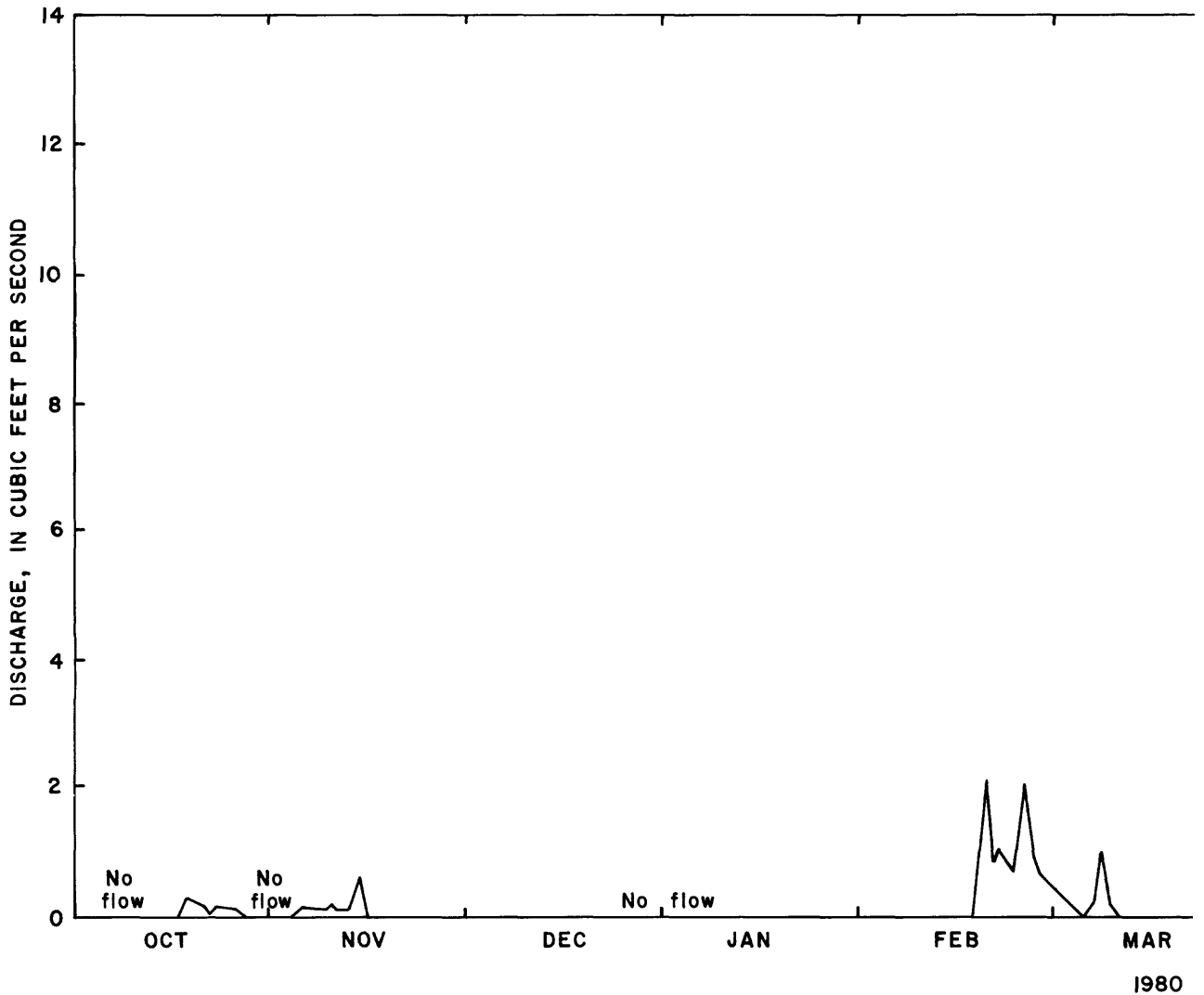
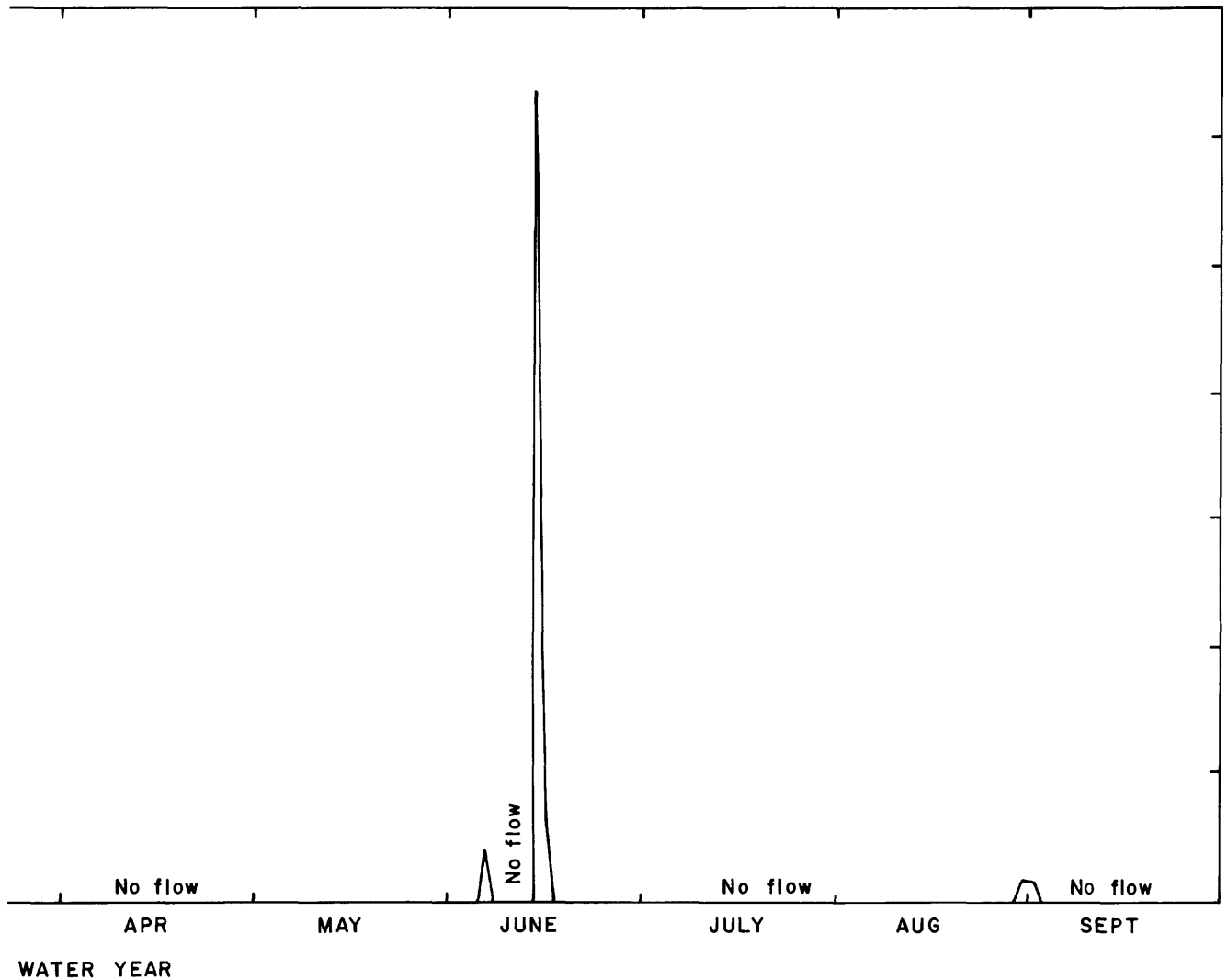


Figure 3.--Hydrograph of mean daily streamflow,

The daily surface runoff during periods of rain is computed using the contributing area concept (Hewlett and Nutter, 1970) and the antecedent soil moisture conditions. The fraction of the area that contributes to surface runoff is computed as a linear function of the antecedent soil moisture in an upper soil layer. This contributing area ranges between a user-specified minimum and maximum contributing area for each response unit.

An energy balance approach is used in the snow subroutines. Solar radiation, long wave radiation, heat conduction and storage in the snowpack, surface melt and crusting, and sensible heat transfer from precipitation are included. Energy balance calculations are made for a 12-hour day and a 12-hour night period. Snowmelt runoff begins when the snowpack is isothermal and the free-water holding capacity is satisfied. Evaporation and sublimation are computed daily as a fraction of potential evapotranspiration. Snowmelt infiltrates until the soil zone is saturated and a user-specified maximum daily infiltration capacity is reached. Any excess becomes surface runoff.



Prairie Dog Creek, 1980 water year.

Daily soil moisture is accounted for using a soil profile whose depth is the average rooting depth of the dominant vegetation in each hydrologic response unit. The profile is divided into an upper and a lower zone. The upper zone thickness is user specified and is the zone in which evaporation to the atmosphere and transpiration occur. Only transpiration occurs from the lower zone. As rainfall or snow-melt infiltrates, the upper, then the lower zones are filled. When the water-holding capacity of the lower zone is exceeded, the excess is added to a subsurface reservoir. Seepage from the subsurface reservoir to a ground-water reservoir is computed from a decay function. A user-specified fraction of the flow becomes streamflow from the subsurface reservoir and the ground-water reservoir.

Actual evapotranspiration is next computed from potential evapotranspiration and a soil-moisture relationship developed by Zahner (1967) for uniformly stocked forest and pasture land. Relationships between the ratio of current to maximum soil moisture and the ratio of actual to potential soil moisture were developed for three general soil texture classes: sand, loam, and clay. Actual evaporation

is then potential evapotranspiration times the soil moisture ratio for the appropriate soil texture class.

After each day's soil moisture accounting has been completed, the base flow and subsurface components of streamflow are computed. Trial runs indicated that the observed delay between the beginning of snowmelt and the beginning of streamflow was not simulated by the model.

Glover (1966) adapted a heat-flow equation to the study of drainage to parallel drains. Aron and Borelli (1973) coupled this equation with a convolution and applied the algorithm to the simulation of base flow from small basins in Pennsylvania. The parameter R in the equation was estimated from hydrograph characteristics. Later, Naney and others (1978) applied this approach in a model of a small basin in Oklahoma. In this study, the parameter R was computed from observed and estimated aquifer characteristics.

This approach was incorporated into the subroutine BASFLW in order to overcome the observed delay problem. The ground-water reservoir routing parameter RCB was redefined to be the parameter R described above. This modification is further described in the Supplemental Information section.

Subsurface flow is the flow from the soil zone, or "quick" flow, following storms. This flow is computed from a quadratic polynomial in the model. The coefficient of the first linear term in the expression used can be estimated from the hydrograph recession limb prior to base flow. The coefficient of the second, non-linear term is initially estimated to be one-third of the first.

#### Storm simulation

The storm mode of model operation is activated on days specified by the user in the storm identification information provided in the basin characteristics data set. Outside this storm period, and also when the storm period is not specified, the model operates in the continuous simulation mode.

When the model is operating in the storm mode, rainfall in excess of that infiltrating into the soil is calculated. The Green and Ampt infiltration equation is used to compute point infiltration. The rainfall excess over an area is computed using a uniform distribution function, wherein areal rainfall excess is a function of maximum infiltration capacity and the rainfall supply rate.

The storm mode execution can be stopped at this point. If stopped, the runoff volumes for the basin are calculated from rainfall in excess of infiltration. If overland, channel, and reservoir routing are desired, kinematic overland flow routing is used to route the rainfall excess over overland flow planes to an associated channel segment. Kinematic channel routing is used to route the rainfall excess contributed by the overland flow planes through each channel segment and into the next segment, continuing until the basin outlet is reached. In this study, the storm volume option was used first, followed by the routing option.

## Optimization and sensitivity analyses

Optimization of selected model parameters is accomplished using the Rosenbrock (1960) or Gauss-Newton technique. One of four objective functions representing the difference between observed and predicted daily streamflow can be selected for use. The step length (a fraction of parameter magnitude) and upper and lower bounds for each parameter are specified by the user.

Sensitivity analysis of user selected parameters is done by estimating the partial derivative of predicted streamflow with respect to each parameter. The increment by which each parameter is varied in order to compute this estimate is user selected. The analysis provides a means of evaluating the extent to which parameter uncertainty is propagated to uncertainty in runoff prediction, the degree of correlation between parameters, and the extent to which daily streamflow affects optimization.

Optimization and sensitivity analyses can be done sequentially. Owing to the number of model parameters that can be optimized (51 total, 38 for continuous simulation, and 13 for storm runoff simulation), sensitivity analysis can be used alone as a tool in defining parameter subsets for subsequent optimization. Parameters to which predicted streamflow is relatively insensitive can be excluded from optimization. Sensitivity analysis can also be used to identify the amount of correlation between pairs of parameters. Use of optimization and sensitivity analyses in the precipitation-runoff modeling system is discussed in greater detail in Leavesley and others (1981).

### Watershed partitioning

Numerous methods have been used to partition watersheds into sub-units for distributed parametric modeling. Many of these methods were reviewed by Leavesley (1973).

The technique used to partition watersheds in the precipitation-runoff modeling system is physically based and uses two levels. The first level pertains to the continuous simulation mode of the model. The second is used in overland flow and channel routing in the event mode. A discussion of this approach, with examples, can be found in Leavesley (1973) and Leavesley and others (1983).

### Daily simulation

The first level of partitioning uses slope, aspect, vegetation, soils, elevation, precipitation, and snow distribution to partition the basin into subunits which are "homogeneous" with respect to these properties. These units are called hydrologic response units (HRU's).

The partitioning of the Prairie Dog Creek basin was complicated by the intermingling of vegetation types and 53 different soil mapping units. Eleven vegetation types were identified and mapped. Frequently, areas of the other vegetation types were included within the mapped boundary of one type.

At the intensity of soil survey used, the mapping units commonly included soil series of dissimilar hydrologic characteristics. Use of 53 soil mapping units with

the other hydrologic response unit criteria would have resulted in a very large number of units. Therefore, the soil units were reduced. The mapping unit descriptions provide the fraction of the area occupied by each soil series. The hydrologic soils group for each series is provided in the soil series description. A numerical score was assigned to each group. Using this score and the percentage of a mapping unit occupied by each series, a weighted score was computed for each unit. The units with similar scores were then grouped.

Overlays of the soil mapping units, of the vegetation types, and of a 1:24,000 slope class map were prepared. Hydrologic response unit overlays were prepared using these overlays and a 1:24,000 topographic base map. The hydrologic response units were delineated on the basis of gross aspect, vegetation type, soils mapping units, and major changes in topography. Color aerial photographs were also used as an aid in interpretation. Because the topographic relief is about 1,400 feet, altitude was considered by dividing the basin using the contours of the average altitude.

Two alternate response unit delineations (A and B) were selected for comparison. Under the first, a unit was defined to be a basin sub-area enclosed by a single boundary, which commonly resulted in the occurrence of more than one vegetation type in a response unit. Although average slope and aspect were determined for each unit, the dissected topography provided, locally, a considerable range in slope and aspect (fig. 4). The general characteristics of these units are given in table 4.

Table 4.--Hydrologic response unit alternative A for the Prairie Dog Creek basin

Hydrologic response unit	Area (percent of total)	Median altitude (feet)	Average slope (percent)	Aspect	Dominant vegetation cover	Soil
1	6	4,405	10	E	Grass	Loam
2	3	4,285	20	S	Shrub	Loam
3	7	4,320	20	NE	Shrub	Loam
4	6	4,360	10	NE	Shrub	Loam
5	1	4,210	20	SE	Trees	Clay
6	1	3,995	10	SE	Shrub	Clay
7	7	4,150	30	S	Trees	Loam
8	5	4,080	30	NE	Trees	Loam
9	6	3,940	40	S	Trees	Loam
10	10	3,740	20	S	Trees	Clay
11	4	3,570	10	SE	Shrub	Loam
12	6	3,795	20	NE	Shrub	Loam
13	4	4,040	20	E	Trees	Clay
14	3	4,000	30	SE	Trees	Clay
15	7	4,000	20	E	Trees	Clay
16	3	3,775	20	S	Trees	Clay
17	5	3,740	30	E	Trees	Clay
18	6	3,605	20	S	Trees	Loam
19	2	3,635	10	SE	Trees	Loam
20	6	3,665	10	NE	Trees	Loam
21	2	3,880	30	E	Trees	Loam

The basin response is the sum of the responses of the units. The units therefore do not have to be single areas. In the second alternative, a hydrologic response unit was defined as above, except it was not required that a response unit consist of a sub-area enclosed by a single boundary. Opposing hill slopes of the smaller tributary drainages to Prairie Dog Creek were assigned to different units. This assignment resulted in more homogeneous vegetation, more representative slope and aspect, and probably less variation in soils in each unit (fig. 5). Their characteristics are identified in table 5.

Table 5.--Hydrologic response unit alternative B for the Prairie Dog Creek basin

Hydrologic response unit	Area (percent of total)	Median altitude (feet)	Average slope (percent)	Aspect	Dominant vegetation cover	Soil
1	5.5	4,420	10	S	Grass	Clay
2	4.5	4,360	20	S	Shrub	Loam
3	6	4,370	20	NE	Shrub	Loam
4	11	4,315	10	NE	Shrub	Loam
5	6	4,040	20	SE	Shrub	Loam
6	3	4,115	30	NE	Trees	Loam
7	5	4,080	20	N	Trees	Loam
8	2	3,945	20	S	Shrub	Loam
9	2	4,210	20	S	Trees	Loam
10	1	4,010	10	SE	Trees	Loam
11	1	3,625	Horizontal	Horizontal	Shrub	Loam
12	2	4,140	30	S	Trees	Loam
13	2	4,020	30	SE	Trees	Loam
14	6.5	3,795	30	SE	Trees	Loam
15	6.5	3,700	20	SE	Trees	Loam
16	5	3,950	30	S	Trees	Loam
17	6	3,690	10	S	Shrub	Loam
18	3	3,660	20	NE	Shrub	Loam
19	2	3,805	20	NE	Trees	Clay
20	2	3,800	20	S	Trees	Clay
21	5	3,780	20	NE	Trees	Clay
22	5	3,865	30	N	Trees	Loam
23	6	3,745	20	NE	Trees	Loam
24	3	3,820	20	S	Trees	Loam

A small basin can be considered to consist of one subsurface flow reservoir and one base-flow reservoir as the simplest case in the precipitation-runoff modeling system. The lack of information or the size of the basin may indicate that one of each of these reservoirs is sufficient. Soils, vegetation, hydrologic, and geologic information available for the Prairie Dog Creek basin indicated that increasing the number of these reservoirs might improve the results of the model simulation. The main valley floor contains significant alluvial deposits, whereas the hill slopes consist of sandstone layers, coal beds, and clinker. Color aerial photographs indicated more extensive clinker in the downstream half of the basin. Prairie Dog Creek loses water to the alluvium in the downstream part of the basin.

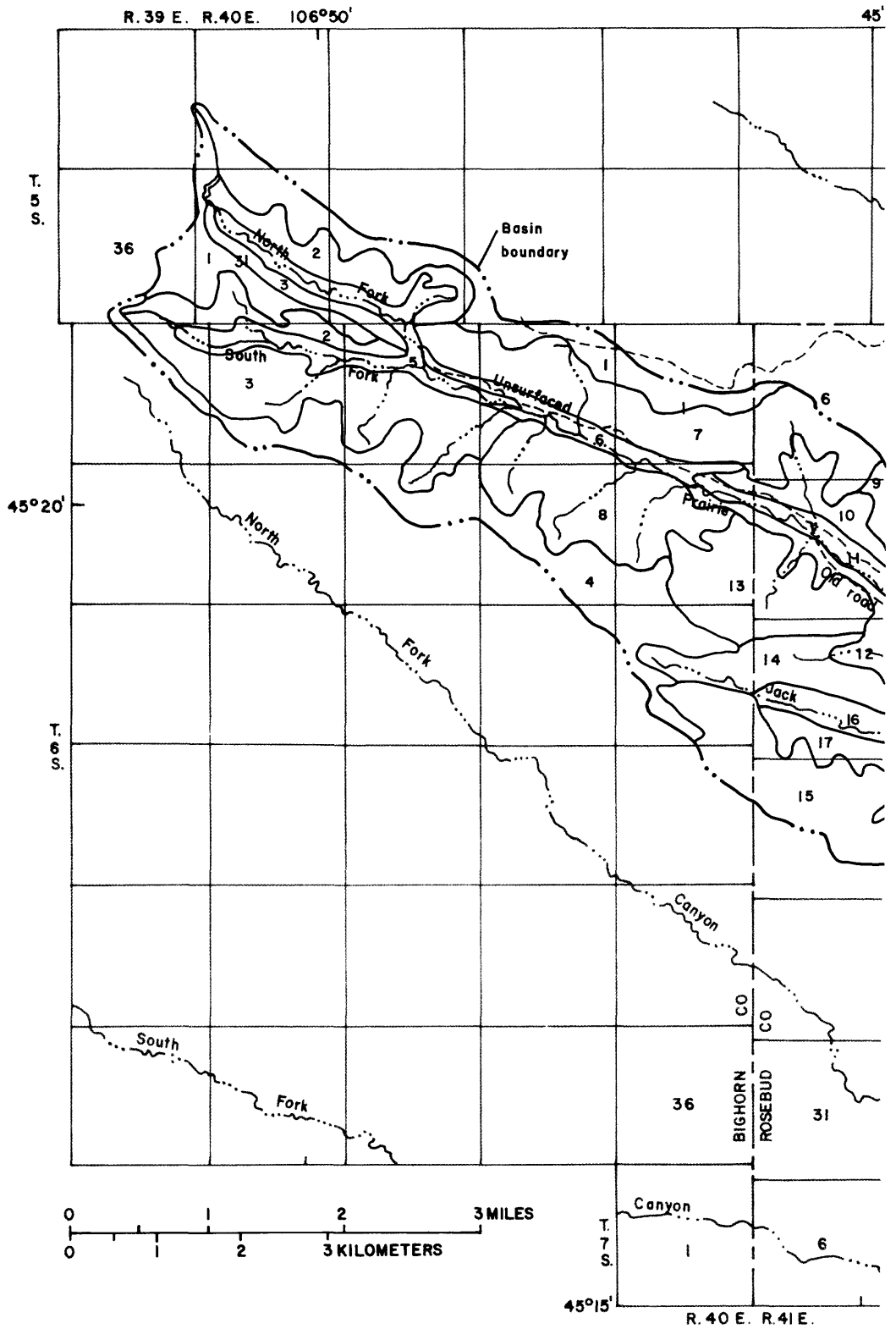


Figure 4.--Hydrologic response units



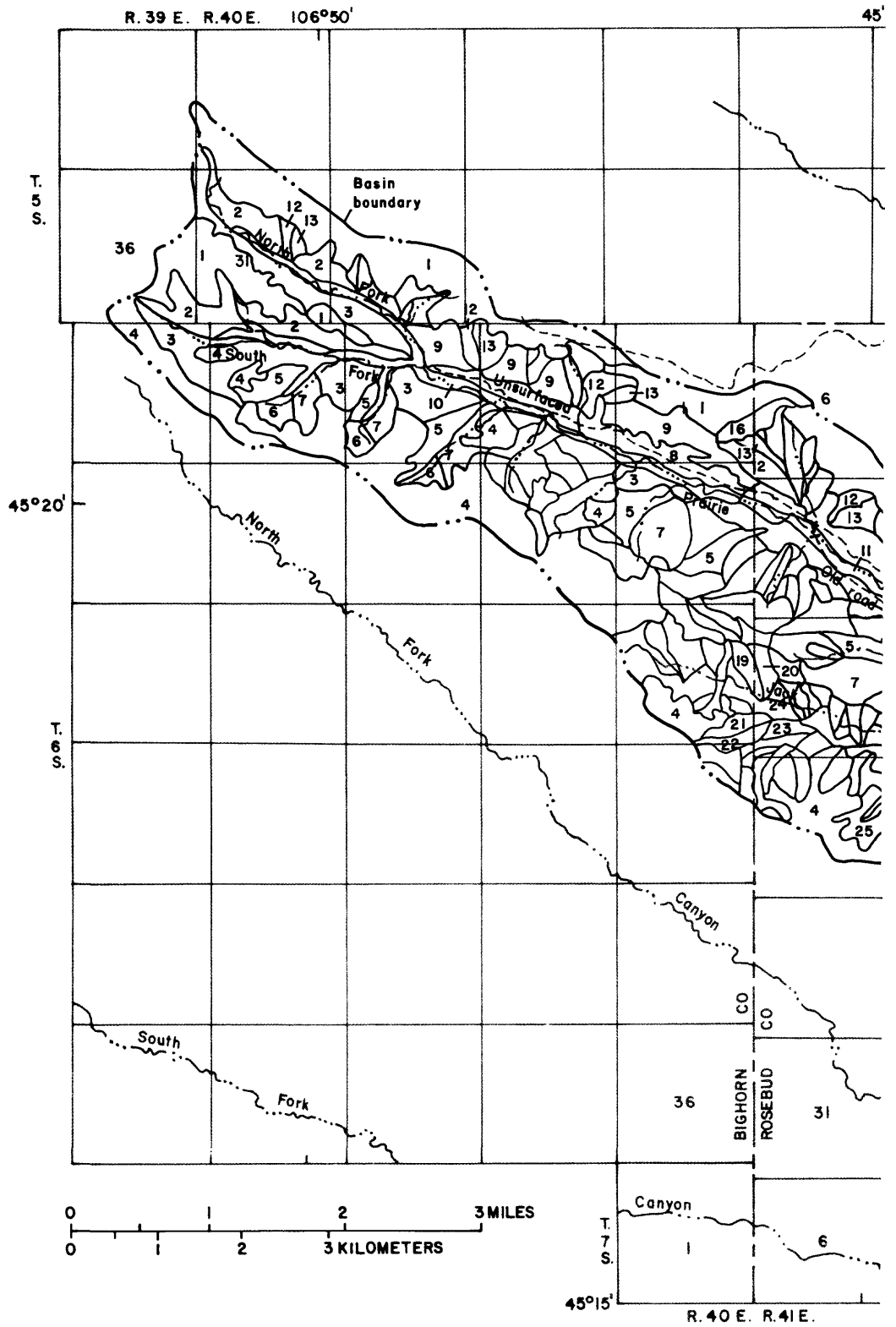
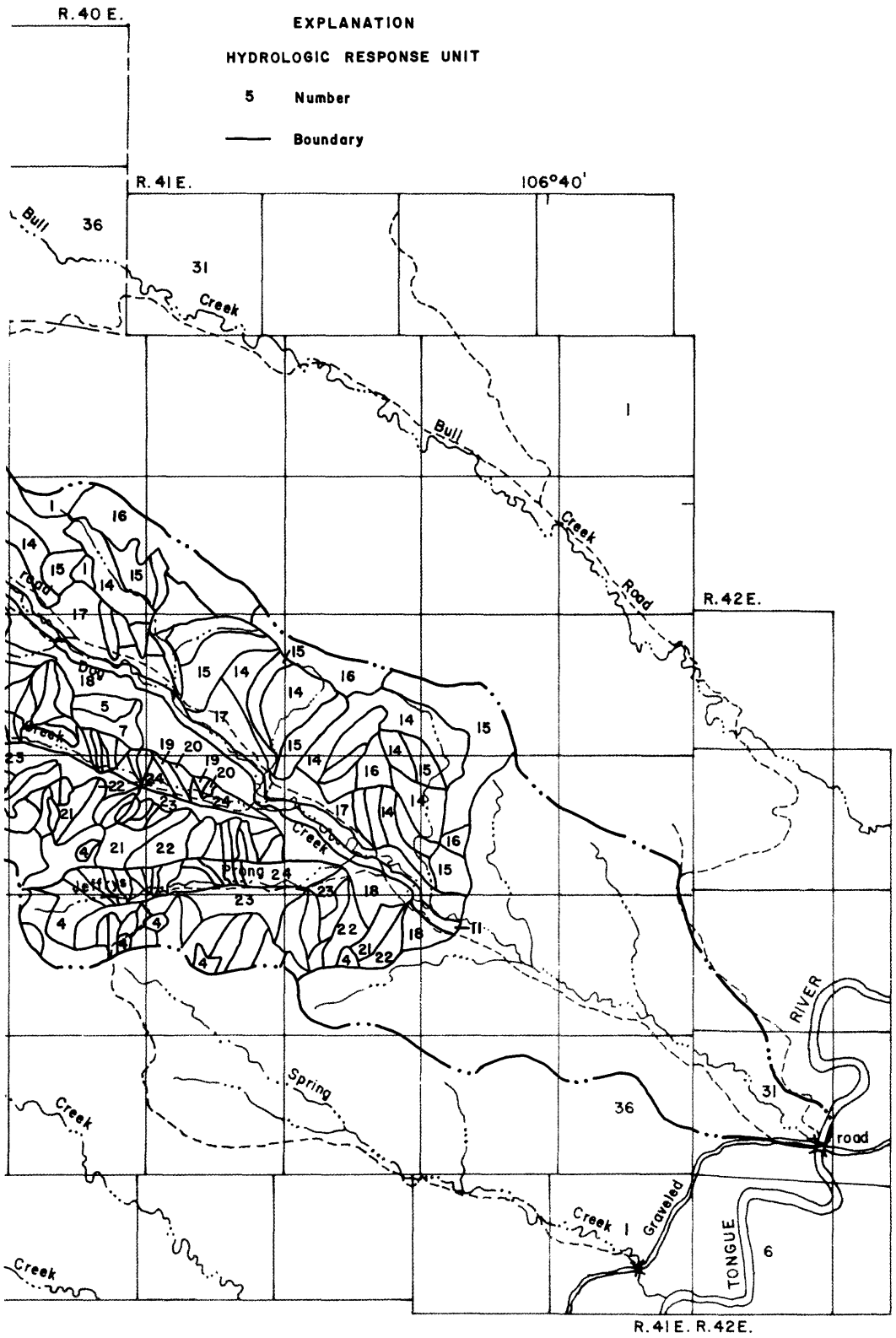


Figure 5.--Hydrologic response units



under alternative B.

The basin, therefore, was divided into four subsurface and base-flow reservoirs. These were the upstream and downstream basin main valley floor and the upstream and downstream basin hillslopes. The division between the upstream and downstream basin was taken to be the altitude contour of the approximate basin average altitude.

#### Storm simulation

The storm mode requires runoff plane and channel segment delineation if flow routing is to be used. A hydrologic response unit may be considered as one or more runoff planes. There is no provision for cascades of planes. Each plane must, therefore, drain directly into a channel segment.

Owing to the criteria used in delineating the hydrologic response units, basin uplands, hillslopes, and the main Prairie Dog Creek valley bottom commonly were included in different response units. To ensure that each plane terminated with a channel segment, without an excessively large number of planes, response unit alternative A was modified to alternative C. The valley bottom response units and upland response units were merged with the nearby hillside response units. Some response unit boundaries were redrawn. The units were divided between the upstream basin and downstream basin, as before. The subsurface and ground-water reservoirs were reduced to two, because the main valley bottom was no longer delineated separately from the hillslopes.

Each hydrologic response unit was considered a surface runoff plane for the storm mode. The stream channels were segmented as indicated by the runoff planes. Each major tributary was considered to be one segment. The main channel between tributary junctions, and between the upstream and downstream basins was considered to be separate segments.

The characteristics of the revised hydrologic response units were determined as before. The surface runoff planes coincided with the response units; therefore, areas, slopes, soil types, and so forth remained the same. The channel segment lengths were measured on the 1:24,000 base map. The effective width of the runoff plane was computed as the area of the plane divided by the associated channel segment length. Channel slope was computed for each segment as the change in altitude divided by its length, both of which were obtained from the base map. The characteristics of the response units and associated runoff planes are summarized in table 6. These units, planes, and channel segments are shown in figure 6.

Because some of the characteristics of the revised response units changed, optimization and sensitivity analyses were made and the results compared with those of hydrologic response unit alternative A with 16 response units. These results are discussed in a later section.

#### Parameter estimation

Each hydrologic response unit is characterized by its vegetation, soils, topography, and climate, which, in turn, are represented by values of parameters. The techniques used to obtain estimates of these parameters are discussed in this section. Some of the values have a strong physical interpretation and are easily estimated from climatic data, soil and vegetation surveys, and topographic maps. Others,

Table 6.--Hydrologic response unit alternative C, modified for the storm mode with associated runoff planes

Hydrologic response unit	Surface runoff plane	Area (percent of total)	Median altitude (feet)	Average slope (percent)	Aspect	Dominant vegetation cover	Soil
1	1	5	3,650	10	N	Trees	Loam
2	2	3	3,770	14	S	Trees	Loam
3	3	13	3,890	11	N	Trees	Loam
4	4	6	3,570	19	S	Trees	Clay
5	5	4	3,750	14	NE	Shrub	Loam
6	6	6	3,960	9	NE	Shrub	Clay
7	7	11	3,940	8	NE	Grass	Clay
8	8	6	4,340	11	NE	Grass	Clay
9	9	3	4,420	14	SW	Shrub	Clay
10	10	3	4,380	12	NE	Shrub	Loam
11	11	4	4,350	10	SW	Shrub	Loam
12	12	7	4,180	23	SW	Trees	Clay
13	13	8	3,860	13	SW	Trees	Loam
14	14	14	3,870	9	SW	Trees	Loam
15	15	4	3,630	15	E	Trees	Loam
16	16	3	3,610	20	W	Trees	Loam

although possessing physical interpretation, are less precisely determined owing to spatial variation and inadequate information. Still others have a weak physical interpretation and pose a considerable problem in estimation. More information is available on the Prairie Dog Creek basin than would usually be available on basins to which the model may be applied. Meteorologic data that are entered in the model are being extensively collected. Soil, vegetation, geologic, and ground-water information was collected as part of the modeling study and the small area reclamation study of McClymonds (1982). Some of this information was used in parameter estimation.

#### Daily simulation

The daily simulation mode parameters are classified as being climatic or land-phase parameters. The methods used to obtain initial parameter estimates are discussed in this section. These parameters are listed (in alphabetical order), along with their definitions, in table 7.

#### Climatic parameters

Parameters related to evaporation and transpiration include EVC, TST, CTS, CTX, and CTW. EVC, the evaporation pan coefficient, is required in the calculation of daily evaporation if the Jensen-Haise equation is not used. Otherwise, EVC is required in the calculation of evaporation from precipitation intercepted by the plant canopy. A coefficient of 0.7 was selected for each month although a larger

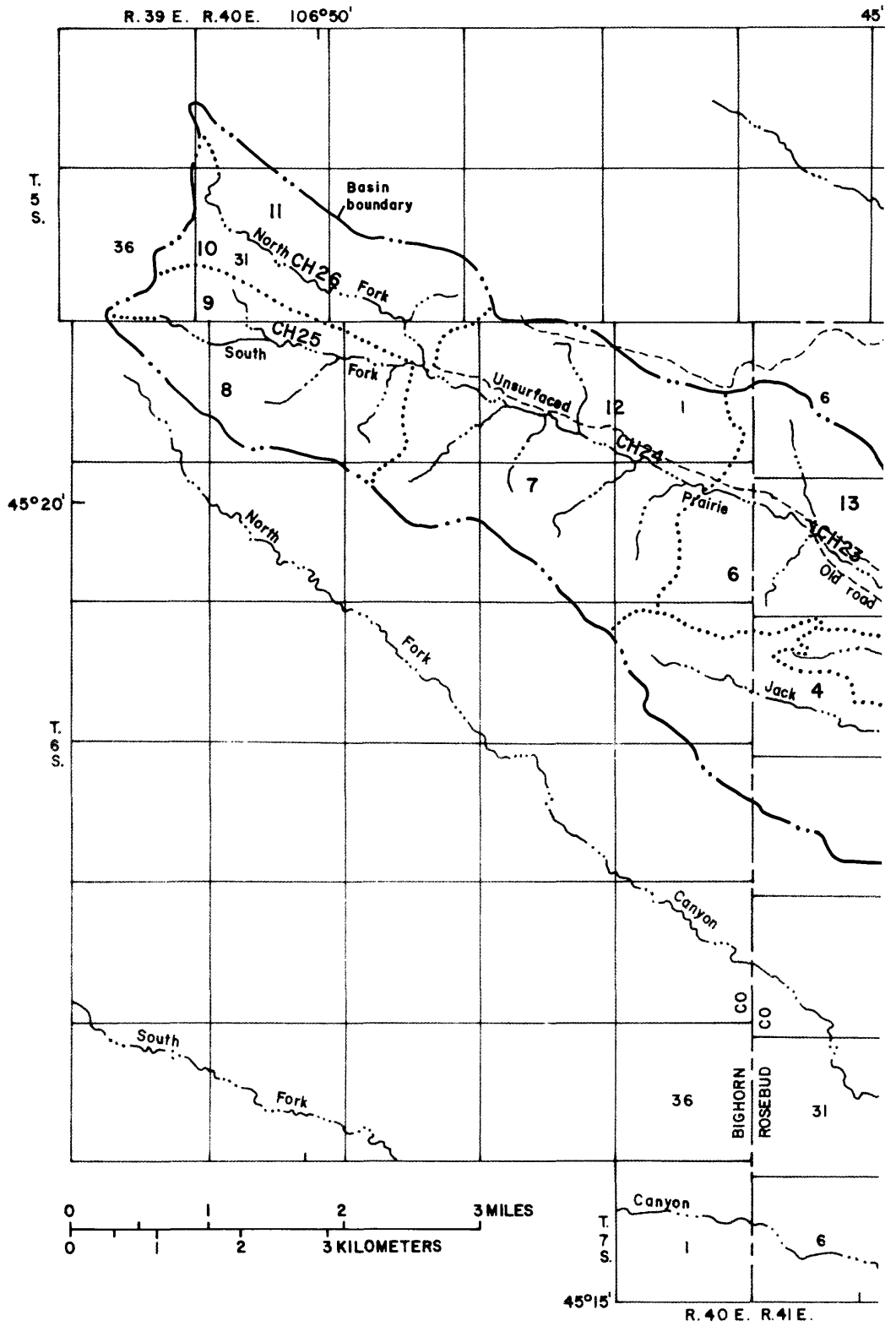


Figure 6.--Hydrologic response units under

EXPLANATION

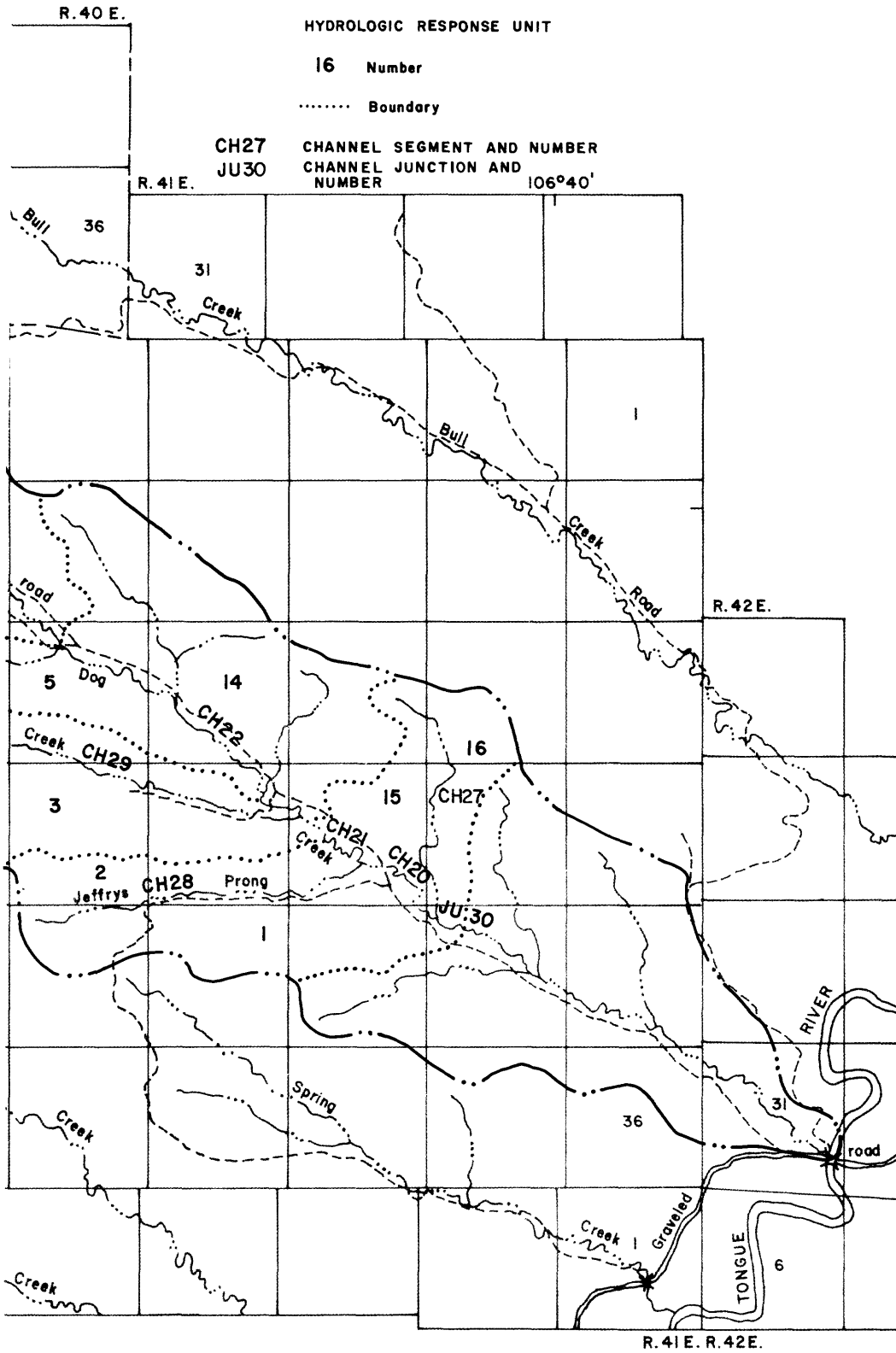
HYDROLOGIC RESPONSE UNIT

16 Number

..... Boundary

CH27 CHANNEL SEGMENT AND NUMBER  
 JU30 CHANNEL JUNCTION AND NUMBER

106°40'



alternative C and associated surface runoff planes.

Table 7.--Precipitation-runoff modeling system parameters  
for the daily simulation mode

[°C, degrees Celsius; °F, degrees Fahrenheit; ft, feet; gm/cm<sup>3</sup>, grams per cubic centimeter; in., inches; in./d, inches per day; HRU, hydrologic response unit]

Parameter	Number of values	Definition
<u>Climatic</u>		
BST	1	Base temperature below which all precipitation is snow, above which it is all rain (°F or °C).
CTS	1	Air temperature coefficient in Jensen-Haise potential evapotranspiration equation.
CTW	1	Proportion of potential evapotranspiration that is sublimated from a snowpack.
CTX	Number of HRU's	Air temperature correction factor in Jensen-Haise potential evapotranspiration equation; constant for a given area (°F).
DENI	1	Initial density of new fallen snow (gm/cm <sup>3</sup> ).
DENMX	1	Maximum snowpack density (gm/cm <sup>3</sup> ).
EVC	12 (monthly values)	Evaporation pan coefficient (in./d).
EAIR	1	Emissivity of dry air.
FWCAP	1	Free-water holding capacity of snowpack (decimal fraction).
PARS	1	Predicted solar radiation correction factor for summer days with precipitation.
PARW	1	Predicted solar radiation correction factor for winter days with precipitation.
PAT	1	Maximum air temperature which, when exceeded, forces all spring and summer precipitation to be rain (°F or °C).
RDC	12 (monthly values)	Intercept of maximum air temperature-degree day function (°F or °C).
RDM	12 (monthly values)	Slope of maximum air temperature-degree day function.

Table 7.--Precipitation-runoff modeling system parameters  
for the daily simulation mode--Continued

Parameter	Number of values	Definition
RMXA	1	Proportion of rain in a mixed rain-snow event above which albedo is not reset (accumulation stage.)
RMXM	1	Proportion of rain in a mixed rain-snow event above which albedo is not reset (melt stage).
SETCON	1	Snowpack settlement constant.
TLN	12 (monthly values)	Lapse rate for daily minimum temperature (°F or °C per 1,000 ft).
TLX	12 (monthly values)	Lapse rate for daily maximum temperature (°F or °C per 1,000 ft).
TNAJ	Number of HRU's	Aspect adjustment factor for daily minimum temperatures (°F or °C).
TST	1	Temperature index to determine start date for transpiration (°F or °C).
TXAJ	Number of HRU's	Aspect adjustment factor for daily maximum temperatures (°F or °C).
<u>Land Phase</u>		
COVDNS	Number of HRU's	Summer vegetation cover density (decimal fraction).
COVDNW	Number of HRU's	Winter vegetation cover density (decimal fraction).
CSEL	1	Meteorological station altitude.
GSNK	Number of ground-water reservoirs	Seepage rate from ground-water reservoir to ground-water sink (in./d).
IMPERV	Number of HRU's	Fraction of HRU that is impervious (decimal).
RCB	Number of ground-water reservoirs	Ground-water routing coefficient.
RCF	Number of sub-surface reservoirs	Subsurface flow routing coefficient.

Table 7.--Precipitation-runoff modeling system parameters  
for the daily simulation mode--Continued

Parameter	Number of values	Definition
RCP	Number of sub-surface reservoirs	Subsurface flow routing coefficient.
REMX	Number of HRU's	Maximum storage in upper soil zone (in.).
RESMX	Number of sub-surface reservoirs	Seepage coefficient from subsurface reservoir to ground-water reservoir.
REXP	Number of sub-surface reservoirs	Exponent of seepage function for seepage from subsurface reservoir to ground-water reservoir.
RNSTS	Number of HRU's	Summer interception storage capacity of major vegetation for rain (in.).
RNSTW	Number of HRU's	Winter interception storage capacity of major vegetation for rain (in.).
SCN	Number of HRU's	Minimum possible contributing area of HRU (decimal fraction).
SCX	Number of HRU's	Maximum possible contributing area of HRU (decimal fraction).
SEP	Number of sub-surface reservoirs	Seepage rate from soil to subsurface reservoir (in./d).
SMAX	Number of HRU's	Maximum soil-moisture storage capacity in soil profile (in.).
SNST	Number of HRU's	Interception storage capacity of major winter vegetation for snow (in. of water equivalent).
SRX	Number of HRU's	Maximum daily snowmelt infiltration capacity of soil profile (in./d).
TRNCF	Number of HRU's	Transmission coefficient for short-wave radiation through the winter vegetation canopy (decimal fraction).

value may be more appropriate for evaporation from the plant canopy. This is the frequently used pan coefficient for large reservoirs. TST, the start actual evaporation parameter, was selected such that actual evapotranspiration began after snowmelt had ended. Current model structure does not permit simultaneous transpiration and snowpack evaporation. Evapotranspiration begins when the sum of maximum daily air temperatures exceeds TST. A value of 392° F (200° C) for TST resulted in evapotranspiration beginning on March 30, 1979, and March 24, 1980. These start dates corresponded reasonably well with the end of snowmelt, especially in 1979.

CTS and CTX are parameters in the Jensen-Haise potential evapotranspiration equation. They were computed using Prairie Dog Creek meteorological station data. A single value of CTS is required for each basin, whereas a value of CTX is required for each hydrologic response unit. Estimates of CTS and CTX were also made using data from the Birney 2SW station for 1954-80. The estimates were corrected for a small difference between the 1979 values at Prairie Dog Creek and the long-term average values at Birney 2SW. There is considerable difference in the 1980 values. When the average temperatures for 1979 and 1980 were used in the calculations, the 2-year averages approximated the long term; the average values were 15.88° F for CTX and 0.0132 for CTS compared to long-term values of 15.61 and 0.0133.

Evaporation from the snowpack is computed as a fraction (CTW) of potential evapotranspiration. An estimate of CTW was computed as follows. Daily net radiation was computed for days in March 1979, assuming clear skies and a snowpack emission temperature of 32°F. An estimate of the fraction of net radiation that is used in snowpack evaporation was obtained from Granger and Male (1978). The average percentage of incoming energy used in evaporation for the three periods reported in their study was applied to the computed net radiation. The ratio of the resulting evaporation to average potential evapotranspiration for the same period resulted in a CTW value of 0.28. The model does not include an advected energy term; therefore, the value of CTW was increased to 0.30 in an attempt to account for this and for vegetation effects.

Air temperature for each hydrologic response unit is corrected for aspect and altitude. A lapse rate of 1.5°F per 1,000 ft was applied to daily maximum and minimum temperatures. The daily temperatures were also increased for east, southeast, south, and southwest aspects by a maximum of 1.1°F for south aspects. This correction was applied to maximum and minimum daily temperatures. These corrections are based upon the assumption that the base station is on an approximately horizontal surface.

The precipitation-runoff modeling system includes an estimation technique for missing solar radiation (Leavesley and others, 1983). The technique requires the slope (RDM) and intercept (RDC) of the maximum air temperature-degree day relationship. These parameters were estimated for each month of the year, using data from 1979 and 1980. A factor SOLF (ratio of observed to potential solar radiation) was estimated for wet and dry days during the summer and winter. Prairie Dog Creek solar radiation data were screened. Days with rain or days with anomalously small solar radiation were included in the rainy-day class, and the other days were considered to be dry. A random sample was drawn for each class for both the summer and winter. The average of the ratio of observed to potential solar radiation for dry days provided the estimates of SOLF. The wet-day correction factors PARS (summer) and PARW (winter) were computed as the ratio of SOLF for wet days (calculated in the same way as SOLF - dry days) and SOLF for dry days.

Two reference temperatures are required in the calculation of precipitation form. The occurrence of rain, snow, or mixed rain and snow is computed from a relationship between maximum daily, minimum daily, and base temperature BST. A value of 32°F was selected for BST. Based upon 2,400 observations of precipitation form and accompanying air temperature, 93 percent of the precipitation occurred as snow at this surface temperature (U.S. Army, 1956). PAT is the base temperature above which all spring and summer precipitation is rain, regardless of minimum air temperatures. PAT was selected to be 39°F based upon the same results used in estimating BST.

The emissivity of dry air over extensive snowfields has been estimated as 0.757 (U.S. Army, 1956). Although extensive and continuous snowfields are not common in the plains, this value was adopted as an estimate.

The initial snowpack density (DENI) was estimated to be 0.1 gm/cm<sup>3</sup> (gram per cubic centimeter). Though variable, depending upon wind and temperature at the time of fall, a new fallen snow density of 0.1 gm/cm<sup>3</sup> is an average value that has been frequently used (U.S. Army, 1956; Garstka, 1964). Maximum snowpack density, DENMX, was estimated from snow-course data acquired during late March 1979 on Prairie Dog Creek. DENMX was estimated to be 0.45 gm/cm<sup>3</sup>. Snowpack free-water holding capacity (FWCAP) ranges from 3 to 5 percent. A value of 4 percent was used for FWCAP (U.S. Army, 1956). In a mixed rain-snow fall, the albedo of the snowpack is decreased. However, rain, followed by snow, may result in fresh snow over old and thus a return to the albedo of fresh snow. Two parameters represent the fractions of rain after which the albedo is not reset. RMXA is the fraction for the snow accumulation season and RMXM the fraction for the melt season. RMXA was estimated to be 0.5 and RMXM, 0.25. Less rain in a mixed storm during the melt season (ripe snowpack) would be required to result in an "old snow" albedo than in the accumulation season. Another snowpack parameter that must be specified is the snowpack settlement time constant, SETCON. A value of 0.1 was obtained from Riley and others (1973).

#### Land phase parameters

Vegetation cover density of a hydrologic response unit affects transpiration, interception, and transmission of solar radiation to the ground. Vegetation cover density of each response unit is represented by a summer density (COVDNS) and a winter density (COVDNW). The cover density for trees and shrubs in each vegetation type was determined from a vegetation survey conducted by F. A. Branson (written commun., 1979). The response unit delineations resulted in some intermingling of vegetation types. The density was therefore computed as the area weighted average. Winter cover density was decreased only for deciduous trees.

The interception storage capacity of vegetation has been the subject of numerous studies, especially for tree and shrub species. Results of some of these studies were used to estimate interception storage capacity for rain and snow. Values of RNSTS (rain interception storage capacity, summer) and RNSTW (rain interception storage capacity, winter) for the tree species occurring in the basin were obtained from Kittredge (1948) and Branson and others (1981). Estimates of the interception storage capacity of big sagebrush was obtained from West and Gifford (1976). The interception storage capacity of silver sagebrush was assumed equal to big sagebrush. Interception by grass was assumed to be negligible. However, in grasslands this assumption may not be valid. Investigations have indicated that interception by grass or grass-like plants can be significant (Branson and others,

1981; Satterlund, 1972). The interception storage capacity for snow (SNST) was estimated as a fraction of the interception storage capacity for rain. Although snow interception can approach 1 inch of water equivalent (Satterlund, 1972), less net energy during winter months, coupled with wind effects and the melt-slide sequence (Miller, 1962; Satterlund and Haupt, 1967), results in a smaller interception loss than for rain. The interception storage capacity, in inches, was computed as the area weighted average of vegetation cover times interception storage capacity for each vegetation type in a hydrologic response unit.

The transmission coefficient (TRNCF) was estimated from figure 24 in Leavesley and others (1983) for tree cover. TRNCF was assumed to be 1 for shrub and grass cover. The transmission coefficient for each response unit was computed as the area weighted average of the vegetation types.

The soil zone in the model is defined as the average rooting depth of the dominant vegetation in a response unit. Soil depths and rooting depths in the basin were obtained from information acquired when the soil moisture access tubes were installed, from soils data acquired in the reclamation study, and from U.S. Soil Conservation Service soil surveys. A rooting depth was defined for each soil series using this information. An average rooting depth was computed for each soil mapping unit using the series composition of each mapping unit. Soil texture was estimated from the texture of soil samples and from soil profile descriptions.

The soils parameters that are required in the daily simulation mode include SMAX, REMX, and SRX. SMAX is the available water-holding capacity in the soil zone, in inches. It is calculated as the difference between soil moisture at field capacity (one-third bar) and at the permanent wilting point (15 bars). REMX is the available water-holding capacity of the upper layer of the soil zone, usually taken as the upper 12 inches. SRX is the maximum daily infiltration capacity for snowmelt.

A large amount of literature pertains to evaluating soil water and to obtaining the hydrologic characteristics of soils from commonly available soil physical properties. Estimates of SMAX, REMX, and SRX can be obtained from the equations of the soil-moisture characteristic curve. The coefficients and exponents in these equations have been related to various soil properties including texture, organic matter, porosity, and bulk density. The parameters in these soil-moisture characteristic equations therefore can be estimated from commonly available soils information and provide a unified means of estimating storm-mode and daily soils parameters in the precipitation-runoff modeling system.

The equation used to describe the soil-moisture characteristic (desorption curve) in Clapp and Hornberger (1978), which was a form used by Campbell (1974), was fitted to the desorption curves of Prairie Dog Creek soil samples. This is the Brooks and Corey (1964) equation when residual soil moisture is zero. The available water-holding capacities computed from the equations were generally less than those reported by Clapp and Hornberger (1978). The greatest difference was in the clay loam texture class where the available water-holding capacity was 11 percent (by volume), compared to 19 percent computed from data presented in Clapp and Hornberger (1978). Estimates of available water-holding capacity for the moisture units were made by estimating the capacities for the soil texture classes of each series, computing an area weighted average for each soil-mapping unit, and subsequently for each response unit. The estimates were multiplied by the average rooting depth to yield an estimate of SMAX, and by 12 in. to yield an estimate of REMX.

Although not model parameters, starting values of average soil moisture in the rooting zone (SMAV) and in the upper soil layer (RECHR) must be specified. Only one soil-moisture observation station had been installed by the beginning of the 1979 water year, near the basin outlet. The observed available water-holding capacity was computed as a ratio of current observed to the available water-holding capacity at that station, for the average rooting depth and for the first 12 in. of soil. These fractions were then multiplied by SMAX and REMX for each hydrologic response unit to provide estimates of SMAV and RECHR.

SRX, the daily snowmelt infiltration capacity, was estimated from the Green and Ampt equation using daily values and assuming a depth to wetting front of 6 in. The parameters in the Green and Ampt equation were, in turn, estimated from the relationships provided in Clapp and Hornberger (1978). Area-weighted averages of SRX were then obtained for each response unit using the same procedures that were used for SMAX and REMX.

As rainfall and snowmelt infiltrate the soil profile, they are added to current soil moisture. When the maximum available water-holding capacity (SMAX) is exceeded, the excess is routed to a user-specified subsurface reservoir. The subsurface reservoir, in turn, transmits water to streamflow or to a ground-water reservoir. If the amount of seepage reaching the subsurface reservoir (RES) exceeds the seepage to ground water (SEP), the excess is routed to streamflow and represents flow from the unsaturated zone. Seepage to ground water is a decay function based upon the ratio of current subsurface storage RES to a maximum storage RESMX raised to a power REXP. The variable RES is computed internally. The parameters SEP, RESMX, and REXP must be estimated. Estimates of SEP were made for each subsurface reservoir using observed values of saturated hydraulic conductivity for the C soil horizon and underlying parent material in each subsurface reservoir. SEP was selected to be one-half of saturated hydraulic conductivity. Estimates of REXP and RESMX were made by trial and error to yield combinations of these two parameters which would represent small storage and rapid drainage for coarse material, intermediate for intermediate textured material, and relatively large storage with slower decay for fine material. Subsurface seepage was assumed to be less in the upland areas and more in the alluvium.

Streamflow from subsurface flow is computed using reservoir routing parameters RCF and RCP. Estimates of these parameters were obtained from hydrograph analysis. RCF was considered to be two-thirds (of the recession coefficient) immediately following the peak (Leavesley and others, 1983). RCP was estimated to be one-third RCF. Hydrographs from both stream-gaging stations were used in the analysis. The more rapid decay was assumed to be from subsurface-flow reservoirs that represented the alluvium of the valley flow. The slower decay was assumed to be due to subsurface flow from the upland reservoirs.

Because the base-flow subroutine was modified, the ground-water reservoir routing coefficient, RCB, is the parameter R in Glover's equation (Aron and Borelli, 1973; Glover, 1966). The parameter RCB (or R) has units one divided by the square root of time. Estimates of  $1/RCB^2$  were made on the basis of the time delay from the onset of snowmelt to the onset of streamflow, and from the onset of snowmelt to the peak of spring runoff. The hydrographs at both stream-gaging stations for spring 1979 were used. Estimates were also calculated, using the approach of Naney, and others (1978). Aquifer-test data obtained at alluvial wells and at coal wells and published by McClymonds (1982) were used. Some average specific-yield values from Walton (1970) were also used. Distances from the watershed divide to stream channels

were estimated from a topographic map. The values so obtained differ between estimating techniques. However, the pattern is the same (table 8). Both techniques suffer from numerous alternative interpretations as well as uncertainty as to which values of transmissivity, specific yield, and distance of flow are most accurate.

Table 8.--Estimates of RCB (R) in Glover's (1966) equation  
[ft<sup>2</sup>/d, feet squared per day]

Type of analysis	Parameter R
Downstream gaging station	
Time to beginning runoff	0.16
Time to peak	.13
Upstream gaging station	
Time to beginning of runoff	.45
Time to peak	.14
Alluvial wells	
Transmissivity (T) = 2,300 ft <sup>2</sup> /d;	
Specific yield (Sy) = 0.10	
Distance of flow (feet): 500	.30
800	.19
1,000	.15
T = 2,300 ft <sup>2</sup> /d;	
Sy = 0.05	
Distance of flow (feet): 500	.43
800	.27
1,000	.21
Coal or sandstone wells	
T = 57 ft <sup>2</sup> /d;	
Sy = 0.001	
Distance of flow (feet): 2,000	.12
2,500	.10
3,500	.07

GSKN is the daily seepage rate from each ground-water reservoir to a ground-water sink. The values assigned to the GSKN parameter for each ground-water reservoir were selected arbitrarily. The values were selected to be small, although this term was increased for the alluvium.

The minimum and maximum contributing areas (SCN and SCX) of each response unit must be specified. Color aerial photographs (scale of 1:24,000) were used to delin-

eate the boundaries of the contributing areas. Changes in vegetation type and shade of green were used in selecting the boundaries. The boundaries were traced on a base map overlay and the maximum area measured. SCX was then computed as a fraction of the area of the hydrologic response unit. SCN was arbitrarily set to 0.01.

The fraction of each hydrologic response unit that is impervious (IMPERV) was selected to be 0. Although rock outcrops result in local impervious areas, they are generally upslope from pervious areas. The impervious areas identified in the basin constitute a small fraction of the total area and therefore were assumed negligible.

#### Storm simulation

The storm simulation mode requires parameter estimates for infiltration and rainfall excess. If overland flow and channel routing are desired, then parameters related to the hydraulic characteristics of the overland flow planes and channel segments must also be provided. A list of these parameters, with definitions, is provided in table 9. The storm mode uses the Green and Ampt infiltration equation. The parameters of the Green and Ampt equation have been derived from equations describing the soil-moisture characteristic curve; for example, Clapp and Hornberger (1978) and McCuen and others (1981).

Table 9.--*Precipitation-runoff modeling system parameters for the storm simulation mode*

Parameter	Number of values	Definition
DRN	Number of HRU's	Drainage factor for redistribution of moisture from saturated moisture storage to unsaturated moisture storage, a fraction of wetting front hydraulic conductivity.
DTM	Number of runoff planes or channel segments	Time interval in the finite difference solution of the kinematic routing equation for each plane and channel segment.
FLGTH	Number of runoff planes or channel segments	Length of overland flow plane or channel segment (feet).
FRN	Number of runoff planes or channel segments	Roughness parameter, Manning or Darcy-Weisbach equation.
KSAT	Number of HRU's	Hydraulic conductivity of transmission zone (inches per hour).

Table 9.--Precipitation-runoff modeling system parameters for  
the storm simulation mode--Continued

Parameter	Number of values	Definition
NDX	Number of runoff planes or channel segments	Number of distance intervals in the finite difference solution of the kinematic routing equation for each runoff plane or channel segment.
PARM1	Number of runoff planes or channel segments	Parameter $a$ in the kinematic approximation to the momentum equation, $Q = aA^m$ .
PARM2	Number of runoff planes or channel segments	Parameter $m$ in the kinematic approximation to the momentum equation, $Q = aA^m$ .
PSP	Number of HRU's	Parameter in Green and Ampt equation. Product of matric suction at wetting front and difference between volumetric soil moisture at effective saturation and field capacity (inches).
RGF	Number of HRU's	Parameter in Green and Ampt equation. Ratio of product of matric suction at wetting front and difference between volumetric soil moisture at effective saturation and permanent wetting point to PSP (dimensionless).
SLOPE	Number of runoff planes or channel segments	Slope of plane or channel segment (foot per foot).
THRES	Number of runoff planes or channel segments	Minimum depth to continue routing overland flow (inches) or minimum discharge to continue channel routing (cubic feet per second).

As was discussed earlier an empirical relationship was fitted to desorption-curve data from the Prairie Dog Creek basin. This relationship was the same as presented by Brooks and Corey (1964), except that residual soil moisture was assumed equal to zero, a form used by Clapp and Hornberger (1978). The assumption was needed because a clearly superior fit to observed data was not obtained using the Brooks and Corey form. The form of the equation used is:

$$\frac{\theta}{\theta_s} = \left( \frac{\psi}{\psi_e} \right)^\lambda \quad (1)$$

where  $\theta$  - volumetric soil moisture,  
 $\theta_s$  - soil moisture at saturation,  
 $\psi_e$  - air entry matric suction,  
 $\psi$  - matric suction at which soil moisture equals  $\theta$ , and  
 $\lambda$  - pore size distribution index.

$\psi_e$  and  $\lambda$  were estimated by nonlinear regression. Average values of  $\psi_e$  and  $\lambda$  were next computed for the texture classes found in the Prairie Dog Creek basin surface soil horizons (loam, silt loam, silty clay loam, and clay loam).

The Green and Ampt equation requires estimates of matric suction and hydraulic conductivity at the wetting front. Wetting front suction was calculated from Brakensiek (1977):

$$\psi_f = \frac{3\lambda + 2}{3\lambda + 1} (\psi_e) \quad (2)$$

Saturated hydraulic conductivity was determined from soil core samples. Therefore, average values were computed from these data for the soil texture classes. Hydraulic conductivity at the wetting front (KSAT) in the Green and Ampt equation was estimated to be one-half the saturated hydraulic conductivity (Bouwer, 1966; Morel-Seytoux and Khanji, 1974).

In the version of the Green and Ampt equation used in the storm mode, the value of the product of wetting front suction times soil moisture at saturation (effective) minus soil moisture at field capacity (PSP) is varied, linearly, to a maximum represented by the difference between soil moisture at saturation (effective) minus soil moisture at the wilting point. This parameter, PSP, was calculated as the product of wetting front suction, computed above, and the difference between soil moisture at saturation and soil moisture at one-third bar for each soil sample. The values of soil moisture were obtained from the model of the desorption curve using the average values of  $\psi_e$  and  $\lambda$  for that class. A second parameter, RGF, was calculated as the ratio of wetting front suction times the soil moisture difference at wilting point to PSP. The soil moisture at wilting point (15 bars) was estimated as above. DRN, the rate of moisture redistribution from saturated to unsaturated soil, was arbitrarily estimated to be one-half the wetting front hydraulic conductivity.

The finite difference method used in solving the kinematic wave equations requires determination of time and distance intervals for each plane and channel segment. Estimates of the roughness parameter (FRN) and the coefficients ALPHA and RM in the kinematic approximation to the momentum equation are required as well.

Dawdy and others (1978) believed that the smallest subarea of interest and the greatest intensity rainfall are needed to estimate the time interval to be used in the finite difference method. The number of distance intervals needed for each overland flow plane and channel segment can be estimated subsequently by dividing the time to equilibrium of the plane or segment by this time interval. The time to equilibrium can be calculated using the approach of Dawdy and others (1978) or Overton and Meadows (1976, p. 89, equation 5-8).

Overland flow was assumed to be turbulent. Estimates of Manning's N (FRN) were obtained from table VIII.13, of Gray and Wigham (1970, p. 8.75). A rainfall

intensity of 2 in./hr was selected for use. This value corresponded to the 100-year 1-hour storm for southeastern Montana including the Prairie Dog Creek basin (Hershfield, 1961).

The smallest surface runoff plane (hydrologic response unit 2) and its associated channel segment were used in equation 5-8 of (Overton and Meadows (1976) to calculate the time of concentration for the plane. The time of concentration (equilibrium) for the channel segment was calculated using equation 14 of Dawdy and others (1978). The time interval for the finite difference method was next estimated using equation 12 of Dawdy and others (1978). A time of concentration was subsequently calculated for each surface runoff plane using the above approach. The number of distance intervals for each plane was estimated as the ratio of the time of concentration to the finite difference time interval.

The parameter, ALPHA, is the coefficient in the kinematic approximation to the momentum equation. It was calculated from the equation for turbulent overland flow in table 9 of Leavesley and others (1983).

A triangular cross section was assumed for channel routing. This assumption was based upon onsite observation and cross sections acquired at the stream-gaging stations. Estimates of Manning's N were obtained as before, except that Barnes (1967) was used for additional guidance. The number of distance intervals was estimated as before, as the time of concentration of the channel segment divided by the finite difference time interval for the basin.

The width of the channel at 1-foot depth is required for a triangular cross section. Estimates were obtained from the cross sections at the stream-gaging stations and onsite observation. Other values were obtained by assuming that the width decreased upstream and was less for small than for large tributaries.

#### MODEL TEST

The daily simulation mode of the precipitation-runoff modeling system was tested using 2 years of data. The storm simulation mode was tested using 3 years of data.

As described earlier, the weather during water years 1979 and 1980 was dissimilar. The first year was characterized by a large snowpack and subsequent runoff that persisted until September. The second year was one of shallow snowpack resulting in a few days of streamflow, much of it occurring over frozen ground. Several periods of runoff resulting from thundershowers occurred during both years. The first year was selected for use in sensitivity and optimization analyses because of the greater duration of flow and a deeper, longer persisting snowpack.

#### Optimization and sensitivity analyses

A parametric model, such as the precipitation-runoff modeling system, is subject to several sources of error, including model error, data error, and parameter error. Model errors occur because of inadequate representation of what is being modeled. Driving variable data errors are inherent to any data-collection effort. Parameter error may occur because of inadequate data used in calculation, poorly determined subsystems, and so forth. In the instance of poorly determined

parameter values, some means of objectively optimizing the parameters is frequently used (Overton and Meadows, 1976). In the precipitation-runoff modeling system, the Rosenbrock (1960) or Gauss-Newton optimization method is used. As many as 42 parameters may be included in optimization in the daily simulation mode, in any combination of as many as 20 parameters. However, not all parameters need be used. Some parameters possess strong physical interpretations and can be well estimated from data. Optimization can result in unrealistic ending values for such parameters and increase difficulty in interpretation. Inclusion of other parameters may increase the difficulty in obtaining an optimum parameter set.

Johnston and Pilgrim (1976), in a study of parameter optimization, identified five potential problems in parameter optimization. Parameter interdependence and indifference of the objective function to the value of a parameter (insensitivity) were two of those. Significant correlation between parameters generates combinations of parameter values that yield apparent optimum values of the objective function. Parameter insensitivity can result in areas of zero gradients in the response surface in which the optimization can be "trapped," resulting in less than optimum parameter sets.

The model parameters were screened. Those parameters that possessed strong physical interpretation and were well estimated were eliminated from the parameter subset that was to be optimized. Other parameters such as those used in the estimation of missing solar radiation data were also eliminated because there was no missing data in the input data set.

Sensitivity analysis was conducted on the remaining parameters. Parameters to which simulated streamflow was not sensitive were removed from the parameter subset.

Following removal of the insensitive parameters, the remaining parameter estimates were optimized using Rosenbrock's (1960) method. Optimizations were performed for each hydrologic response unit alternative at each level of partitioning. Eight cycles were used in each optimization. A value of 5 percent was chosen for the initial change in parameter values. The first 4 months of water year 1979 were excluded from the optimization period and considered to be the "warmup period" suggested by Johnston and Pilgrim (1976).

Sensitivity analysis following optimization provides information in addition to that provided by sensitivity analysis alone. Estimates of the parameter standard error, the parameter correlation matrix, the hat matrix<sup>2</sup>, and the variance of prediction are provided (Leavesley and others, 1981 and 1983). A comparison of how well parameters have been determined, when their mean values differ by orders of magnitude, is facilitated by use of their coefficients of variation (parameter standard error divided by mean value). The correlation matrix can be used to evaluate the degree of parameter interdependence. The diagonal elements (H) of the hat matrix provide a means of evaluating the effect of each day on the optimized values. Sensitivity analysis was therefore conducted following each of the above optimizations.

---

<sup>2</sup> A matrix computed as the product of the sensitivity matrix, inverse of the information matrix, and the transpose of the sensitivity matrix. The diagonal elements give an indication of the relative effect of a day or a storm on an optimization, with values closer to 1 signifying greater effect.

Model runs were made using the results of optimization analysis and the reduced parameter set. A run was made using each response unit alternative with similar levels of basin partitioning. The results of these simulation runs were compared.

### Objective function

The selection of the objective function to be used in optimization depends upon the flow characteristics that are to be emphasized (for example, peak flow, mean daily flow, flow volume). Numerous investigations have been made into various expressions for objective functions. Johnston and Pilgrim (1976) evaluated three forms of the sum of the absolute differences between observed and predicted flows in which the exponent on the differences was selected to be 1/2, 1, or 2. They also reviewed other work and concluded that little information was available on the merits of different objective functions. They concluded from their study that use of the sums of squares of the differences favored reproduction of large events, and the use of the square root of the differences favored small events. Dawdy and others (1972) used the sum of squares of differences in the logs of flow because streamflow errors are generally more equal in percentage than in absolute terms. Dawdy and others (1978) used the same objective function in a revision of their earlier model.

The precipitation-runoff modeling system provides four alternate objective functions. These are the sum of absolute values of the differences between predicted and observed flows, the sum of squares of the differences, and the same forms using the natural logarithms of flows. The sum of squares of the differences between the logarithms of flows was selected as the objective function to be used in the continuous simulation mode, and the sum of squares of the differences between observed and simulated flows was selected for use in the storm mode.

### Hydrologic response units

The evaluation was made by concurrent optimization and sensitivity analyses of the two response unit alternatives. The reduction in number of response units in a search for an optimum number was also performed, with each reduction being subjected to optimization and sensitivity analyses. Comparisons were then made using the hydrographs, the objective function, and the parameter values.

In an evaluation of the optimum number of response units, Leavesley (1973) began with 25, then reduced this number by combining, using area weighted averages of the climatic and physical characteristics. A similar approach was used in this study, except that the units were combined in a manner that preserved the distinction between the two alternatives. Four combinations of response units were used with each definition. The fourth set represented the lumped model case (one hydrologic response unit). The recombination of response units has been summarized in table 10.

### Model components

The primary means of model evaluation is the comparison between observed and simulated streamflow. However, the precipitation-runoff modeling system is a pro-

Table 10.--Consolidation of hydrologic response units (HRU's)  
alternatives A and B

Alternative A, reduction (24 percent) to 16 HRU's		Alternative A, reduction (62 percent) to 8 HRU's	
New HRU's	Old HRU's	New HRU's	Old HRU's
1	1	1	1, 4
2	2, 7	2	2, 7, 9, 10, 18
3	3, 8, 13	3	3, 8, 12, 13
4	4	4	5, 6, 11
5	5	5	14, 16
6	6, 11	6	15, 17
7	9	7	19, (21)
8	10, 18	8	20, (21)
9	12		
10	14		
11	15		
12	16		
13	17		
14	19		
15	20		
16	21		

Alternative B, reduction (25 percent) to 18 HRU's		Alternative B, reduction (58 percent) to 10 HRU's	
New HRU's	Old HRU's	New HRU's	Old HRU's
1	1	1	1, 4
2	2, 8	2	2, 8, 17
3	3, 18	3	3, 18, 24
4	4	4	5, 21
5	5	5	6, 22
6	6	6	7, 23
7	7	7	9, 16
8	9, 16	8	10, 11
9	10, 11	9	12, 14, 19
10	12, 14	10	13, 15, 20
11	13, 15		
12	17		
13	19		
14	20		
15	21		
16	22		
17	23		
18	24		

cess model and as such, simulates each component of the hydrologic cycle that is important in the basin. Some of the components, such as evapotranspiration, deep seepage, and ground-water discharge, are difficult to evaluate without detailed and difficult-to-obtain data. Snow-course data and soil-moisture data were acquired periodically in the basin. These data, although spatially and temporally discrete, provide a means of comparison between observed and simulated snowpack water equivalent and soil moisture. These comparisons were, therefore, made as an additional means of model evaluation.

The precipitation-runoff modeling system provides a means of adjusting the simulated snowpack water equivalent to observed data once each year of model operation. Corrections in the water equivalent of the snowpack can be made internally. This option was not used, so that the simulated and observed water equivalent data would be independent.

## RESULTS

### Daily simulation

#### Results of initial sensitivity analysis

The parameter subsets were defined from the sensitivity analysis using the error propagation table. The results of the error propagation analysis for both of the hydrologic response unit alternatives have been presented in table 11. The values in the table are the mean squared runoff prediction error of the logarithms of flow associated with a 20-percent change in parameter value. The estimated residual variance is provided at the bottom of the table for comparison. A 10-percent error in parameter values will generally result in an increase in runoff prediction error of about 10 percent of the residual variance. The parameters included in the table are those that remained following initial screening. Based upon the results in table 11, TRNCF, CTX, SMAX, SEP, RESMX, REXP, RCB, CTS, and BST were selected for further analysis. All the parameters retained except CTX and CTS contributed more to prediction error under alternative A than alternative B, which may reflect the more detailed land area subdivision permitted under B. The contribution to prediction error by errors in RCB was much greater than the other parameters under both alternatives, which might reflect either an inadequate model or poorly determined parameter estimates. However, the model of base flow used here has been used successfully elsewhere (Aron and Borelli, 1973; Naney and others, 1978).

Certain pairs of parameters could be expected to have high correlations. TRNCF was estimated from vegetation cover density. Therefore, COVDNW was excluded because its contribution to prediction error was less than that of TRNCF.

CTX and CTS, parameters in the Jensen-Haise equation, were both retained because of their effects on prediction error under both alternatives. However, the two parameters were highly correlated. Similarly high correlation could be expected among the parameters in the subsurface reservoir seepage relationship. Again, these were retained because of their relative contribution to the error.

After the reduced parameter set was identified, optimization followed by sensitivity analysis was completed using the reduced set and alternative A. The parameter standard errors and correlations were examined. SEP and RESMX were highly correlated, as were CTX and CTS (both pairs exceed 0.9). Therefore, RESMX and CTX were removed from the reduced parameter set.

Table 11.--Mean squared runoff prediction error<sup>1</sup> resulting from a 20-percent parameter error, hydrologic response unit (HRU) alternatives A and B

Parameter	HRU, alternative A	HRU, alternative B
COVDNW	0.001	0.001
TRNCF <sup>2</sup>	.079	.051
CTX <sup>2</sup>	.006	.004
TNAJ	.000	.000
SMAX <sup>2</sup>	.061	.041
REMX	.000	.000
SCX	.000	.000
SCN	.000	.000
RCF	.002	.000
RCP	.000	.000
SEP <sup>2</sup>	.057	.001
RESMX <sup>2</sup>	.010	.002
REXP <sup>2</sup>	.010	.003
RCB <sup>2</sup>	1.81	1.22
TLX	.000	.001
CTS <sup>2</sup>	.002	.003
BST <sup>2</sup>	.058	.037
SRX	.000	.000
Residual variance	.951	.386

<sup>1</sup> Based on natural logarithms of flow.

<sup>2</sup> Selected for further analysis

Of the parameters remaining, six were the same as those reported in Leavesley and others (1981). These were TRNCF, SMAX, SEP, RCB, CTS, and BST. REXP was included in the parameter subset in this study, but was not in the study of Leavesley and others (1981). Conversely, they retained COVDN, TLX, and TST.

#### Results of daily optimization

The effects of optimization upon average values of the parameters are given in table 12 for alternative A and table 13 for alternative B. The initial and optimized values are presented along with the percentage change in value. These data are shown for each level of hydrologic response unit delineation. Distributed parameters were adjusted by equal percentages in the optimizations.

The change in the value of TRNCF was consistently small for each level of delineation and response unit definition. The values under alternative B were consistently less than under alternative A. The changes in value under alternative B are probably too small to result in any detectable change in snowmelt or runoff. Under alternative A, TRNCF increased by 8 percent under 16 response units but decreased by 18 percent under 8 response units, which would result in noticeable changes in the snowmelt rate and hydrograph. The generally small changes may be a

Table 12.--Results of optimization on average parameter values, hydrologic response unit (HRU) alternative A

Parameter	21 HRU's			16 HRU's			8 HRU's			1 HRU		
	Initial value	Optimized value	Change (percent)	Initial value	Optimized value	Change (percent)	Initial value	Optimized value	Change (percent)	Initial value	Optimized value	Change (percent)
TRNCF	0.87	0.84	- 3	0.87	0.94	+ 8	0.88	0.72	-18	0.65	0.65	0
SMAX	4.39	6.22	+42	4.44	6.28	+41	4.53	4.93	+ 9	4.48	4.95	+11
SEP	1.00	.99	- 1	1.00	.71	-29	1.16	.85	-27	1.11	.83	-25
REXP	1.39	1.08	-22	1.39	1.39	0	1.28	2.03	+59	1.40	2.34	+67
RCB	.13	.19	+46	.13	.20	+54	.12	.19	+58	.12	.17	+42
CTS	.0133	.0081	-39	.0133	.0081	-39	.0133	.0193	+45	.0133	.0185	-39
BST	32.1	31.1	- 3	32.1	38.3	+19	32.1	33.4	+ 4	32.1	37.5	+17
Objective function	142.4	20.2	-86	131	19.3	-85	121.8	19.8	-84	136.5	21.6	-84

Table 13.--Results of optimization on average parameter values, hydrologic response unit (HRU) alternative B

Parameter	24 HRU's			18 HRU's			10 HRU's			1 HRU		
	Initial value	Optimized value	Change (percent)	Initial value	Optimized value	Change (percent)	Initial value	Optimized value	Change (percent)	Initial value	Optimized value	Change (percent)
TRNCF	0.69	0.69	0	0.68	0.67	- 1	0.69	0.68	- 1	0.71	0.73	+ 3
SMAX	3.90	5.16	+32	3.74	5.53	+48	3.94	5.26	+34	3.71	5.60	+51
SEP	1.00	1.15	+15	1.00	.63	- 7	1.00	.88	-15	.95	.94	- 1
REXP	1.34	1.99	+49	1.34	1.42	+ 6	1.39	2.10	+51	1.51	1.00	-34
RCB	.13	.20	+54	.13	.20	+54	.15	.23	+53	.11	.17	+55
CTS	.0133	.0127	- 5	.0133	.0113	-15	.0133	.0127	- 5	.0133	.0113	-15
BST	33.8	30.0	-11	33.8	30.0	-11	33.8	33.8	0	33.8	32.2	- 5
Objective function	86.5	20.7	-76	93.2	19.0	-80	95.9	27.4	-71	185.8	21.01	-89

reflection of the use of observed values of vegetation cover density as well as the predominance of sagebrush-grassland vegetation types in the basin.

Relatively large changes in SMAX occurred under both alternatives, and in every instance, the optimized value was greater than the initial value. The available water-holding capacity was usually somewhat less than the estimates derived from Clapp and Hornberger (1978). Also, average rooting depths were estimated from on-site data and soil-survey-profile descriptions. In some instances, particularly sagebrush, the rooting depths may have been underestimated. Increasing SMAX increases the storage capacity in the soil, providing greater opportunity for transpiration, and reducing seepage to the subsurface reservoir and subsequently to the ground-water reservoir.

Moderate decreases in SEP occurred with optimization, except for alternative B, 24 units. Smaller values would result in a lessened rate of seepage to ground water and a greater chance for occurrence of streamflow from the subsurface reservoir. Most of the streamflow resulting from snowmelt during 1979 occurred as base flow. Reducing SEP is not in accordance with this observation. However, increasing SMAX would reduce the frequency and amount of seepage from the soil zone to the subsurface reservoir.

REXP, the exponent in the subsurface reservoir seepage function, was changed both small and large amounts by optimization. The smallest changes were no change for alternative A (16 units) and 6 percent for alternative B (18 units). The change was usually positive, which would result in a lessened rate of seepage to the ground-water reservoir.

The largest consistent percentage change was in RCB. The optimized value was greater than the initial value for all response unit delineations, for both alternatives. Increasing RCB reduces the time delay between an increment to ground water and the beginning of subsequent base flow. It also reduces the flow duration, but increases the peak daily flow resulting from that increment to ground water.

CTS was decreased under alternative B for each set of response units. Under alternative A, it was decreased for 21 and 16 units, but increased for 8 and 1 units. The relative changes were consistently greater under alternative A, ranging from 39 to 45 percent. Under alternative B, the greatest change was a 15 percent decrease for both 18 units and 1 unit. Changes in the value of CTS result in the same percentage change in potential evapotranspiration. A value of 0.0145 (after optimization) was reported by Leavesley and others (1981). An initial value of 0.0133 was computed in this study. Considering the difference in latitude between the basin used in their study and the Prairie Dog Creek basin, as well as the value of CTS computed from the records of Birney 2SW, it was concluded that the value of CTS would be somewhat less than the value reported by them. However, the value of 0.0081 (obtained after optimization) is probably too small.

BST either remained unchanged or decreased moderately under alternative B. It generally increased under alternative A; for 16 units, it increased by 19 percent. An increase in BST results in a smaller frequency of simulated mixed rain-snow events and a smaller fraction of rain in each such event. If a value of 35°F were used as the temperature above which all precipitation was rain, a correct classification of form would result 90 percent of the time (U.S. Army, 1956). An optimized value of BST near this, therefore, could be considered reasonable.

The value of the objective function (differences between logarithms of flows) before and after optimization for each set of response units is presented in the last row of tables 12 and 13. In each instance, optimization resulted in at least a 71-percent reduction. The minimum value of the objective function was obtained when 16 units were used under alternative A and 18 units under alternative B. The minimum values under both alternatives were nearly equal. The initial value of the objective function was less under alternative B than A. This relationship may indicate that the units were more homogeneous under alternative B than under A.

The effects of optimization on simulated streamflow are summarized in tables 14 (alternative A) and 15 (alternative B). The observed and simulated mean monthly stream discharge for each level of partitioning is given, along with the value of the objective function for each month.

Table 14.--Simulated mean monthly streamflow before and after optimization for hydrologic response unit (HRU) alternative A

Stream discharge, in cubic feet per second													
Month (1979 water year)	Observed	21 HRU's			16 HRU's			8 HRU's			1 HRU		
		Initial	Optimum	Objective function <sup>2</sup>	Initial	Optimum	Objective function <sup>2</sup>	Initial	Optimum	Objective function <sup>2</sup>	Initial	Optimum	Objective function <sup>2</sup>
Oct.	0.44	0.16	0.20	--	0.17	0.20	--	0.41	0.51	--	0.54	0.65	--
Nov.	.27	.05	.01	--	.05	.01	--	.12	.02	--	.15	.02	--
Dec.	.05	.01	0	--	.02	0	--	.04	0	--	.02	0	--
Jan.	0	0	0	--	0	0	--	0	0	--	0	0	--
Feb. <sup>1</sup>	0	0	0	0	0	0	0	0	0	0	0	0	0
Mar. <sup>1</sup>	0	.10	.05	.50	.04	.05	.44	.05	.04	.35	.05	.05	.48
Apr. <sup>1</sup>	1.02	.73	1.37	6.65	.55	1.14	6.38	.51	1.59	6.54	.53	1.76	7.85
May <sup>1</sup>	2.03	.28	2.45	4.86	.35	1.66	4.66	.64	1.47	6.89	4.16	1.56	6.40
June <sup>1</sup>	1.02	5.02	1.01	1.91	5.22	.53	3.62	6.17	.66	2.35	5.24	.49	3.59
July <sup>1</sup>	.34	3.29	.19	2.36	3.06	.31	1.41	2.26	.56	1.88	1.85	.40	1.35
Aug. <sup>1</sup>	.40	1.37	.04	3.75	1.24	.12	2.41	.72	.29	1.02	.07	.20	1.56
Sept. <sup>1</sup>	.03	.44	.03	.17	.36	.05	.14	.05	.19	.78	.03	.13	.34
Annual	.47	.96	.45	20.2	.92	.34	19.3	.91	.45	19.8	1.06	.44	21.6

<sup>1</sup> Period used in objective function calculation

<sup>2</sup> Sum of squares of the differences between the natural logarithms of flows

The poorest agreement between observed and simulated mean monthly flow for the year occurred with a level of partitioning of 16 units under alternative A and 18 units under alternative B, even though these two partitioning levels had the lowest values of the objective function. All other levels of partitioning, including the lumped parameter case (1 unit), resulted in closer correspondence. The monthly value of the objective function was generally largest in April, although the peak streamflow occurred in May. More precipitation occurred in April than in May from more storms (11 rainy days versus 9). These storms resulted in much larger simulated flows on rainy days than were observed. Under some levels of partitioning, simulated flow began in late March, whereas observed flows did not begin until the 6th of April. There were several days of relatively large (greater than 1 ft<sup>3</sup>/s) simulated flow during this period, which further increased the objective function.

Consistent improvement was obtained through optimization for both alternatives and each level of delineation. No large changes in the value of the objective function occurred with changing levels of basin delineation under either alternative, however. The minimum value occurred with 16 units under alternative A and 18 units under alternative B. The objective function under alternative B was slightly less than under A at these levels of delineation. The monthly value of the objective function generally decreased through the season. The decrease is primarily a reflection of decreasing flow through the season and, subsequently, smaller sums of squares. It does not necessarily reflect improved fit of the model later in the season. The absence of large differences in objective-function values indicates that the model is not highly sensitive to the degree of basin

Table 15.--Simulated mean monthly streamflow before and after optimization for hydrologic response unit (HRU) alternative B

Month (1979 water year)	Stream discharge, in cubic feet per second												
	Observed	24 HRU's			18 HRU's			10 HRU's			1 HRU		
		Initial	Optimum	Objective function <sup>2</sup>	Initial	Optimum	Objective function <sup>2</sup>	Initial	Optimum	Objective function <sup>2</sup>	Initial	Optimum	Objective function <sup>2</sup>
Oct.	0.44	0.22	0.29	--	0.20	0.26	--	0.44	0.54	--	0.50	0.67	--
Nov.	.27	.06	.01	--	.05	.01	--	.12	.02	--	.16	.02	--
Dec.	.05	.02	0	--	.02	0	--	.04	0	--	.05	0	--
Jan.	0	0	0	--	0	0	--	0	0	--	0	0	--
Feb. <sup>1</sup>	0	0	0	0	0	0	0	0	0	0	0	0	--
Mar. <sup>1</sup>	0	0	.25	3.63	0	.06	.87	.02	.02	.16	1.0	0	0
Apr. <sup>1</sup>	1.02	1.57	1.48	9.33	1.73	1.12	6.38	2.52	1.48	14.3	.09	1.32	4.12
May <sup>1</sup>	2.03	.90	1.94	3.05	.76	1.66	4.57	.64	1.60	5.86	.18	1.98	3.12
June <sup>1</sup>	1.02	3.22	.75	1.62	2.86	.58	3.32	4.03	.59	3.55	8.03	.36	6.49
July <sup>1</sup>	.34	2.53	.45	1.29	2.68	.30	1.45	2.26	.51	1.62	3.28	.12	3.24
Aug. <sup>1</sup>	.40	1.12	.26	1.06	1.15	.15	1.97	.81	.26	1.23	1.14	.04	3.80
Sept. <sup>1</sup>	.03	.36	.18	.76	.40	.10	.42	.11	.17	.70	.05	.03	.25
Annual	.47	.83	.47	20.7	.82	.36	19.0	.89	.43	27.4	1.21	.38	21.0

<sup>1</sup> Period used in objective function calculation  
<sup>2</sup> Sum of squares of the differences between the logarithms of flows

delineation or to response unit alternatives in the Prairie Dog Creek basin. Within each response unit, considerable averaging of soils and vegetation characteristics took place. Averaging may have offset the potential increased sensitivity that may have been realized by higher levels of basin delineation.

The optimum number of response units appears to be 15-22, regardless of basin size, at least in the Rocky Mountain region. Leavesley (1973) concluded that 15 units was an optimum number for the 12.4-mi<sup>2</sup> montane-subalpine Little Beaver Creek watershed in Colorado. Weeks and others (1974) used 22 units in a study of part of the Piceance Basin in Colorado, a considerably larger basin. More recently Leavesley and others (1981) used 19 units in an application of the model to a 2.7-mi<sup>2</sup> basin in northwestern Colorado. In this study, 16 and 18 units were found to be the optimum numbers for the 19.4-mi<sup>2</sup> Prairie Dog Creek basin.

#### Results of final sensitivity analysis

The results of the sensitivity analyses were summarized and placed in tables 16-18. The effects of a 20-percent error in parameter estimates for each alternative and level of partitioning were included in table 16. SMAX and RCB contributed most to prediction error in both alternatives, and SEP contributed the least. The effects of decreased partitioning were variable, although the greatest contribution to error frequently occurred for the lumped parameter case, and the joint error was greatest under both alternatives. The contribution to prediction error by SEP did

Table 16.--Effects of a 20-percent error in parameter value upon mean squared prediction error, hydrologic response unit (HRU) alternatives A and B

Parameter	Alternative A				Alternative B			
	21 HRU's	16 HRU's	8 HRU's	1 HRU	24 HRU's	18 HRU's	10 HRU's	1 HRU
TRNCF	0.005	0.003	0.023	0.114	0.060	0.049	0.091	0.143
SMAX	.198	.207	.182	.335	.090	.099	.191	.287
SEP	.001	.001	.001	.001	.000	.001	.001	.000
REXP	.005	.007	.005	.007	.005	.005	.005	.005
RCB	.281	.251	.426	.308	.222	.181	.217	.693
CTS	.010	.008	.005	.009	.004	.005	.009	.025
BST	.011	.001	.007	.004	.163	.174	.045	.211
Joint error	.585	.646	.681	.995	.570	.523	.548	1.567

Table 17.--Parameter coefficients of variation (percent), hydrologic response unit (HRU) alternatives A and B

Parameter	Alternative A				Alternative B			
	21 HRU's	16 HRU's	8 HRU's	1 HRU	24 HRU's	18 HRU's	10 HRU's	1 HRU
TRNCF	5.0	7.0	2.5	1.2	1.6	1.7	1.5	1.0
SMAX	.9	1.0	.9	.7	1.3	1.2	1.0	.7
SEP	15.2	13.0	15.9	14.8	17.4	15.4	16.6	18.0
REXP	5.4	4.0	5.3	4.7	5.6	5.2	6.0	6.0
RCB	.7	1.0	.6	.7	.8	.8	.9	.5
CTS	3.7	4.0	5.2	4.3	6.3	5.3	4.8	3.0
BST	3.6	13.0	4.5	5.8	.9	.9	2.1	.8

Table 18.--Correlation coefficients greater than 0.75 in absolute value under various levels of basin partitioning, hydrologic response unit (HRU) alternatives A and B

Parameter pairs	Alternative A				Alternative B			
	21 HRU's	16 HRU's	8 HRU's	1 HRU	24 HRU's	18 HRU's	10 HRU's	1 HRU
TRNCF-SMAX	--	--	--	--	--	--	--	0.78
TRNCF-RCB	--	--	--	--	--	-0.82	--	--
TRNCF-BST	--	--	--	0.84	--	--	--	--
SMAX-CTS	--	--	-0.95	-0.89	-0.79	--	-0.76	--
SEP-REXP	0.84	0.93	.95	.98	.86	.94	.87	.87
SEP-CTS	.80	--	--	--	--	--	--	--
REXP-CTS	--	--	--	--	--	--	--	-.79

not change noticeably between levels of partitioning or between alternatives. The stability indicates that the initial estimates of SEP were sufficiently large that changing their value did not significantly affect prediction error. Smaller estimated values of SEP may result in increased sensitivity. Otherwise, SEP could be eliminated from optimization. The sensitivity of REXP did not change noticeably with levels of partitioning, although its contribution to error was somewhat greater than SEP. The sensitivity of the model to SMAX and RCB was consistently high and

usually greater for alternative A than B. The effects of the remaining parameters were more variable.

The coefficients of variation of the parameters for each alternative and each level of partitioning are presented in table 17. None of the parameters exceed the 25-percent level indicated in Mein and Brown (1978). SEP exhibited the largest coefficient of variation and SMAX and RCB the least. Comparison of table 17 with table 16 reveals that the parameters having the greatest effect upon runoff prediction error had small coefficients of variation. Mein and Brown (1978) indicated that large coefficients of variation could be due to least-squares estimates failing to provide good estimates of the true parameter set or to a larger number of parameters than necessary to simulate the characteristics of the watershed. The large values of coefficient of variation especially for SEP and REXP, may reflect inadequate estimation techniques and subsequent inability to determine a parameter set through optimization that was near the "true" set.

The value of correlation coefficients which would indicate a high degree of correlation between parameters is somewhat arbitrary. A value greater than 0.75 has been suggested (Mein and Brown, 1978). Parameter correlation coefficients greater than 0.75 changed with the level of partitioning for both alternatives. The largest number of correlation coefficients greater than 0.75 occurred in the lumped parameter (1 unit) case under both alternatives (table 18). A correlation coefficient of greater than 0.75 between SEP and REXP occurred with all levels of partitioning under both alternatives. The second most frequent "significant" correlation coefficient occurred four times between SMAX and CTS. The remaining large correlation coefficients occurred once each between different pairs of parameters. Many of these were unpredictable and reflect changes in relationships between parameters with varying levels of partitioning and response unit definition.

The hat matrices for all levels of partitioning under each alternative were inspected in order to determine the sensitivity of each day in the modeled period. Generally, the effect upon the objective function was greatest ( $h_1$  greater than 0.1) early in the period included in the objective function calculation (Feb.-Sept.) and corresponded to peak snowmelt runoff.

The occurrence of rainfall could result in increased effect upon the objective function. The relative frequencies of rainy days and of the total days affecting the objective function were computed. These days accounted for as few as 30 percent and as many as 60 percent of the total days. However, the values of the hat matrices did not change significantly on these days compared to those on the dry days.

In no instance did the number of days with elements greater than 0.5 exceed 2. The larger values of the hat matrix usually occurred early, then gradually decreased through the season. Although individual days did not affect the objective function greatly, the earlier days included in its calculation had greater effect than later days. Most of the streamflow during this time was the result of snowmelt. Thus, the greatest effect occurred earlier in the season, during and soon after snowmelt.

The model was run using data from both the 1979 and 1980 water years, and optimized parameter values. Model runs were made using alternative A (16 units) and alternative B (18 units). These two levels of basin partitioning were selected as being "optimum" levels of partitioning based upon the previous results.

## Mean daily streamflow

The hydrographs of simulated and observed mean daily streamflow for the 1979 water year are presented in figure 7. There was some carryover base flow from the previous water year, which lasted until about mid-December, ending with winter freezeup. Simulated streamflow during the same period decreased more rapidly, ending more than a month before observed streamflow. This period was part of the initialization period for simulation, so was not used in optimization. The poor fit is the result of uncertainty as to the soil, and subsurface and ground-water reservoir contents at the beginning of the simulation.

Spring snowmelt runoff began about April 6. Simulated runoff began April 16 under alternative A. There were several periods of runoff before this time, but they were directly attributable to rainfall occurring on those days. Under alternative B, runoff began earlier, on March 20. Beginning about April 15, both simulations approximated the observed hydrograph, except they both lagged large changes by 3 to 5 days. Observed peak flow occurred on May 23. Simulated peak flow occurred on May 17 under alternative A and on the 22d to the 25th under alternative B. The peak flow under alternative A was nearer to the observed than was that of alternative B.

During June through August, simulated flow was generally less than observed flow. During August, there was a period of increased flow that was not reflected in changes in simulated flow. During September, simulated flow was greater than observed. No flow occurred on the 9th and 10th. A storm later on the 10th and on the 11th resulted in streamflow for 10 days. By the 21st, flow ceased. During this period, both alternatives gave the same simulated flow, and indicated flow throughout the month.

Both alternatives produced simulated streamflow during the fall and winter of the 1980 water year (fig. 8), although the flows were too small to delineate on the graph. Under alternative A, flow ended on December 27, while under alternative B flow continued through March 4. During this time, fall storms produced three short periods of streamflow, two in October and one in November. The first storm in October resulted in increased simulated flow, but the remaining storms didn't. The model considered all remaining precipitation to be snow, most of which accumulated on the ground.

The first streamflow to occur during the late winter of 1980 began February 20 and ended on February 28. Soil-temperature and soil-frost observations made near this period indicated that the first streamflow was runoff over frozen ground. Alternative A did not simulate any streamflow during this period. Alternative B simulated a small amount of base flow but no increase in flow due to snowmelt or precipitation during this period. A second period of streamflow occurred during March 6-9, probably in response to precipitation that occurred March 3-5 and again March 9. Alternative A simulated streamflow on March 10, 15, 19, and 24. Alternative B simulated streamflow only on March 31.

Actual streamflow occurred only in direct response to rainstorms during the rest of the year. Under alternative A, base flow from snowmelt was simulated, beginning April 26 and lasting until May 27. One rainstorm during this period resulted in relatively high simulated peak flows ( $2.5 \text{ ft}^3/\text{s}$ ) for both alternatives. These flows were of short duration, however. Under alternative B simulated streamflow from snowmelt began March 31 and continued through the end of June, peaking

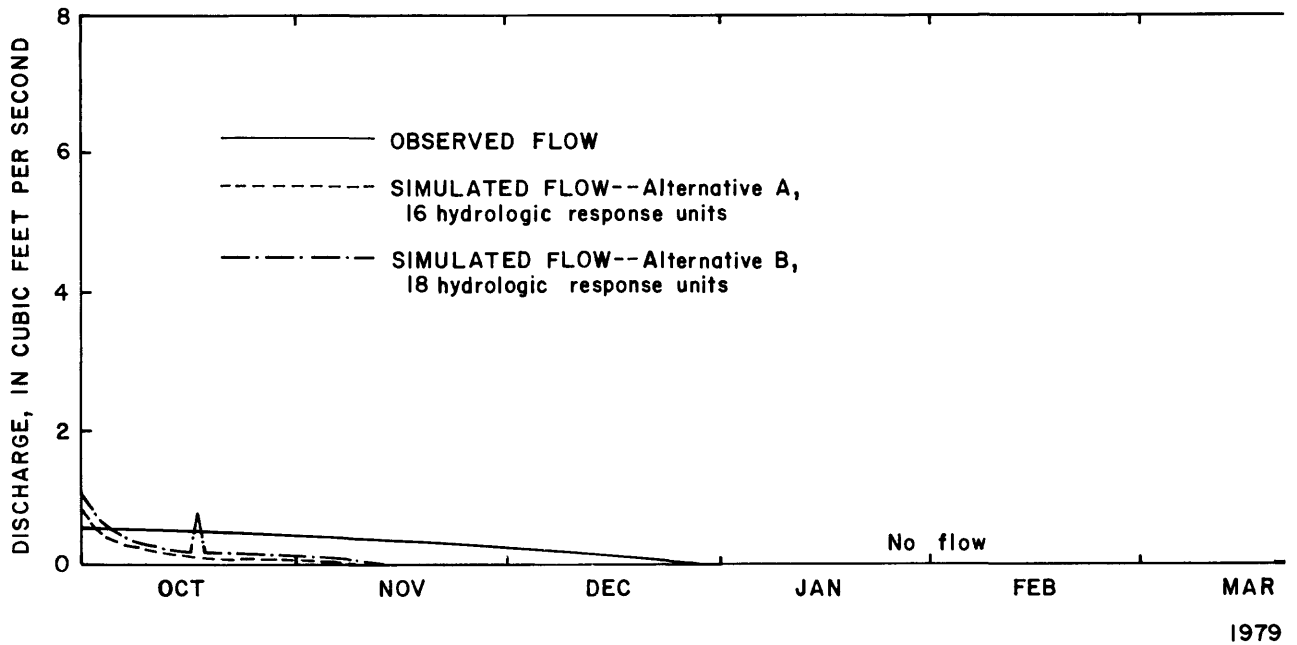
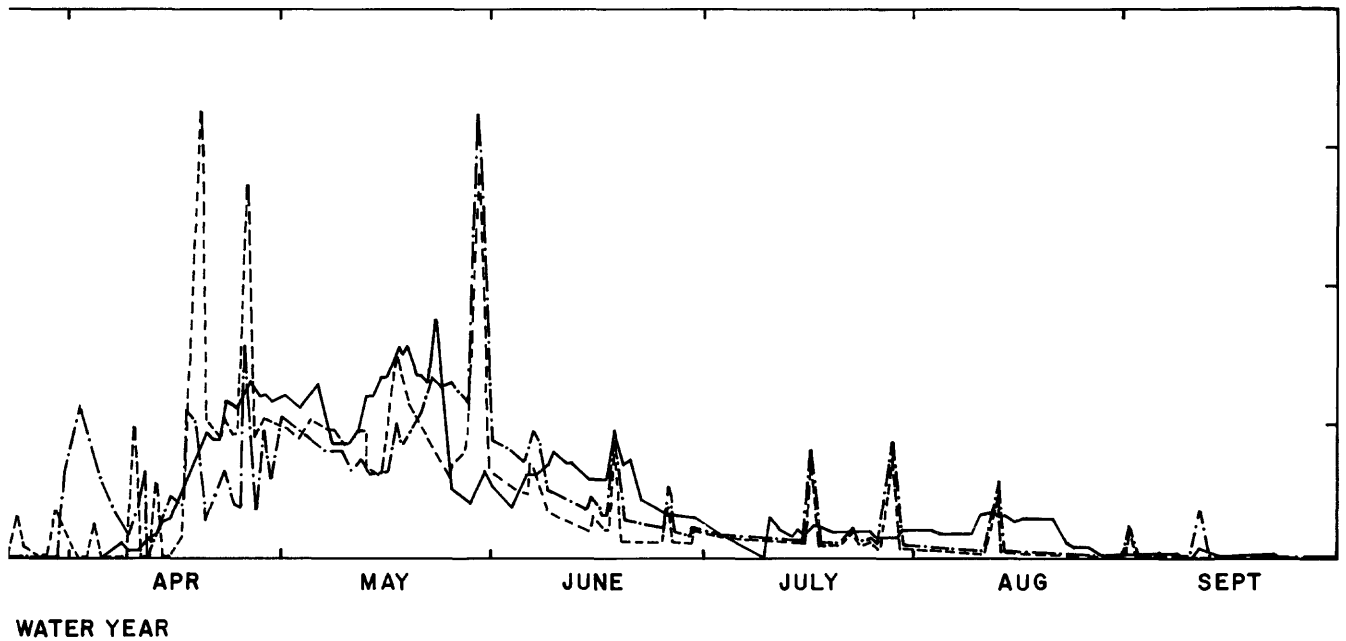


Figure 7.--Observed and simulated mean daily streamflow,

May 17 ( $0.94 \text{ ft}^3/\text{s}$ ). In July, this base flow was augmented by base flow from rainstorms that occurred in May and June. Base flow continued under this alternative until the end of the year.

Neither alternative simulated rainstorms well. During both years many more runoff events were simulated than actually occurred. Although changing the daily soil moisture accounting method and reducing the contributing area so that less surface runoff could occur would improve the simulation somewhat, the problem would not be eliminated. Daily simulation does not take into account rainfall intensity and duration, only total precipitation for the day; therefore, it cannot simulate the resulting variable response. Mean daily flows on rainy days are directly proportional to total daily rainfall in the daily simulation mode. Because intensity and duration of precipitation are not considered, high simulated flows can occur with lower observed flows or low simulated flows when actual flows are high. A good example of this situation occurred in June 1980. On June 6, 1.19 inches of rain fell, resulting in simulated mean daily flows of  $11.9 \text{ ft}^3/\text{s}$  (alternative A) and  $12.2 \text{ ft}^3/\text{s}$  (alternative B) and an observed flow of  $0.78 \text{ ft}^3/\text{s}$ . Eight days later 0.37 inch of rain fell, resulting in a mean daily flow of  $12.8 \text{ ft}^3/\text{s}$  on the same day, and simulated flows of  $2.81 \text{ ft}^3/\text{s}$  (alternative A) and  $3.14 \text{ ft}^3/\text{s}$  (alternative B). Much better simulation results can be obtained through the use of the storm mode for each rainstorm. This mode takes into account storm duration and intensity, as well as basin antecedent conditions.

Tests of the slopes of the regressions of monthly predicted flows on monthly observed flows failed to reject the hypothesis that the slopes were equal to 1 ( $\alpha=0.05$ ). It was concluded that the model provided good estimates of monthly flows.



Prairie Dog Creek, 1979 water year.

#### Snow accumulation and melt

The 1978-79 snow season was one of above average snowpack accumulation. The melt season began in early March and lasted until late March or early April. Few occurrences of significant melt and evaporation occurred during the accumulation period. This pattern is characteristic of mountain snowpacks in this region. The total precipitation during November through March was 5.05 inches.

The simulated snowpacks of each alternative have been plotted in figure 9 for the 1978-79 snow season and figure 10 for the 1979-80 snow season. The average snowpack water equivalents from snow surveys were also plotted. Both simulations provide a reasonable approximation to the basin snowpack, as represented by the average snowpack water equivalent data during the first season. The simulated snowpack under alternative A overestimated snowpack water equivalent during the 1978-79 accumulation season, and that from alternative B underestimated it. Both alternatives indicated more rapid melt and evaporation early in the melt season than did the snow surveys. The last snow survey was made on March 24. Again, both alternatives resulted in less water equivalent than did the snow survey. The beginning of snow accumulation was correctly identified under both alternatives. Peak accumulation seemed to be adequately simulated. Onsite observations indicated that only a few isolated snow drifts remained by March 31. Alternative A simulated the end of melt better than did alternative B, under which the snowpack persisted until April 18.

The snowpack did not exhibit the same pattern of accumulation and melt during the 1979-80 snow season. The snowpack accumulated and ablated several times during the season. The "peak" accumulation occurred as the result of three storms occurring about 1 week apart, beginning the last of February and ending the second

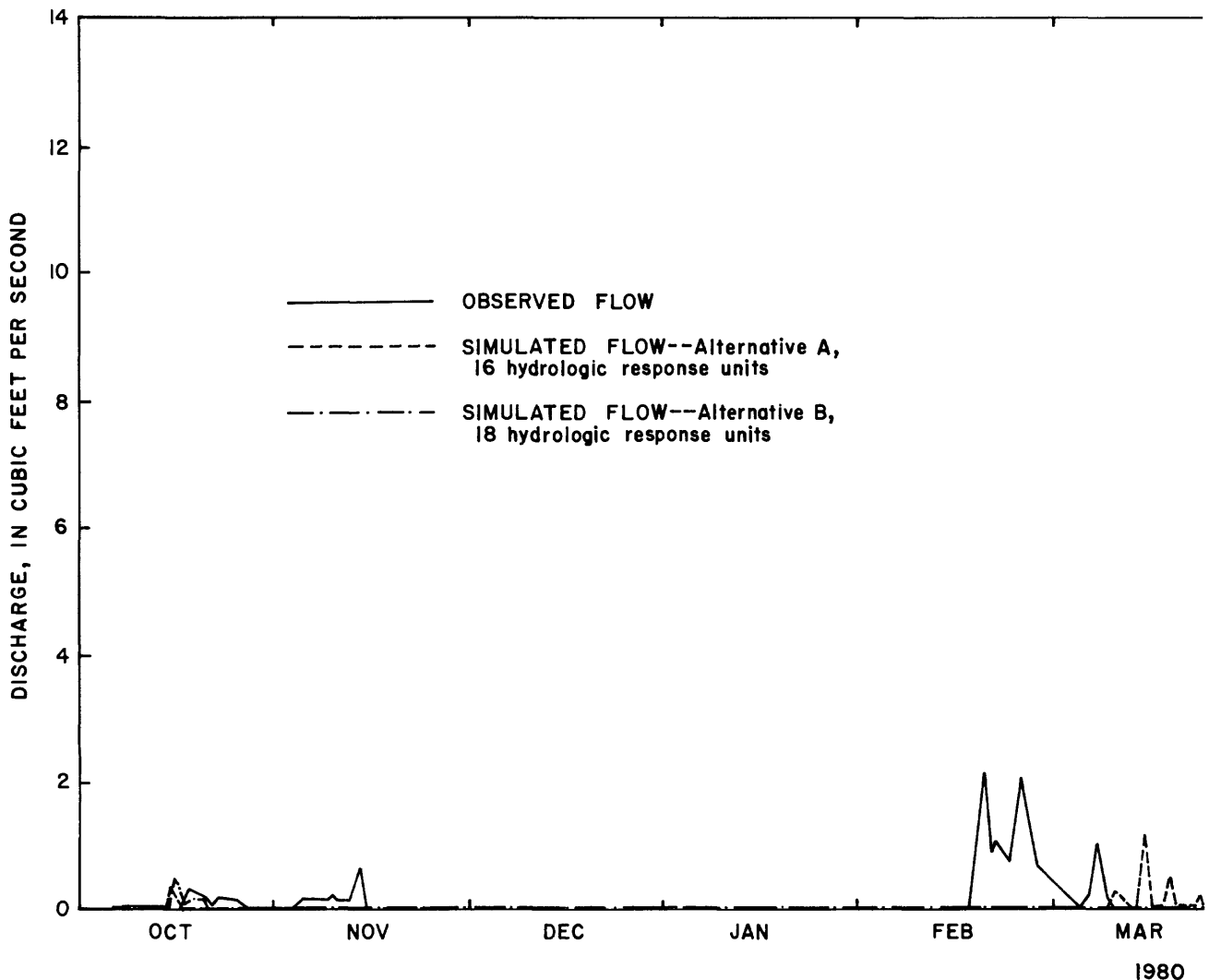
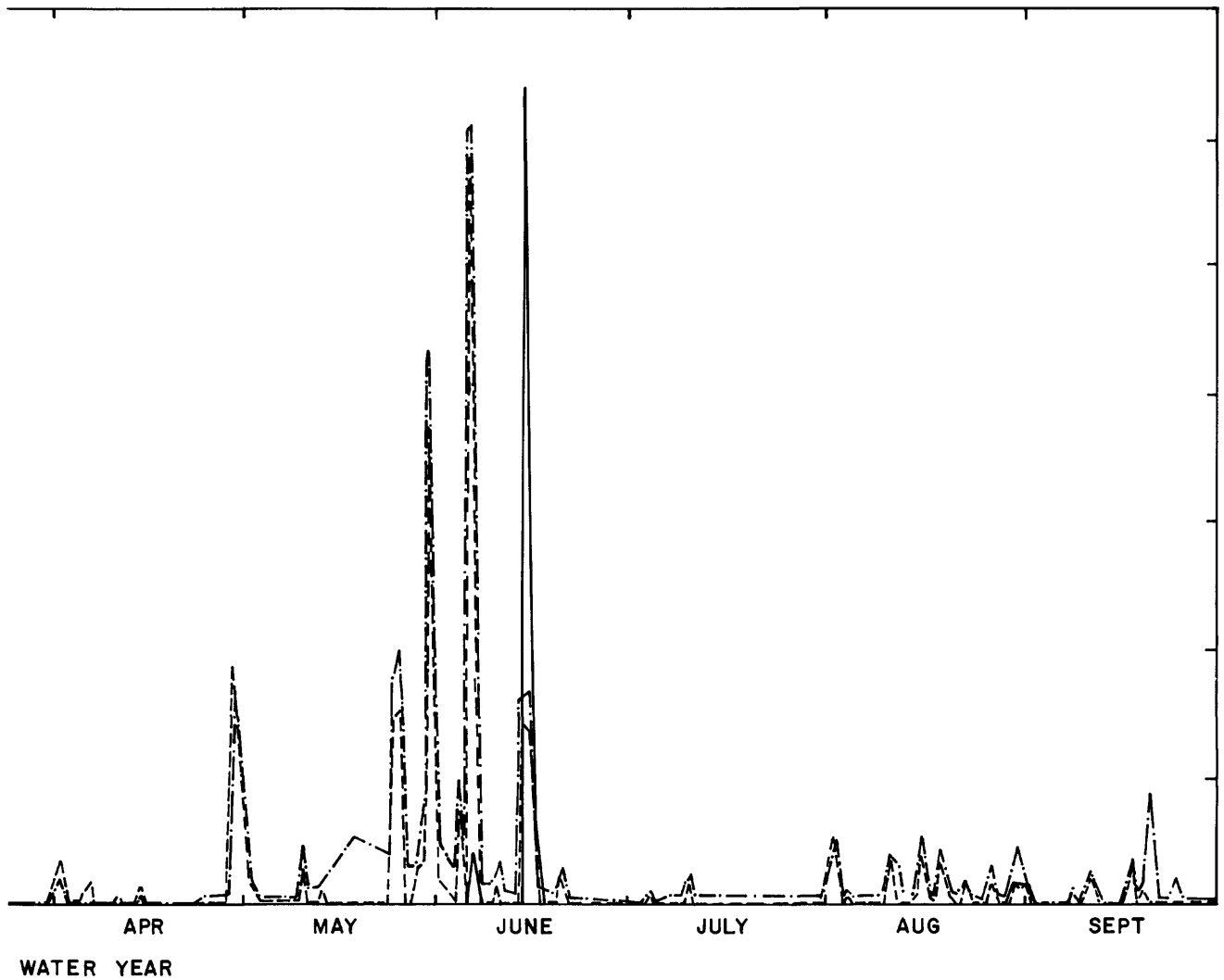


Figure 8.--Observed and simulated mean daily streamflow,

week in March. This type of accumulation is in contrast to the previous year when snow accumulated continuously to the beginning of melt.

The model overestimated snowpack water equivalent under both alternatives during the 1979-80 snow season. Alternative A usually gave closer correspondence to the observed snowpack water equivalent than did alternative B. The snowpack began forming on November 4 under both alternatives. Streamflow records and snow-course data collected during the second week in November indicated that the actual snowpack did not persist, if it formed at all. Neither alternative reflected the cycles of accumulation and melt although alternative A came closer than B. Both alternatives resulted in peak snow accumulation occurring by March 5th. It is not clear which alternative provided the better fit to the actual peak. The basin snowpack had ablated completely by April 4 and probably as early as the third week in March. The simulated snowpack ablated by March 10 under alternative A and April 13 under alternative B. As during the previous year, alternative A appeared to simulate the end of snowmelt better than alternative B.



Prairie Dog Creek, 1980 water year.

The snow components of the model were developed for application to the central Rocky Mountains (Leaf and Brink, 1973a, 1973b; Leavesley, 1973). A study on the prairie in Canada indicated that prairie snowpacks or otherwise intermittent snowpacks may require model modification to obtain better simulation (Granger and others, 1977). For example, the snowpack is assumed to be continuous and of great areal extent. However, a continuous snowpack is exceptional in the Prairie Dog Creek basin. The frequent occurrence of bare ground, rock, and exposed vegetation provides opportunity for local advection. The decrease in albedo with age of the snow surface is based upon results obtained from deep snowpacks (U.S. Army, 1956). Male and Granger (1979) reviewed literature pertaining to the albedo of prairie snowpacks and concluded that there were considerable differences due to the effects of the underlying surface, foreign matter in the snowpack, and spatial discontinuity of the snowpack. Solomon and others (1976) found that the snow model of Leaf and Brink (1973a, 1973b) had to be modified because it kept intermittent Arizona snowpacks too "cold." The 1979-80 season in the Prairie Dog Creek basin yielded similar results in that the simulated snowpacks did not ablate as did the observed.

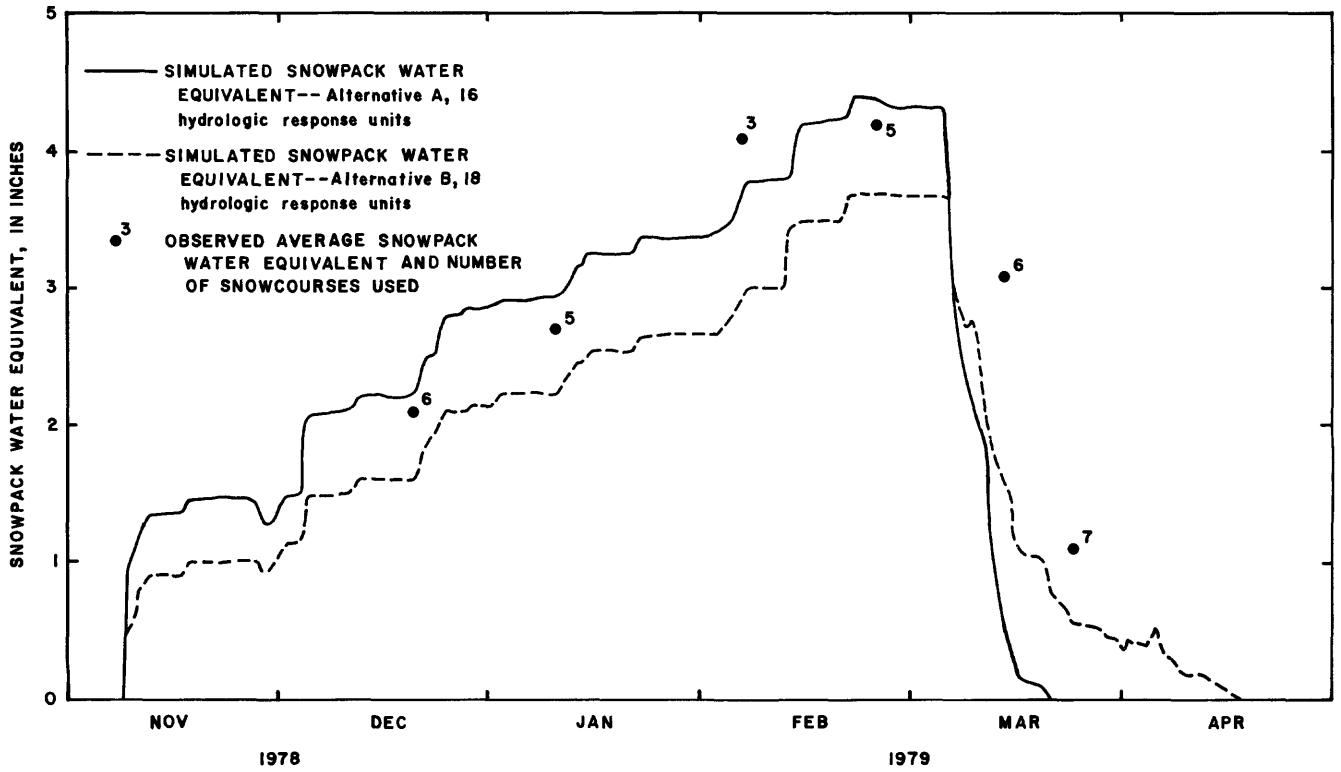


Figure 9.--Observed and simulated snowpack water equivalent, Prairie Dog Creek basin, November 1978 through April 1979.

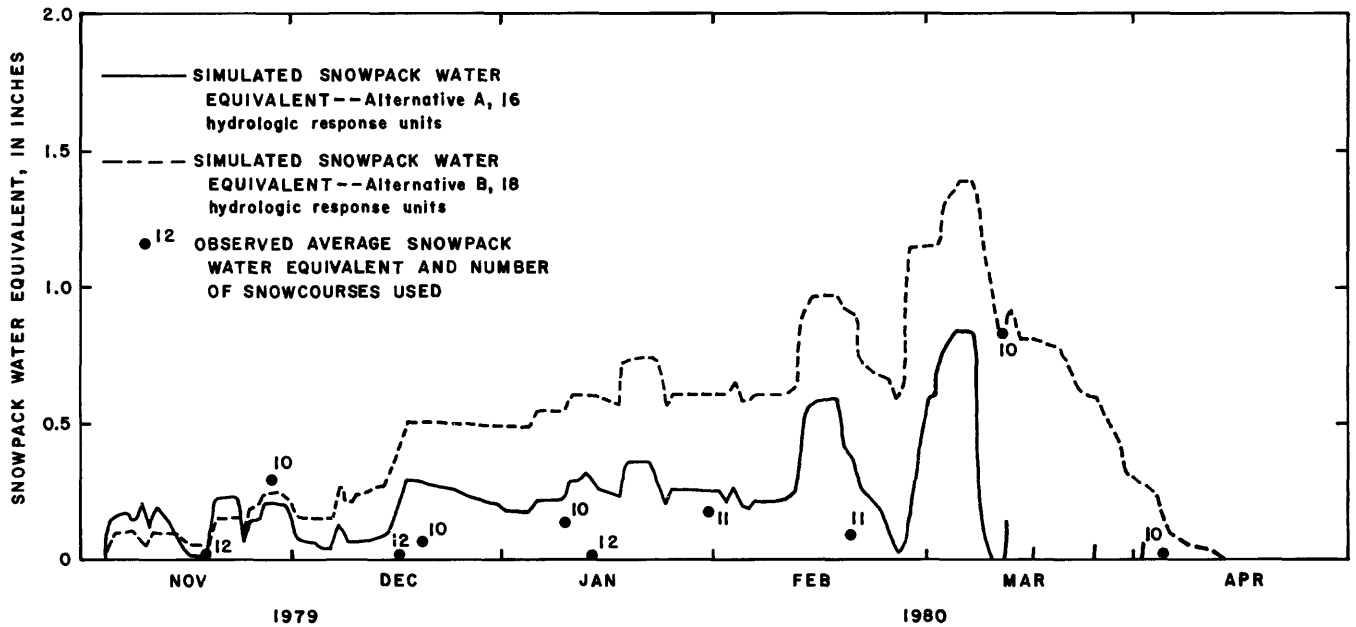


Figure 10.--Observed and simulated snowpack water equivalent, Prairie Dog Creek basin, November 1979 through April 1980.

During the second snow season, snowmelt runoff over frozen ground occurred at least twice. The model does not consider soil freezing and thus cannot simulate resultant runoff. Soil freezing occurs frequently in the northern Great Plains. Conditions favorable to rapid snowmelt such as chinook winds or rain on snow in conjunction with frozen soil can result in rapid runoff and high peak flows. If prairie snowpacks are to be adequately simulated, frozen soils need to be simulated. Algorithms using commonly acquired meteorological variables in frozen soil simulation have been developed, and may provide adequate means of simulation (see for example, Cary and others, 1978).

### Soil moisture

Soil-moisture observations were made periodically through the 2 years of this study. These data provide a means of evaluating the soil moisture. The average soil moisture retained at 20 bars suction was subtracted from the average observed soil moisture at each station to account for unavailable soil moisture. When data from more than one station were available, the data from all stations were averaged. This average "available" soil moisture was then multiplied by the average rooting depth for each alternative to yield the average basin soil moisture in the rooting zone, in inches. The basin-wide average rooting depth was 34 inches under alternative A and 30 inches under B. These data are compared to simulated soil moisture in figures 11 and 12.

Simulated and observed soil moisture were in reasonably close agreement in February 1979 (fig. 11). Both alternatives overestimated soil moisture for March through April and underestimated soil moisture from mid-May through the rest of the year. Alternative A provided closer agreement between observed and simulated soil moisture than alternative B. Both alternatives yielded peak soil moisture in early March, and soil moisture observations indicated that the peak occurred in mid-May. A secondary peak occurred in July, but was not well reflected in the simulations. Simulated and observed soil moisture agreed more closely when an average rooting depth of 30 inches was used than when 34 inches was used.

Simulation under both alternatives underestimated observed soil moisture during the second year (fig. 12). Again, closer correspondence occurred between alternative A and the observed soil moisture with alternative B's rooting depth. The peak soil moisture accumulation was simulated more closely in this year and a secondary peak was correctly simulated in June. The rate of decrease in simulated soil moisture was greater than observed during the periods April-May and June-July, but was nearly parallel in August-September.

The approximate shape of the observed soil moisture graph was maintained in both years. That simulated soil moisture under alternative A agreed more closely with the observed soil moisture in which the average rooting depth from alternative B was used in its calculation indicates that either rooting depths or available water-holding capacities were overestimated, or both. This result does not agree with the results of optimization which consistently indicated that storage capacity (SMAX) needed to be increased. The increase in optimized values of SMAX reflects the compensation for reductions in simulated flows as the result of optimization.

The two simulations produced nearly identical soil moisture graphs, differing by a nearly constant amount. Much of this difference can be accounted for by the difference in rooting depths. The effects of changing hydrologic response unit

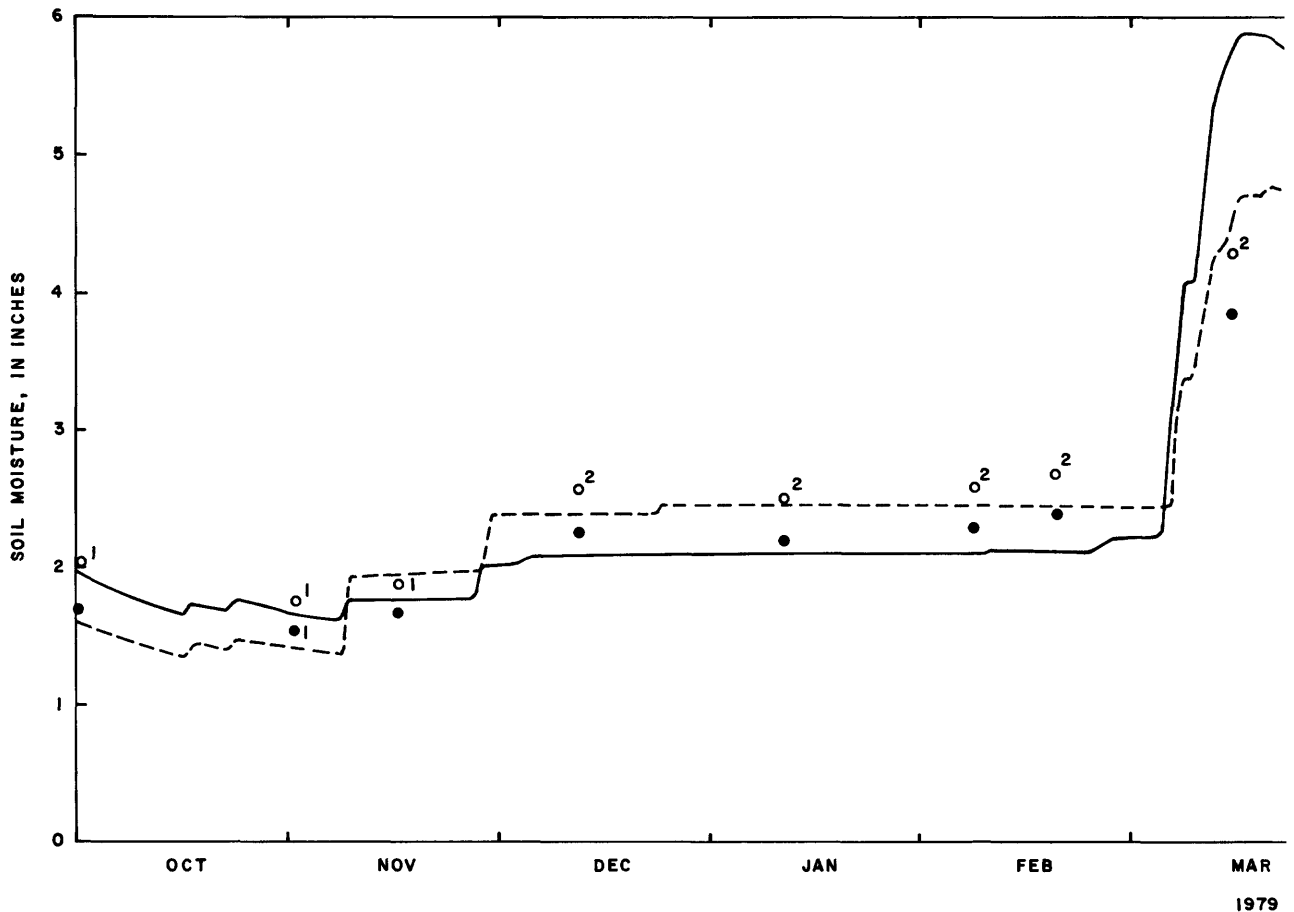


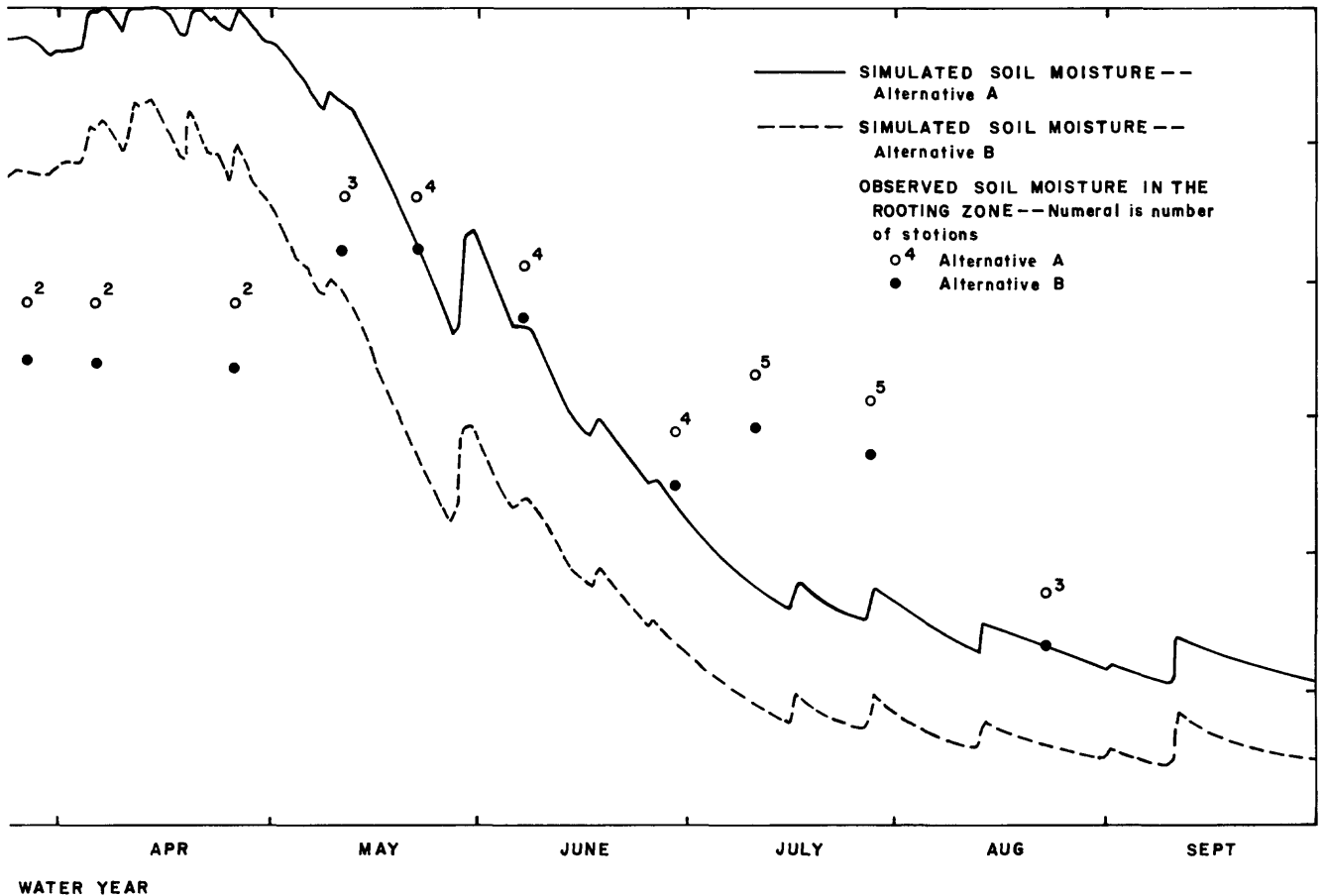
Figure 11.--Observed and simulated soil moisture, Prairie

definitions were apparently negligible, or were masked by the averaging of soils and vegetation characteristics.

In the current soil-moisture accounting method, percolation through the soil does not occur. Soil moisture in excess of SMAX is added to a subsurface reservoir as it occurs. When soil moisture is equal to or less than SMAX, soil moisture is extracted by evaporation and transpiration from the upper 12 inches, and by transpiration from the rest of the rooting zone.

#### Evapotranspiration

Simulated evapotranspiration approximately followed the annual cycle of solar radiation. Evapotranspiration decreased in October of the first year, and ended early in November. From December through February daily mean temperatures commonly were less than CTX (table 1). Thus, the potential and actual evapotranspiration were 0 and there was no snowpack evaporation. Evapotranspiration began in March and increased through June. Thereafter, it decreased through the end of September (fig. 13).



Dog Creek basin, 1979 water year.

During the second year, a somewhat different pattern emerged (fig. 14). The annual cycle of solar radiation was again apparent. However, the period October through February was warmer (table 1), resulting in periods of evapotranspiration, which consisted of snowpack evaporation after October (fig. 10). Evapotranspiration began to increase in March, declined early in May, increased to an annual peak in June, and decreased until mid-September when it began to increase through the end of the month.

Evapotranspiration generally decreased sharply on rainy days, because of lessened solar radiation. There generally was a significant increase immediately following rainy days resulting from increased soil moisture available for evaporation. The higher peaks in evapotranspiration the second year were associated with frequent storms, with greater magnitudes occurring in late May and June (fig. 14).

The difference in patterns in evapotranspiration between years was similar to the differing pattern in soil moisture (figs. 11 and 12). After peaking in March, soil moisture decreased in April and May, then increased as a result of the May-June storm. Evapotranspiration similarly decreased from mid-April to mid-May as a result of less soil moisture, in spite of greater solar radiation during this period in 1980 than in 1979. The increase in evapotranspiration in September 1980 was asso-

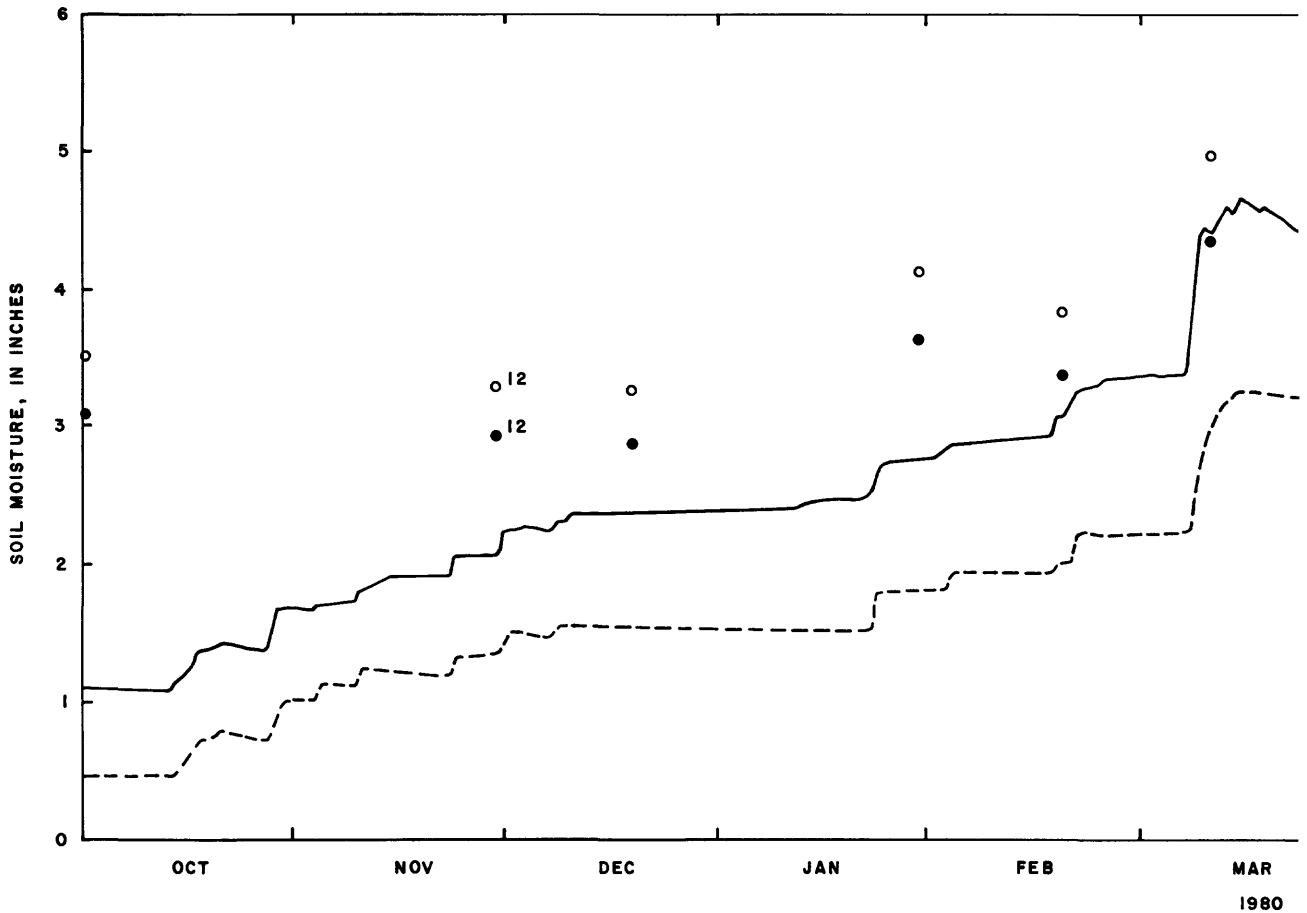
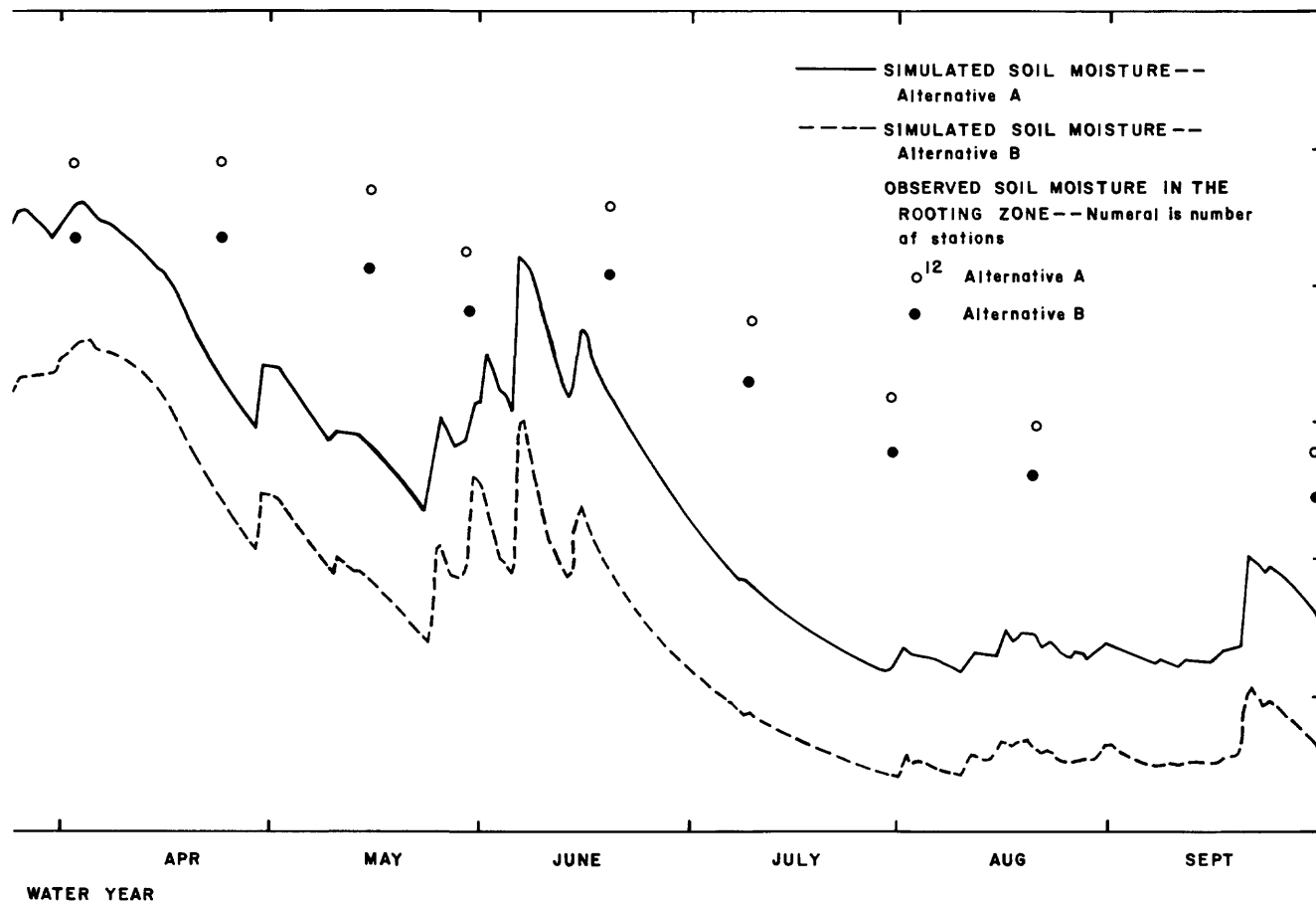


Figure 12.--Observed and simulated soil moisture, Prairie

ciated with several days of rain in mid-month. Solar radiation was somewhat less in 1980 than in 1979 as a result of the greater frequency of rainy (cloudy) days.

Much of the difference between evapotranspiration computed under alternative A and that computed under alternative B is explained by the smaller optimum value of CTS under A than under B. Until after the peak in evapotranspiration during both years, somewhat larger values were computed under B than under A. Following the peak, computed evapotranspiration under alternative B was somewhat less than that under A, and followed the patterns of soil moisture under these two alternatives.

Most of the decrease in soil moisture can be attributed to evapotranspiration. Inspection of a monthly summary of net precipitation, evapotranspiration, and changes in soil moisture reflect this. Monthly total evapotranspiration generally accounted for most monthly precipitation and soil moisture decreases. The soil moisture accounting method affects runoff from the surface as well as the subsurface and ground-water reservoirs. Overestimation of evapotranspiration results in reduced soil-moisture storage in the rooting zone. Similarly, underestimation results in more simulated soil moisture than actually exists. During peak soil moisture accumulation in 1979, soil-moisture observations indicated a smaller peak and a decrease in late March (fig. 11). During this time, evapotranspiration was relatively small and several short-term decreases occurred. The soil zone is consid-



Dog Creek basin, 1980 water year.

ered to be a reservoir in which soil moisture can be removed only by evapotranspiration when SMAV is less than SMAX. There is no opportunity for soil moisture to be redistributed during times of small evapotranspiration under this condition.

Total annual evapotranspiration was nearly the same for each alternative for both years. The annual total simulated was 10.22 in 1979 and 11.26 in 1980 for alternative A and 10.32 in 1979 and 11.32 inches in 1980 for alternative B. DeJong and McDonald (1975) reported a 4-year average soil-water use by plants of 11.57 inches in southwestern Saskatchewan. These determinations were made in a native rangeland type of vegetation.

The calculation of actual evapotranspiration is based on three soil-moisture depletion functions representing sand, loam, and clay soils. These functions were derived by Zahner (1967) for fully stocked forest stands in which the rooting zone is fully occupied by roots near the surface, and decreasing density with depth. Because of this assumption, this approach is not suitable for sparsely stocked forests or rangelands such as occur in the western United States and Canada. Over-depletion of soil moisture in the model simulations reflects the assumed root distribution. The basin forest cover is sparse ponderosa pine and Rocky Mountain juniper. Most of the basin is covered with sagebrush and bunch grass. The rooting density in this vegetation is less than that assumed by Zahner.

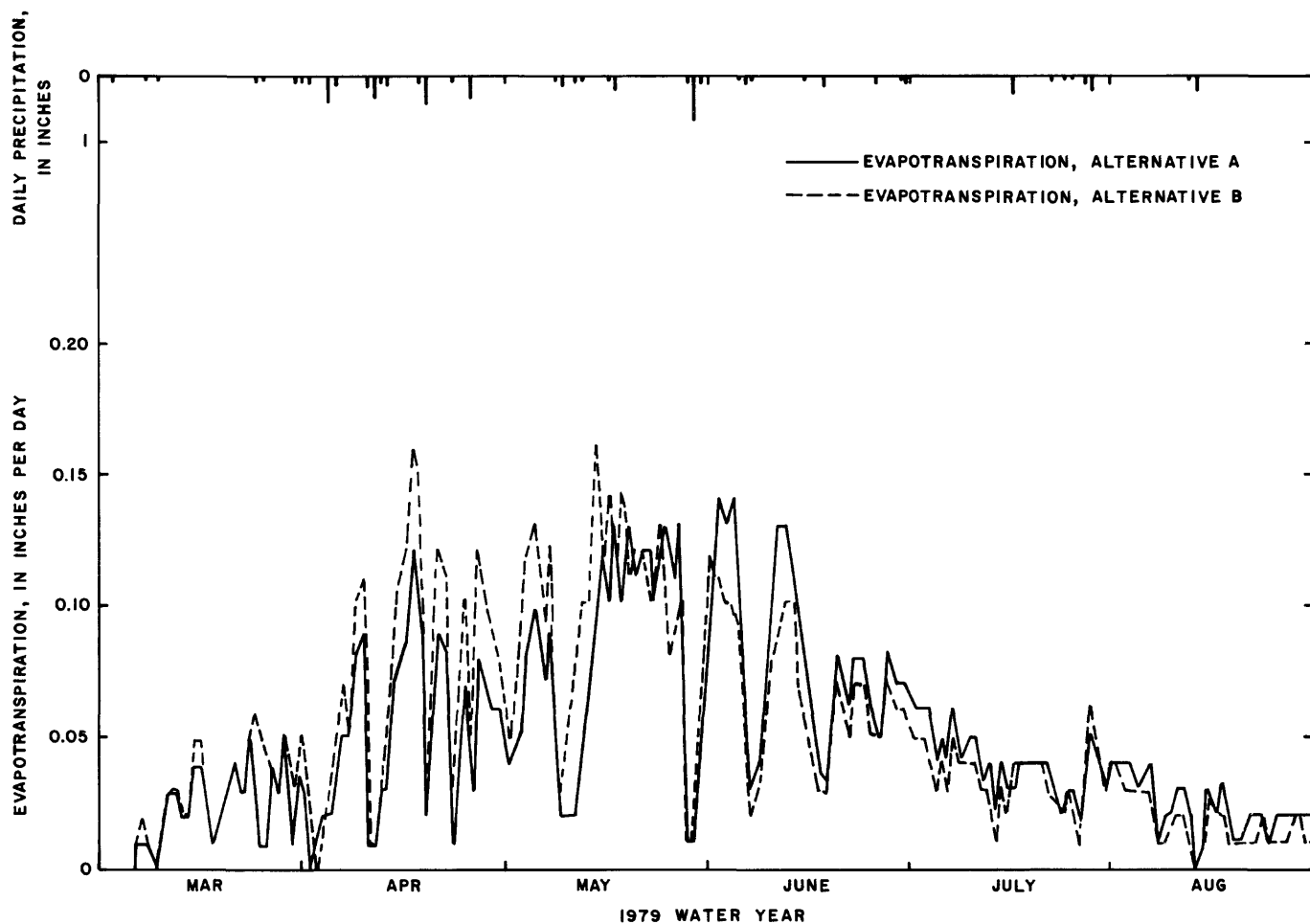


Figure 13.--Simulated evapotranspiration, Prairie Dog Creek basin, 1979 water year.

Depletion functions could be derived which would reflect the decreased root density. Increasing the number of the functions used to better reflect the existing diversity of soil textures could also improve the soil moisture-evapotranspiration simulation.

#### Subsurface and ground-water reservoirs

The basin was divided into four subsurface and ground-water reservoirs in an attempt to better describe the conditions observed. McClymonds (1982) discussed the basin ground-water conditions during 1978 and 1979 and the hydrogeology of the basin. Most of the streamflow from snowmelt originated from coal and sandstone aquifers in the upstream part of the basin. The stream lost water to the alluvium in the lower two-thirds of the valley. There was little, if any, contribution to streamflow from snowmelt in the downstream half of the basin. The change from a gaining to a losing stream was accompanied by a change in the riparian vegetation from nearly continuous cottonwood, green ash, and chokecherry to discontinuous, becoming isolated, stands of cottonwood. This change was used as guidance in delineating the upstream and downstream basin subsurface and ground-water reservoirs.

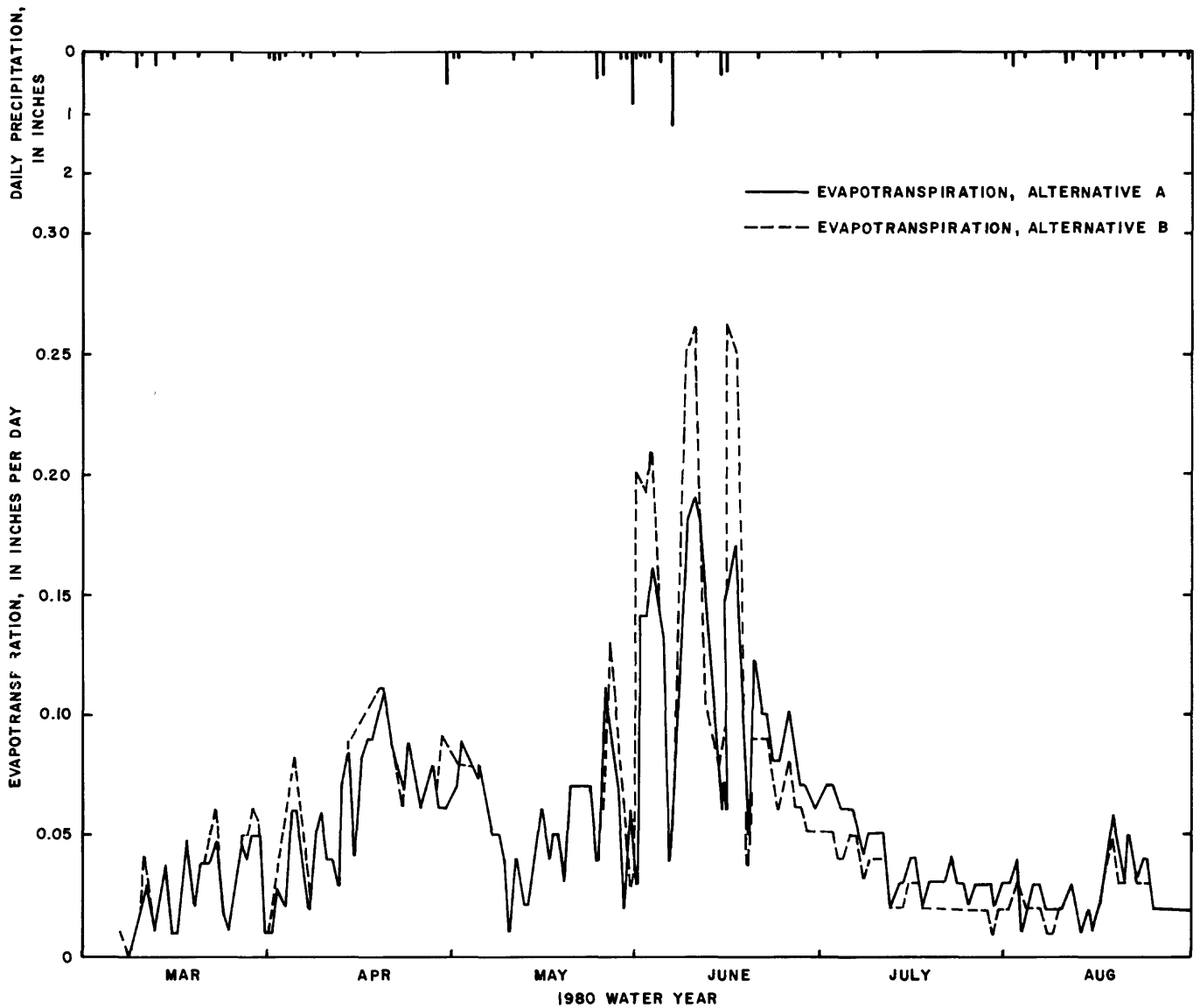


Figure 14.--Simulated evapotranspiration, Prairie Dog Creek basin, 1980 water year.

The model simulations resulted in base flow originating from hydrologic response units 1 and 3 under alternative A and units 1 and 2 under alternative B. Under alternative A, these units include the original units 1, 3, 8, 13—all in the upstream half of the basin (fig. 4). Under alternative B, these included the original units 1, 2, and 8, which are upstream basin units, except 8, which is a mid-basin downstream slope unit (fig. 5). Several units in the upstream basin that were known to contribute to streamflow were not identified as such in the simulation. More were identified under alternative A than under B. The selection of areas of the basin from which subsurface flow and base flow originate is controlled by the selection of parameter values for these reservoirs. However, which units contribute to these reservoirs depends upon their soils, vegetation, and topographic characteristics. Those that were not identified as contributing may have had more shallow soils than were estimated. Overestimation could result in less opportunity for deep seepage to the subsurface and ground-water reservoirs.

The deep seepage that does not become subsurface reservoir flow or base flow is added to a ground-water reservoir. Seepage is controlled by the seepage coefficient GSNK. McClymonds (1982) estimated that an average of 110 acre-feet of water flows from the basin through the alluvium each year. The amount of water added to the ground-water reservoir was computed for each year and for each hydrologic moisture unit alternative. Under alternative A, 1,648 acre-feet of water was added the first year and 10 acre-feet the second. Under alternative B, 2,923 and 498 acre-feet were added in these years. Soil-moisture observations made at the beginning of the second year resulted in an average soil moisture of about 3.5 inches under alternative A and simulated moisture of 1.1 inches (fig. 11), whereas alternative B yielded observed average soil moisture of 3.1 inches and 0.5 inch of simulated soil moisture (fig. 12). The difference amounts to 2,488 acre-feet of water under alternative A and 2,695 acre-feet under B. At the end of the second year, these differences were 1,192 acre-feet under alternative A and 778 acre-feet under B. If soil-moisture storage were increased in the model simulation, most, if not all, the water added to the ground-water sink could be retained as soil moisture. Increased storage would result in a better correlation between observed and simulated soil moisture as well as a better correlation with the observation made by McClymonds (1982).

#### Annual water balance

An overall check on model performance is provided by the calculation of an annual water balance; that is, inflow minus outflow equals change in basin storage. Inflow included net precipitation and initial contents of the subsurface and ground-water reservoirs. Outflows included evapotranspiration, surface runoff, subsurface reservoir flow, base flow, and seepage to the ground-water reservoir. The change in storage in the basin is the change in soil moisture and in the subsurface and ground-water reservoirs between the beginning and end of the year. The annual water balance under each alternative was calculated for each year (table 19). The difference in inflow and outflow agreed with the change in soil moisture within the limits of roundoff error in all instances except the first year under alternative B. Here the error (inflow minus outflow plus or minus changes in storage divided by precipitation) was 9.0 percent--greater than would be expected for roundoff error. Seepage to the base-flow reservoir is stored in an array until an appropriate time has passed (the lag time). It is then released as base flow. Water in storage may be held over from one year to the next, becoming base flow the following year. Values in the temporary array were not printed. Therefore, the change in storage may differ from the difference between inflow and outflow by this amount.

#### Storm simulation

##### Interfacing with daily simulation

The revision that was made to the hydrologic response unit alternative A, referred to hereafter as alternative C, was tested. Because some of the response-unit characteristics changed as a result of the revision, a second analysis included initial parameter screening using sensitivity analysis.

Of the 19 parameters evaluated using sensitivity analysis, the sensitivity of 10 increased, 3 decreased, and 6 remained unchanged. Overall, there was a slight increase in sensitivity of simulated runoff to changes in parameter values, com-

Table 19.--Annual water balance of the model simulations in inches  
[<, less than]

	Hydrologic response unit, alternative A, 16 units		Hydrologic response unit, alternative B, 18 units	
	1979	1980	1979	1980
<b>Inflow</b>				
Precipitation	10.77	12.55	10.58	12.29
Subsurface reservoir	.83	.01	1.01	.22
Ground-water reservoir	.16	.00	.10	.02
Total	<u>11.76</u>	<u>12.56</u>	<u>11.69</u>	<u>12.53</u>
<b>Outflow</b>				
Evapotranspiration	10.22	11.26	10.32	11.33
Interception	.57	.76	.31	.44
Surface runoff	.06	.10	.05	.10
Subsurface flow	.00	.00	.00	.00
Base flow	.20	.00	.24	.06
Ground-water sink	<u>1.59</u>	<u>.01</u>	<u>2.82</u>	<u>.48</u>
Total	<u>12.64</u>	<u>12.13</u>	<u>13.74</u>	<u>12.41</u>
Inflow minus outflow	- .88	.43	-2.05	.12
<b>Change in storage</b>				
Change in soil moisture	- .86	.43	-1.09	.19
Change in subsurface reservoir	<.005	<.005	-.01	<.005
Change in ground-water reservoir	-.01	<.005	<.005	<.005
Error, in percent	.1	0	9.0	.6

pared to alternative A. Most of the changes in parameter sensitivity were not large enough (or small enough) to warrant additions or deletions to the original parameter subset. Three exceptions did occur, however. The lapse rate for maximum daily air temperatures (TLX) increased sufficiently to warrant further analysis. The transmission coefficient (TRNCF) doubled its effect on simulated streamflow. The seepage rate from the soil to the subsurface reservoirs increased by an order of magnitude, from 0.001 to 0.017.

TLX and TLN, the lapse rates for maximum and minimum daily air temperatures, were added. A trial model run was made using alternative C. Optimization resulted in a nearly identical increase in lapse rates TLX and TLN, from 1.5°C per 1,000 feet to 3.99 and 3.98°C, respectively. These values are greater than the dry adiabatic lapse rate (3°C or 5.4°F per 1,000 feet). These lapse rates therefore, were, truncated to 3°C per 1,000 feet.

Although highly correlated ( $r > 0.9$ ), CTX and CTS were both retained in the parameter subset. They are estimated from temperature and vapor-pressure data. It was felt that both needed to be subject to optimization analysis to increase the chance that the optimized values could be related to regional climatic data. Use

of only one would have resulted in the change between original estimates and optimized values occurring in one parameter, increasing the difficulty in relating the parameter values to the same climatic data.

A summary of parameter values following optimization is given in table 20. The changes in subsurface and ground-water parameters (SEP, REXP, and RCB) between the two alternatives are probably due to a reduction from four subsurface and ground-water reservoirs to two. When the number was reduced, parameter estimates were made by averaging the earlier estimates.

Table 20.--Average values of parameters before and after optimization for hydrologic response unit alternatives A and C

Parameter	Alternative A			Alternative C		
	Initial	Optimized	Change (percent)	Initial	Optimized	Change (percent)
TRNCF	0.87	0.99	+14	0.75	0.69	-8
CTX	15.62	16.37	+5	15.48	17.41	+12
SMAX	4.39	6.24	+42	4.73	5.76	+22
SEP	1.00	.78	-22	.65	.72	+11
REXP	1.39	1.47	+6	1.40	3.00	+114
RCB	.13	.20	+54	.23	.14	-39
CTS	.0133	.0096	-28	.0135	.0098	-27
BST	32.10	32.25	+5	37.94	34.97	-8
Objective function	131	11	-92	100	14	-86

#### Rainfall excess and storm runoff

Seventeen rainstorms were selected from the 3 years of data. Although a greater number of rainstorms occurred, these 17 produced noticeable changes (greater than 0.1 ft<sup>3</sup>/s) in the hydrograph. The 17 storms represented a mixture of storm types, including frontal and convective.

In the storm mode of model operation, infiltration and rainfall in excess of the infiltration capacity are calculated using the Green and Ampt infiltration equation. These calculations are made for each hydrologic response unit. The excess from each response unit is summed to obtain the storm-runoff volume.

Individual parameter values are specified for each response unit. Average soil texture classes were derived for each hydrologic response unit. Six average texture classes were determined for the Prairie Dog Creek basin. As a rather thin layer of soil is generally important in infiltration, the average texture class of the A horizon was determined. In instances of an undeveloped or very thin A hori-

zon, the upper B horizon was included. Although soil texture varied considerably within each hydrologic response unit, the number of "average" soil texture classes of this upper soil layer was reduced from six to three: silty clay loam, silt loam, and loam. The infiltration parameters were estimated for each of these three classes.

Initially, the sum of squares of the logarithms of storm-runoff volumes was selected for use. Of the four parameters available for optimization of runoff volumes, three (KSAT, PSP, and RGF) are used directly in the calculation of infiltration rate. The fourth, DRN, is used in the calculation of percolation of water from the wetting front to greater depths. The degree of parameter correlations was not known beforehand; therefore, all four were used in the first optimization and sensitivity analyses.

Storm volumes in the precipitation-runoff modeling system are expressed as inches of runoff. After extraction of infiltration, the resultant storm runoff may be a small fraction of an inch. If a sum of squares of logarithms objective function is used, an inordinately large amount of weight will be given to smaller storms.

The values on the diagonal of the hat matrix provides information as to the degree of effect of each simulated storm volume upon the objective function, and, then, the optimized parameter values. The simulated and observed storm runoff volumes, together with the values from the diagonal of the hat matrix, have been placed in table 21. The high degree of effect of the smaller storms relative to

Table 21.--*Simulated and observed storm-runoff volumes and values of the hat matrix following optimization of the sums of squares of the logarithms of flows*

Storm number	Precipitation (inches)	Simulated runoff (inches)	Observed runoff (inches)	Diagonal elements of hat matrix
1	0.52	0.0002	0.0004	0.185
2	.30	.0002	.0014	.379
3	.89	.0003	.0028	.456
4	.57	.0349	.0048	.296
5	.26	.0000	.0001	.192
6	.26	.0005	.0001	.145
7	1.02	.0083	.0012	.195
8	.39	.0116	.0256	.160
9	.55	.0003	.0001	.123
10	.22	.0000	.0003	.162
11	.36	.0007	.0004	.162
12	.22	.0002	.0001	.205
13	.70	.0094	.0067	.785
14	.41	.0044	.0020	.106
15	.27	.0006	.0007	.181
16	1.28	.0020	.0019	.097
17	.27	.0001	.0001	.117

the large storms can be seen. The objective function was changed to the sum of squares, and the parameters reanalyzed. A comparison between the two objective functions was made (fig. 15). The objective function values were normalized and their values at the end of each cycle plotted. The rate of reduction was consistently greater for the sum of squares, which may indicate that the initial values were closer to the optimum set for the sum of squares. In both instances, most of the reduction occurred by the fourth cycle, indicating that, regardless of the form of the objective function, four to five optimization cycles are probably adequate.

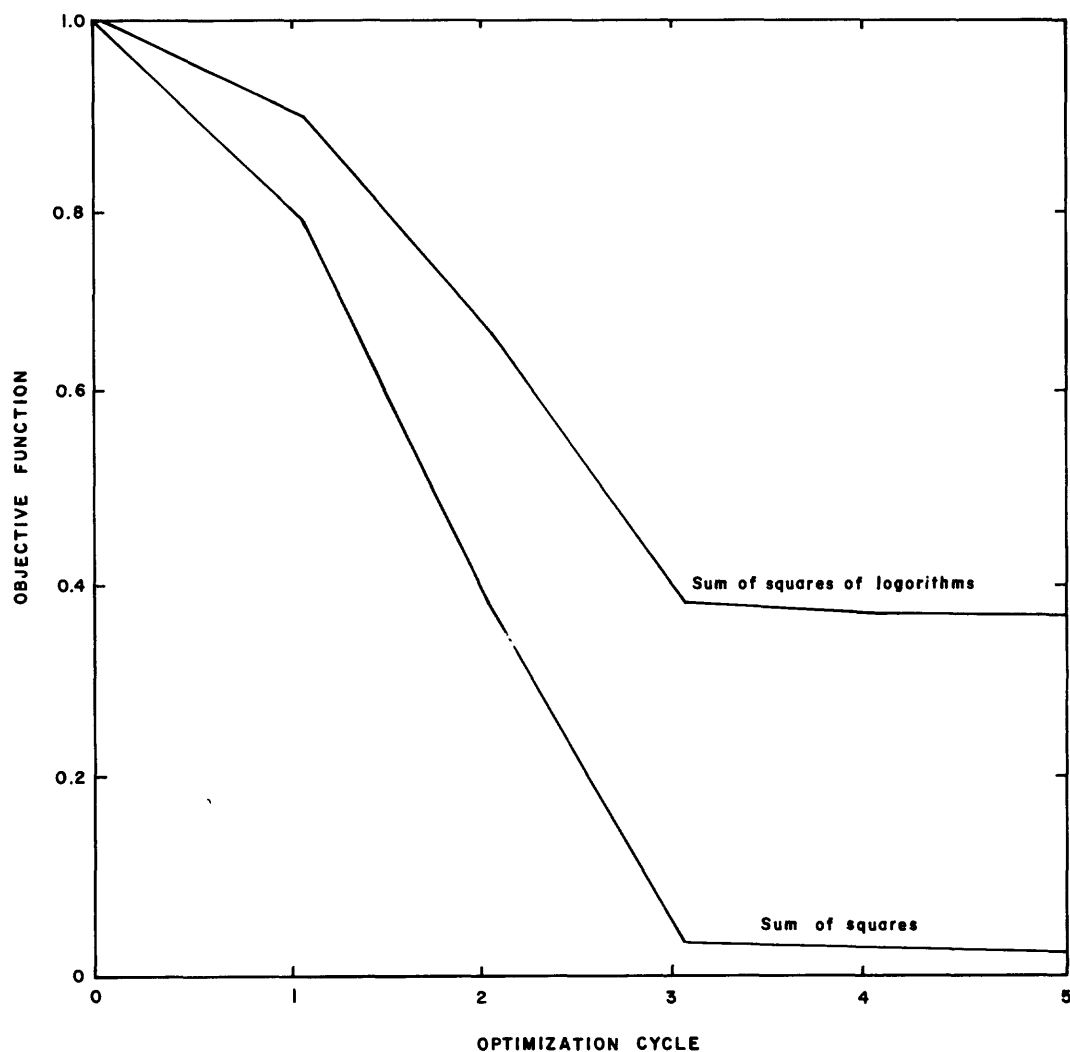


Figure 15.--Reduction in objective function during optimization of four storm simulation parameters and 17 storms.

The initial and optimized values of the parameters for each "average" texture class, together with the objective function values, have been placed in table 22. The option selected for use changes the logarithms of the parameter values by the same percentage. Therefore, the percentage change for each hydrologic response unit, or in this instance, each texture class, will be the same. Large increases in value occurred for all four parameters, particularly hydraulic conductivity at

Table 22.--Initial and final parameter values following optimization using 17 storms and the sum of squares objective function

Parameter	Soil texture class <sup>1</sup> of surface horizon	Initial	Optimized	Change (percent)
KSAT	SiL	0.69	5.10	+739
	L	.26	1.92	+739
	SiCL	.79	5.84	+739
PSP	SiL	1.59	2.17	+136
	L	1.33	1.82	+136
	SiCL	1.14	1.56	+136
DRN	SiL	1.0	1.92	+192
	L	1.0	1.92	+192
	SiCL	1.0	1.92	+192
RGF	SiL	4.43	8.49	+192
	L	5.12	9.81	+192
	SiCL	3.26	6.24	+192
Objective function	---	.026378	.000545	-98

<sup>1</sup>SiCL - silty clay loam, L - loam, SiL - silt loam.

the wetting front (KSAT). These changes were accompanied by a 98-percent reduction in the objective function.

The drainage coefficient (DRN) was initially set equal to 1.0, meaning that percolation to greater depths following infiltration would occur at a rate equal to wetting front hydraulic conductivity. The drainage coefficient was nearly doubled in optimization. However, the model was not sensitive to this parameter. Furthermore, DRN was not correlated with any of the other parameters.

Inspection of the sensitivity and hat matrices revealed that parameter sensitivity was proportional to storm-runoff volume. Among the three remaining parameters, the order of sensitivity was PSP, KSAT, and RGF. KSAT and PSP were highly correlated (-0.988). However, the correlation between these two and RGF was only intermediate (0.493 and -0.542, respectively). Although high correlations can create false minima in the response surface of the objective function, the amount of reduction in the objective function indicated that this condition may not have occurred.

Because of the insensitivity of DRN, the initial value was reduced to 0.5, which is about the median of its suggested range (Dawdy and others, 1978). The parameters were reanalyzed using the original initial conditions for the remaining

parameters. The results of the reanalyses were identical to the first, except the optimized value of DRN was 0.94. This change had no effect and the model remained insensitive to DRN.

The parameters PSP and RGF are used in an expression to calculate PS, where PS is a function of matric (or capillary) suction at the wetting front and current soil moisture in the upper soil zone. PS is subsequently used, with KSAT, in the calculation of the current infiltration capacity. Thus KSAT, PSP, and RGF are functionally related and highly correlated. In order to study the effects of optimizing KSAT and PSP individually with RGF, optimization and sensitivity-analysis runs were made first with KSAT and RGF, next with PSP and RGF. In both instances, the parameter not being used was kept at its original values. DRN was left equal to 0.5. The results of optimization are summarized in tables 23 and 24.

In both analyses, the optimized parameter values were greater than initial values. KSAT increased 739 percent, the largest increase in either analysis. In the second analysis RGF increased the most. The final value of the objective function was slightly smaller in the optimization of parameter pair PSP-RGF. However, the difference was small enough that either parameter pair could be used. The relative value of the objective function at the end of each optimization cycle is greater for each of the two parameter analyses than the four-parameter analysis for the first three cycles (fig. 16). However, they converge in relative (and actual) value by the end of the fourth cycle. At least in this instance, little is gained by use of the four-parameter optimization compared to either of the two-parameter optimizations.

Sensitivity analyses indicated that simulated runoff volumes were generally more sensitive to changes in parameter pair KSAT-RGF than to changes in parameter pair PSP-RGF. In all instances, the change in simulated runoff was negative, reflecting decreases in simulated runoff with changes (increases) in parameter values. The larger storms experienced the greater changes. The coefficients of variation (standard error divided by the mean) were slightly less for pair PSP-RGF than for KSAT-RGF, indicating that pair PSP-RGF may have been somewhat better determined. These small differences may not be significant. In the former analysis the coefficient of variation of PSP was 37 percent and RGF was 41 percent compared to 41 percent for KSAT and 49 percent for RGF in the latter. These coefficients of variation were consistently less than the corresponding values in the four-parameter analysis: KSAT - 52 percent, PSP - 56 percent, and RGF - 60 percent. The correlation between the parameters was very high in both analyses, -0.967 between PSP and RGF, and -0.982 between KSAT and RGF. In both analyses, simulated storm runoff was less sensitive to RGF than to KSAT or PSP.

KSAT and PSP have somewhat stronger physical interpretation than does RGF. Because of the weaker physical interpretation for RGF and the high correlation with the other two, RGF was subjected to optimization and sensitivity analysis alone, again using all 17 storms. After five cycles, a 90-percent reduction in the objective function was achieved accompanied by a 327 percent increase in RGF, to an average value of 18. Reflecting the effects of optimization on a single parameter, the effect of error in RGF on runoff error increased by an order of magnitude. In this instance, the coefficient of variation was 27 percent--less than in any of the previous analyses. Although a substantial reduction in the objective function was realized, the additional reduction obtained using a two-parameter optimization warrants using two parameters.

Table 23.--Optimization of the parameter pair KSAT-RGF, using 17 storms

Parameter	Soil texture class <sup>1</sup> of surface horizon	Initial	Optimized	Change (percent)
KSAT	SiL	0.69	5.79	+739
	L	.26	2.18	+738
	SiCL	.79	6.63	+739
RGF	SiL	4.43	8.48	+91
	L	5.12	9.81	+92
	SiCL	3.26	6.24	+91
Objective function	---	.026434	.000561	-98

<sup>1</sup>SiCL - silty clay loam, L - loam, SiL - silt loam.

Table 24.--Optimization of the parameter pair PSP-RGF, using 17 storms

Parameter	Soil texture class <sup>1</sup> of surface horizon	Initial	Optimized	Change (percent)
PSP	SiL	1.59	6.08	+282
	L	1.33	5.08	+282
	SiCL	1.14	4.36	+282
RGF	SiL	4.43	18.92	+327
	L	5.12	21.86	+327
	SiCL	3.26	13.92	+327
Objective function	---	.026434	.000541	-98

<sup>1</sup>SiCL - silty clay loam, L - loam, SiL - silt loam.

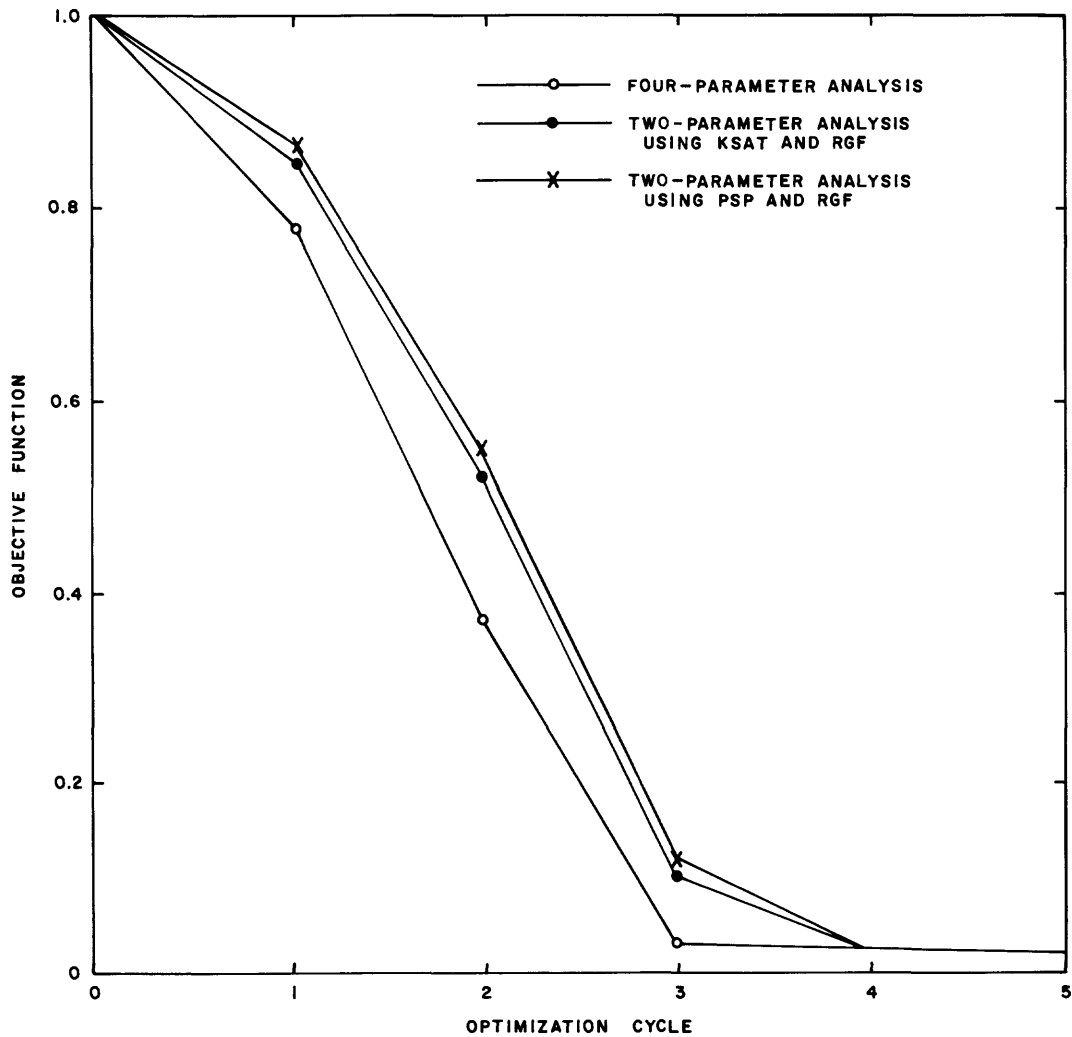


Figure 16.--Reduction in objective function with number of optimization cycles.

A large reduction in the value of the objective function was realized in each of the above analyses. However, the objective function measures the agreement between simulated and observed runoff volumes over all storms. A storm-by-storm comparison will provide better insight into the ability of the model to simulate a range in runoff volumes, generated by different storm magnitudes and types.

Inspection of table 25 reveals a generally poor ability of the model to simulate storm-runoff volumes even following optimization. Only three simulated storms agreed with observed runoff to within 50 percent. Optimization of four and two parameters increased the agreement to four storms each, even though the overall fit as measured by the objective function improved by 98 percent each time. The one-parameter optimization did not increase the number of periods of simulated runoff that agreed with the observed to within 50 percent.

Closer agreement was obtained between simulated and observed runoff for the small and intermediate storms. Prior to optimization, the model simulated more runoff than was observed. All changes in parameter values were in the direction of

Table 25.--Observed and simulated storm runoff for 17 storms  
[<, less than]

Storm No.	Date storm started	Observed runoff (inches x 10 <sup>-4</sup> )	Simulated runoff before optimization (inches x 10 <sup>-4</sup> )	Four-parameter optimization [KSAT, PSP, RGF, DRN] (inches x 10 <sup>-4</sup> )	Two-parameter optimization [KSAT, RGF] (inches x 10 <sup>-4</sup> )	Two-parameter optimization [PSP, RGF] (inches x 10 <sup>-4</sup> )	One-parameter optimization [RGF] (inches x 10 <sup>-4</sup> )
1	4-18-79	4	18	1	1	2	7
2	4-26-79	14	11	1	1	2	7
3	5-28-79	28	23	1	1	2	6
4	6-18-79	48	1,531	110	129	138	491
5	7-16-79	1	3	<1	<1	<1	1
6	7-28-79	1	31	2	2	2	8
7	6-06-80	12	391	35	41	71	240
8	6-14-80	256	562	37	44	48	173
9	10-15-80	1	21	1	1	1	5
10	10-22-80	3	2	<1	<1	<1	1
11	3-27-81	4	37	2	3	4	13
12	3-31-81	1	11	1	1	2	6
13	5-28-81	67	454	32	39	54	188
14	6-12-81	20	226	17	19	20	73
15	7-14-81	7	43	2	3	3	10
16	7-25-81	19	127	7	9	10	36
17	9-06-81	1	4	<1	<1	<1	1

increasing infiltration and thus reducing simulated runoff. Following optimization, the largest storm volume was consistently undersimulated. Of the intermediate storms (greater than 10 x 10<sup>-4</sup> inch), storms 2 and 3 were considerably underestimated. Storm 4 was overestimated, as was storm 12. The remaining intermediate storm volumes were consistently underestimated, although storm 14 resulted in simulated runoff that was very close to the observed (except the single-parameter optimization). In general, optimization resulted in an order of magnitude decrease in simulated runoff.

The diagonals of the hat matrices for each optimization and storm are presented in table 26. Generally, the parameters were affected more by the larger, summer storms. During these storms, much of the runoff occurred as surface runoff, as evidenced by the rapid rise in the hydrograph, occurring at most within a very few hours of the onset of rainfall. Storms 2 and 3, although intermediate in size, were early spring frontal storms as were many of the small volume storms. Consistently the greatest effect was by storm 4, the first convective storm in the sequence. Storm 7 also affected the parameters, except for the one-parameter sensitivity analysis. Storm 8, the largest storm in the sequence, did not exhibit a great amount of leverage under any of the sensitivity analyses. Why this occurred is not clear. Storm 13 was the last storm whose simulated runoff volume strongly affected

Table 26.--Diagonal elements of the hat matrices for four sensitivity analyses of storm runoff

Storm No.	Date storm started	Four-parameter optimization [KSAT, PSP, RGF, DRN]	Two-parameter optimization [KSAT, RGF]	Two-parameter optimization [PSP, RGF]	One-parameter optimization [RGF]
1	4-18-79	0.001	0.000	0.000	0.000
2	4-26-79	.002	.001	.001	.000
3	5-28-79	.001	.000	.000	.000
4	6-18-79	.883	.885	.823	.772
5	7-16-79	.000	.000	.000	.000
6	7-28-79	.003	.000	.000	.000
7	6-06-80	.950	.751	.967	.027
8	6-14-80	.220	.091	.092	.099
9	10-15-80	.001	.000	.000	.000
10	10-22-80	.000	.000	.000	.000
11	3-27-81	.001	.001	.000	.000
12	3-31-81	.000	.000	.000	.000
13	5-26-81	.856	.237	.098	.080
14	6-12-81	.045	.028	.014	.017
15	7-14-81	.008	.001	.000	.000
16	7-25-81	.029	.004	.004	.005
17	9-06-81	.000	.000	.000	.000

the parameters, although this was only true for the four-parameter sensitivity analysis. Storms 4 and 7 had, in general, the most effect, and produced the largest simulated storm runoff volumes.

The difference between observed and simulated runoff was greatest for storms 4, 7, and 13. Optimization resulted in parameter values that reduced simulated runoff, particularly for these three storms. The reduction in simulated runoff from the three storms resulted in the underestimation of runoff from the remaining storms.

A variation of the Green and Ampt infiltration equation proposed by Philip (1954) is used to model infiltration. With certain simplifying assumptions, this equation has been widely used with satisfactory results. Some of these applications were referenced by Brakenseik (1977) and McCuen and others (1981).

A large amount of effort has also been spent providing physically based interpretations of this equation and its parameters (for example, Morel-Seytoux and Khanji, 1974). Additional work has involved providing estimating techniques for these parameters (for example, Clapp and Hornberger, 1978; McCuen and others, 1981). These studies provide estimates based upon physical properties of the soils, especially texture and texture classes. If reliable parameter estimates could be obtained, then a large body of soils information would become available for use in future model applications. Rawls and others (1983) provided five methods of parameter estimation in order of accuracy, including use of U.S. Soil Conservation Ser-

vice soil surveys. Much additional information is available in the coal regions because of recent data collection by various universities, mining companies, and various Federal and State agencies, including the Department of the Interior's interagency studies funded through the U.S. Bureau of Land Management's EMRIA (Energy Minerals Rehabilitation Inventory and Analysis) program.

KSAT, the hydraulic conductivity at the wetting front, was estimated as one-half of hydraulic conductivity at saturation. The observed values of hydraulic conductivity for the texture classes observed in the Prairie Dog Creek basin along with values computed from average parameter values by texture class are presented in table 27. Published values from two sources are also provided. Although the observed values are very variable (the smallest coefficient of variation is more than 100 percent), they compare favorably with the values in the rest of the table. One exception was the value for fine sandy loam class, which was considerably less than the other values. The coefficients of variation probably reflect sampling error coupled with the inherent variability of soil properties, including the range in particle composition within each class and differences in structure. Furthermore, samples from all horizons were grouped to increase sample sizes.

Table 27.--Hydraulic conductivity at the wetting front (KSAT) by soil texture class

Soil texture class <sup>1</sup> (sample size)	Mean of observed (Standard deviation) (inches per hour)	KSAT		
		Cal- culated (inches per hour)	Li and others (1976) (inches per hour)	McCuen and others (1981) (inches per hour)
SiCL(14) <sup>2, 3</sup>	0.79 (1.13)	0.55	0.12	0.21
CL(15) <sup>2</sup>	.35 (0.73)	.45	.18	.71
L(25) <sup>2, 3</sup>	.26 (0.37)	.92	.50	1.18
FSL(13) <sup>2</sup>	.55 (0.61)	2.69	2.46	3.53
SiL(11) <sup>2, 3</sup>	.69 (0.75)	.65	.51	.32
SCL(1) <sup>2</sup>	.52	.26	.45	.93

<sup>1</sup> SiCL - silty clay loam, CL - clay loam, L - loam, FSL - fine sandy loam, SiL - silt loam, SCL - sandy clay loam.

<sup>2</sup> Soil texture classes of the soils in the Prairie Dog Creek basin.

<sup>3</sup> Soil texture classes of the surface horizons in the Prairie Dog Creek basin.

As with the other parameters, optimization resulted in consistent increases in KSAT and subsequently in infiltration rates. For KSAT, optimized values were unrealistically large (tables 22 and 23), often larger than published ranges in values for the given soil texture. In other studies using the rainfall-runoff model, KSAT typically ranged between 0.05 and 1.0 in./hr (Dawdy and others, 1972 and 1978). The values obtained above, from acquired data or estimated for texture classes, are

within this range, as well as other published ranges for texture classes. If optimization is conducted on KSAT, the maximum and minimum bounds need to be established by the range in values typical for that soil. Otherwise, KSAT need not be subject to optimization.

PSP was calculated from wetting front matric suction and soil moisture at saturation and at "field capacity." The values are listed in table 28 along with values of PSP calculated from data presented in the literature for the six texture classes represented in the basin. The values calculated from Prairie Dog Creek data generally agreed with those calculated from data presented by Clapp and Hornberger (1978) and McCuen and others (1981). Most of the values calculated from other source data were within one standard deviation of the Prairie Dog Creek data. The sandy clay loam class was much larger for Prairie Dog Creek; however, the calculated value was from a single sample.

Table 28.--Values of the product of matric suction at the wetting front and moisture deficit at field capacity (calculated as soil moisture at saturation minus soil moisture at one-third bar suction), PSP

Soil texture class <sup>1</sup> (sample size)	Mean values (standard deviation) for Prairie Dog Creek soils (inches)	Calculated from Clapp and Hornberger, 1978 <sup>2</sup> (inches)	Calculated from Clapp and Hornberger 1978 <sup>3</sup> (inches)	Calculated from McCuen and others, 1981 <sup>4</sup> (inches)
SiCL(14) <sup>5,6</sup>	1.14 (1.13)	0.91	1.41	1.74
CL(15) <sup>5</sup>	1.09 (0.70)	1.63	1.86	1.91
L(25) <sup>5,6</sup>	1.33 (0.90)	1.11	2.18	1.60
FSL(13) <sup>5</sup>	.71 (0.77)	.69	1.29	1.38
SiL(11) <sup>5,6</sup>	1.59 (0.85)	3.41	2.92	2.26
SCL(1) <sup>5</sup>	2.13	.55	1.20	1.80

<sup>1</sup> SiCL - silty clay loam, CL - clay loam, L - loam, FSL - fine sandy loam, SiL - silt loam, SCL - sandy clay loam.

<sup>2</sup> Calculated from wetting front suction, soil moisture at saturation from their table 3; soil moisture at one-third bar suction calculated from their equation 1.

<sup>3</sup> Calculated from average matric suction at saturation and average exponent, b, using their equation 6. Soil moisture determined as before.

<sup>4</sup> Calculated from antilog of mean log suction at the wetting front and total porosity, obtained from their figures 2 and 3. Soil moisture at one-third bar calculated using their equation 4.

<sup>5</sup> Soil texture classes of the soils in the Prairie Dog Creek basin.

<sup>6</sup> Soil texture classes of the surface horizons in the Prairie Dog Creek basin.

As with KSAT, optimization resulted in much larger than initial values of PSP. Dawdy and others (1972) reported values of PSP (their SWF) ranging from 1.75 to about 20 inches following optimization. In a later report (Dawdy and others, 1978), the range was 1 to 15 inches. In the first instance almost all initial values were

less than the minimum value. The optimized values were within the range determined in the former study and were close to the suggested initial value of 5.0 inches in the latter. When estimating Green and Ampt parameters from soil moisture data, a logarithmic regression commonly is used. The logarithms of matric suction are regressed on the ratio of soil moisture to soil moisture at saturation (after subtracting residual soil moisture from each in the case of the Brooks and Corey form). When desorption data are used, the intercept is taken to be air entry or bubbling suction. According to Clapp and Hornberger (1978), the intercept was considered to be matric suction at saturation. The slope of the regression line is the pore size distribution index,  $\lambda$ . Because the process of sorption is of concern in calculating infiltration, the air exit suction is desired. Bouwer (1966) indicated that an exit suction could be estimated as one-half the air entry value. Later, Aggelides and Youngs (1978) further substantiated the approximation. This approximation was used in the calculation of wetting front suction from data acquired on the Prairie Dog Creek basin.

Philip (1954) indicated a range of wetting front suction values of 31.5 inches (80 cm) in coarse textured soils to 55.1 inches (140 cm) in clay. Hillel (1980) reported a range for initially dry soils of 19.7 to 39.4 inches (50 to 100 cm). The values calculated from Prairie Dog Creek soils data were smaller than these ranges, as were most of the values reported in Clapp and Hornberger (1978) and McCuen and others (1981). Although many other factors would need to be considered in a complete evaluation of the infiltration components of the precipitation-runoff modeling system, the above ranges and the values of PSP resulting from optimization may indicate that wetting front suction is being underestimated by the approach used here.

The product of wetting front suction and soil moisture (PS) is varied linearly between a maximum at wilting point and a minimum at field capacity (PSP). An assumption is that field capacity is the soil moisture retained at one-third bar. That field capacity is not an intrinsic property of the soil is generally recognized (see, for example, Hillel, 1980, p. 67-72). Furthermore, the soil moisture level at which rapid drainage ceases (field capacity) will vary considerably between soils. The arbitrary use of soil moisture at one-third bar suction can introduce additional errors in infiltration calculations. Similar remarks also apply to the concept of wilting point.

RGF, the ratio of the product of wetting front suction and soil moisture deficit at wilting point to PSP was consistently increased by optimization. An assumption in the Green and Ampt infiltration equation is that wetting front suction is constant for a given soil. With this assumption, the ratio reduces to the ratio of moisture deficit at wilting point to moisture deficit at field capacity. These values are much smaller than those obtained when RGF is optimized (tables 22-24), and also are smaller than the typical range of values reported in Dawdy and others (1972) of 4.4 to 14.

If matric suction at wilting point, for example, 15 bars, is substituted into the numerator and suction at field capacity, one-third bar, is substituted in the calculation of PSP, large values of RGF result. These far exceed published values and the optimized values presented in tables 22-24. At this point, the technique used to estimate RGF does not provide results that correspond to optimized values.

The areal net infiltration rate over each hydrologic response unit is calculated as rainfall rate minus one-half the rainfall rate squared over point infil-

tration capacity when rainfall rate is less than capacity. When rainfall rate exceeds the point infiltration capacity, net areal infiltration is taken as one-half the point capacity. Thus, even for the smallest storms, there will be rainfall excess. The assumption that areal net infiltration is equal to one-half the point infiltration capacity could result in doubling the Green and Ampt parameters by optimization.

Estimates of KSAT, PSP, and RGF based upon average soil texture classes for each hydrologic response unit could result in anomalous infiltration capacities. The parameter estimates were made using data from soil samples collected in the basin and soil survey information. Rock outcrops, if extensive enough, are identified in soil survey maps. Clinker outcrops are common in the Prairie Dog Creek basin. These outcrops have been recognized as frequently being sink areas because of their permeable nature (for example, McClymonds, 1982). When hydrologic response units were delineated, the clinker outcrops were not separately identified. The large permeability of these outcrops was ignored. Optimization of infiltration parameters for a basin comprised of significant areas of clinker could result in unrealistically large parameter values as the model attempted to compensate for large differences between observed and simulated runoff. The permeability could be accounted for by assigning arbitrarily large values to the parameters for the clinker areas. The parameter values for the response unit could then be determined by area-weighted averages of these estimates with those estimated for the soil types.

There are numerous livestock reservoirs in the basin. The storage capacity of these reservoirs and the delay and attenuation of peak flows by them was not considered in the model runs. Runoff stored in the reservoirs was probably accounted for by increased infiltration on the response units. In future model tests, the reservoir component of the model will be used to evaluate the effects upon simulated runoff.

At the beginning of a storm period, the antecedent base-moisture storage (BMS) is set equal to RECHR, the current soil moisture of the upper soil zone in the daily mode of the model. Similarly, the maximum storage in this zone (BMSN) is set equal to REMX, the maximum storage capacity in the daily mode. At the end of a storm period, RECHR is updated by the ending value of BMS. Correspondence between the storm and daily soil moisture accounting is thus maintained. The current value of PS is controlled by the ratio BMS/BMSN. If BMS is overestimated, current infiltration capacity will be underestimated. An earlier comparison between soil moisture observations and simulated soil moisture revealed that generally, simulated soil moisture was small during many of the storm periods. Therefore, overestimation of BMS usually didn't occur.

#### Precipitation variability

Unaccounted precipitation variability can result in large errors in simulated runoff as well as the other processes being modeled. The first version of the precipitation-runoff modeling system used input from three precipitation gages. Data input was later increased to five gages. Because the earlier version of the model was used in the evaluation of the daily mode, use of data from three gages instead of five was continued in the test of the storm runoff mode. In addition to multiple gage input, precipitation correction factors can be used in the model to change the amount of precipitation received on particular hydrologic response units as a fraction of the precipitation from the gage to which the response unit is assigned.

Although storm characteristics will vary from storm to storm, some observations can be made from the storm summary (table 29) that are relevant to possible errors in the results presented above. The storms cannot be classified by type without more detailed observations, but those thought to be primarily convective have been separated on the basis of season and the length of storm. Storms 4, 5, 6, 8, 12, and 15 have durations indicating that they are of the convective type.

Table 29.--Characteristics of storms used in model testing

Storm No.	Dates of storm <sup>1</sup>	Duration of precipitation <sup>2</sup> (hours)	Length of storm (hours)	Three-gage mean precipitation, inches (coefficient of variation, percent)	Five-gage mean precipitation, inches (coefficient of variation, percent)
<u>1979</u>					
1	4/18-4/20	9.25	24	0.52 (19)	-----
2	4/26-4/27	4.25	8	.30 (43)	-----
3	5/28-6/1	12.0	38	.89 (8)	0.84 (14) <sup>3</sup>
4	6/18-6/18	.50	1	.57 (107)	.49 (108)
5	7/16-7/16	2.75	5	.26 (15)	.24 (29)
6	7/28-7/28	.50	.50	.26 (24)	.34 (35)
<u>1980</u>					
7	6/6-6/7	6.50	20	1.02 (36)	1.02 (27)
8	6/14-6/16	2.75	3	.39 (103)	.31 (98)
9	10/15-10/15	7.25	11	.55 (61)	.56 (44)
10	10/22-10/23	4.50	12	.22 (13)	.33 (71)
<u>1981</u>					
11	3/27-3/28	3.75	18	.36 (35)	.38 (25)
12	3/31-3/31	3.25	6	.22 (47)	.23 (32)
13	5/26-5/27	5.75	12	.70 (58)	.97 (50)
14	6/12-6/14	4.25	17	.41 (29)	.55 (42)
15	7/14-7/15	.25	.25	.27 (14)	.35 (30)
16	7/25-7/29	7.75	33	1.28 (6)	1.27 (5)
17	9/6-9/6	4.25	11	.27 (18)	.27 (14)

<sup>1</sup> Includes precipitation and runoff

<sup>2</sup> Does not include time intervals in which no precipitation fell

<sup>3</sup> Mean of four gages

Precipitation variability over the basin was evaluated using the coefficients of variation of total storm precipitation. Although the coefficients of variation were calculated from small samples (three and five gage amounts), they provide some

measure of the spatial variability. The results could change if more gages were used. The largest coefficients of variation occurred in this group of storms (storms 4 and 8). Some of the smaller coefficients also were associated with the three-gage network in this group of storms. The coefficients of variation of the remaining storms ranged from the smallest of 6 percent, reflecting a very uniform distribution of precipitation amounts over the basin, to intermediate values (61 percent) reflecting considerably more variability.

The effects of assuming a particular mean precipitation over the basin using data from a few gages can be assessed from the changes in mean precipitation between the three- and five-gage network. Of the 15 storms for which a five-gage network was available, the mean precipitation decreased in five instances, increased in eight, and remained unchanged in two. Mean precipitation amounts changed between the three- and five-gage networks in excess of 10 percent in 7 of 15 storms, or 47 percent of the time.

Precipitation variability can be assessed by the change in the coefficient of variation between the three- and five-gage network. The coefficient of variation increased in four of the six short-duration storms or 67 percent of the time. It increased in three of nine storms in the group of long-duration storms. Considering all storms, precipitation variability increased in 7 of 15 storms or 47 percent of the time.

The frequent occurrence of large coefficients of variation indicates that the use of data from few gages in a basin of this size as driving variable input to a model may result in anomalous storm-runoff simulations. A comparison of the diagonals of the hat matrices (table 26) with the information presented in table 29 indicates that the storms exhibiting the greatest effect upon the optimization of parameters were also those with relatively large coefficients of variation. Failure to account for this variability could result in optimized parameter values that differ considerably from the original estimates (unless constrained), even though they may have been adequately determined.

Storm 7, a long-duration storm, produced 1.24 acre-feet (0.0012 in.) of runoff with a peak discharge of 18.7 ft<sup>3</sup>/s. It produced an intermediate volume of runoff and the precipitation variability was not large (coefficient of variation 27 percent for the five-gage network). Therefore, this storm was selected for an evaluation of the effects of precipitation variability. A storm with relatively small areal variation was desirable in the evaluation in order to increase the chance that interpolation of precipitation amounts between gages would provide accurate estimates of the precipitation falling on each hydrologic response unit. The precipitation amounts for each gage were plotted on a base map. Lines of equal precipitation were sketched using interpolated precipitation amounts. Using the lines of equal precipitation, a unit precipitation correction factor (UPCOR) was calculated for each hydrologic response unit. A model run was made using the initial infiltration parameter estimates. Although the simulated runoff volume was still much greater than the observed, the simulated volume was reduced by 41 percent, from 0.0391 to 0.0232 in.

Parameters PSP and RGF were subsequently optimized, using storm 7 only. The simulated runoff was reduced to the observed (0.0012 in.). The reduction was accomplished by an increase in the average value of PSP of 633 percent, and an increase in RGF of 347 percent. Even though unaccounted precipitation variability

will introduce considerable error in the simulation, the current uncertainty in the calculation of infiltration remains a major consideration.

### Routing of storm runoff

A comprehensive evaluation of the rainfall excess routing and sediment transport components was deferred until the simulation of rainfall excess could be improved. A preliminary test of the rainfall excess routing was conducted, however.

Rainfall excess from 16 of the 17 storms used above was routed to the basin outlet. The optimized parameter values from the two-parameter optimization of PSP and RGF were used in the calculation of infiltration and rainfall excess. The initial values of the routing parameters were used. Owing to the uncertainty in the calculation of infiltration, the routing parameters were not optimized. However, the routing time interval was reduced from 10 minutes to 5 because of numerical instability.

Simulated peak flows were greater than observed flows for storms 1, 2, 3, 6, and 16 (table 30). Simulated peaks were less than observed for the rest of the storms. The difference was particularly pronounced for storm 8, which had the largest observed peak flow, 240 ft<sup>3</sup>/s, compared to a simulated peak flow of 1.67 ft<sup>3</sup>/s. No routing occurred for storms 5, 9, and 15 because the threshold flow rate for routing was selected to be 0.1 ft<sup>3</sup>/s and these storms had less flow than this.

Table 30.--A summary of the results of routing rainfall excess to the basin outlet  
[<, less than]

Storm number	Peak flow, in cubic feet per second		Time to simulated peak (hours)	Time to observed peak (hours)
	Simulated	Observed		
1	6.5	1.8	14-3/4	19
2	4.9	.57	15-1/4	2
3	2.1	.60	18-1/2 (day 2)	21-1/2
4	24	76	20-1/2	17-3/4
5	<.10	.13	--	20-1/4
6	.49	.32	1/4	20-1/4
7	.10	19	18	21
8	1.7	240	18	18-3/4
9	<.10	.66	--	16-3/4
10	.51	1.4	16-1/2 (day 2)	4-1/4 (day 2)
11	1.6	1.6	13-1/4	4-3/4
12	12	24	22-1/2	24
13	.81	4.5	1/4 (day 1)	7-3/4 (day 2)
14	.71	2.4	1/4 (day 1)	6-3/4 (day 2)
15	<.10	3.4	--	22
16	.69	.28	1/4	2-3/4

Correlation coefficients were calculated between runoff error (observed-simulated peak flows) and the coefficients of variation of precipitation amounts for the three-gage network. The correlation between the error and the coefficients of variation of precipitation was 0.73. Because the sample was small and contained one or two very large values relative to the remaining data, there is a chance of spurious correlation. Furthermore, a high correlation does not imply cause and effect. However, a correlation of 0.73 between peak flow error and the coefficient of variation of precipitation amounts indicates that large error is associated with large spatial variability of precipitation.

The times to peak of the simulated and observed hydrographs are given in the last two columns of table 30. The error (time to observed peak minus time to simulated peak) did not appear to be strongly related to storm characteristics or to error in peak flow. The correlation between time error and infiltration (as the percent of net precipitation) was 0.60. Although subject to the same qualifications above, the correlation is a reflection of less surface runoff resulting from greater infiltration, and therefore a greater time lag. The times that the simulated peak preceded the observed peak were times of less relative infiltration. Conversely, the times when simulated peaks lagged the observed were generally associated with greater relative infiltration. As is indicated by the small correlation coefficient, other factors must also be considered in a detailed analysis of timing error, including the effects of detention and storage by livestock reservoirs.

#### IMPROVEMENT OF SIMULATION RESULTS

Every model is a simplified representation of actual occurrence. As such, each one can be improved. Based upon the results of the model test, certain components of the precipitation-runoff modeling system that could be modified to improve simulation results in semiarid regions similar to eastern Montana can be identified.

The frequency with which parameters related to soil moisture, percolation, and evapotranspiration were identified as being sensitive indicates that the soil moisture accounting and evapotranspiration methods are relatively important. A more complex model of the soil mantle is possibly needed. The model could include multiple soil layers with more complex texture. Allowance could be made for redistribution of soil moisture between occurrences of infiltration.

Allowance could be made for a more complex vegetation composition. Variation of plant activity through the season including growth and dormancy might be considered. The cover provided as well as extraction of water from the soil are greatly affected by growth stage as well as soil moisture. Some current models use concepts of leaf area index and root activity-soil temperature relationships in this regard. Rooting depths and rooting densities can be quite variable. For example, certain bunch grasses and shrubs such as big sagebrush can root to considerable depth.

The Green and Ampt equation has provided useful estimates of infiltration. The parameters have been given physical interpretation. The variable results obtained in this study need to be investigated. Better identification of average soil characteristics over a response unit might help. Use of the current scheme in calculating areal infiltration capacity from point capacity could be evaluated in this light. Use of average soil characteristics of a unit might reduce the need to

convert point infiltration to areal infiltration using the current uniform distribution function.

Modification of the snowmelt and evaporation component of the model is needed in order to better simulate prairie and foothills snowpacks. The spatial variability caused by blowing snow could be incorporated. An expanded energy budget could include exchanges between adjacent bare ground and vegetation, advected energy, energy exchange with the soil, and changes in shallow snow characteristics such as albedo. Concurrently, development of a soil frost algorithm would permit simulation of soil freezing and runoff over frozen soils.

Two alternate hydrologic response unit delineations were studied. Although one gave slightly better results than the other, it is felt that the considerable averaging of dissimilar vegetation and soils characteristics in both instances may have masked larger differences. Defining hydrologic response units to include only similar soils and single vegetation types would result in an excessive number of response units on basins such as Prairie Dog Creek. Other approaches could be evaluated. An evaluation of the effects of using average soil and vegetation characteristics for response units comprised of intermingled soils and vegetation types might provide important results.

Various parameter estimation techniques were employed. Knowledge of parameters to which simulated runoff is sensitive and which do not possess a strong physical interpretation is important. If modifications to components such as soil moisture accounting were being made, parameter definition and estimation techniques could be incorporated.

Application of the model to ungaged basins and to the simulation of land-use change would be an important addition to any future study. A study of model transferability could be conducted wherein the model is run using another gaged basin and regionalized parameter estimates. The ability (or inability) to transfer the model to an ungaged basin using regionalized parameters thus could be assessed.

How well the model can simulate land-use changes will depend upon parameter sensitivity. Simulation of land-use changes involves changing values of selected parameters to represent the land-use change and studying the results. If the degree of change in value of the parameters necessary to simulate the change in land use is less than the error in parameter estimates, the results would be indistinguishable from the results prior to the change. Such a study therefore, would include parameter sensitivity and the detection of significant changes in results using statistical theory.

The lack of long-term data from small basins, particularly arid and semiarid western basins, will make simulation of a wide range of events difficult. Synthetic driving variable data sets could be generated using stochastic process theory. A long period of record which would include events with various probabilities of occurrence could be synthesized. The sequences of the long record that included events of interest could then be used as model input. For example, the effects of rare, intense storms or winters with very large snow accumulation (and small probability of occurrence) upon a basin could be studied this way. Numerous such data-generation methods are available.

## SUMMARY

The continuous simulation mode of the precipitation-runoff modeling system was tested with 2 years of data (1979 and 1980 water years) acquired from a small, semi-arid basin in southeastern Montana. Two alternate hydrologic moisture unit definitions, with four levels of basin partitioning each, were evaluated. The first year was used in optimization and sensitivity analysis as it included larger snow accumulation and melt, several frontal and convective rainstorms, and a relatively long period of streamflow. The parameters were screened and a reduced parameter set defined which was subsequently used in the evaluation of the hydrologic moisture unit alternatives and levels of basin partitioning. This evaluation was conducted through the use of optimization and sensitivity analyses of each alternative and level of partitioning. An optimum level of basin partitioning was selected for each alternative. These two were then used along with the optimum values of the parameters and both years of data to study the model simulation. Observed streamflow, snow-survey, and soil-moisture data were used in this study.

The parameters TRNCF, CTX, SMAX, SEP, RESMX, REXP, RCB, CTS, and BST contributed more to runoff prediction error than did the others and were retained as the parameter subset to be used in subsequent analyses. Subsequent analysis revealed consistently good correlations between CTX and CTS, and between SEP and RESMX. CTX and RESMX were subsequently removed from the subset. When tested using the hydrologic moisture unit alternatives and levels of partitioning, SMAX, RCB, SEP, and CTS had the largest changes between initial and optimized values. The first three are related to basin soils and geology. The last is a climatic parameter, but it is a parameter in the Jensen-Haise equation, and thus is indirectly related to soil moisture.

Large reductions in the value of the objective function were realized through optimization, the least being 71 percent. Large changes in the objective function reflect the inability to obtain good estimates of "true" parameter values for some parameters and, subsequently, the need for objective optimization plans in such instances. There were no large differences between optimized values of the objective function for the hydrologic moisture unit alternatives at any level of partitioning. The model is not greatly sensitive to levels of partitioning under either alternative when this test basin is used. The difficulty in obtaining homogeneous moisture units owing to intermingling of soils and vegetation types as well as heterogeneous topography may cause the insensitivity. The minimum value of the objective function occurred with 16 hydrologic moisture units under alternative A and 18 hydrologic moisture units under alternative B. These levels were selected as the optimum levels of partitioning.

Simulated hydrographs under alternatives A and B approximated the observed hydrograph during the first year, although the relative error was frequently large. However, this was the year used in optimization. During the second year simulated flow continued through most of the winter under alternative B. There was also significant and prolonged snowmelt runoff under this alternative owing to greater simulated snowpack accumulation than under A. During this time, there was no actual streamflow except for isolated periods. During these periods, the streamflow was directly attributable to rainstorms or to runoff over frozen ground. There was no simulated streamflow during the time of runoff over frozen ground, which was expected because there is no provision in precipitation-runoff modeling system to simulate soil freezing.

Most rainfall produced simulated runoff, often when there was no actual streamflow. When streamflow did occur, the peaks were frequently subdued compared to the simulated peak flows. The opposite also occurred in which observed peak flows far exceeded the simulated flow; this condition reflects the inability of the model to account for variations in rainstorm intensity and duration in the daily mode because only total daily precipitation is considered.

The snow components of the model simulated snowpack accumulation reasonably well during the first snow season. The simulations resulted in more rapid melt than was observed. The simulated snowpack under alternative B persisted until mid-April, whereas the actual snowpack disappeared by the end of March.

The second season was one in which a snowpack accumulated and ablated several times. Neither alternative simulated these snowpacks well. The simulation under alternative A produced results somewhat closer to observed than did B. Both alternatives resulted in continuous snowpacks through the season. The snowmelt components of the precipitation-runoff modeling system do not permit as large evaporation and melt as can occur in shallow prairie snowpack.

The simulated soil moisture was greater than observed during the peak soil moisture accumulation period of the first year. During the rest of the year and all the next year, simulated soil moisture was less than observed for both alternatives. Alternative A provided somewhat closer agreement between simulated and observed soil moisture than did alternative B. The times of peak soil moisture were reasonably well simulated even though the amounts were not.

The change in rate of evapotranspiration followed, in general, the annual cycle of solar radiation. Within this cycle, the pattern of changes in evapotranspiration were related to concurrent changes in soil moisture.

Little direct information was available to check the operation of the subsurface and ground-water reservoir components. Annual volumes of water seeping to ground water were compared with the computed average amount leaving the basin in the alluvium and with the differences between simulated and observed soil moisture. Increasing simulated soil moisture storage and decreasing seepage to ground water would result in closer agreement to soil moisture and alluvial ground-water observations.

The storm mode of the precipitation-runoff modeling system was tested with 17 storms selected from 3 years of data. These storms were selected from the period late March through October and included various storm types. The first hydrologic response unit alternative was modified by combining such that a single unit extended from the drainage divide to the stream channel. These units were then considered overland flow planes in the storm mode.

Parameter estimates were made for the Green and Ampt equation for each hydrologic response unit on the basis of the average texture of the surface horizon. The estimates were made using equations describing the soil moisture characteristic and soils data collected in the basin. The routing parameters were estimated using the slope, length, and roughness characteristics of the overland flow planes and associated channel segments.

The four parameters associated with infiltration were optimized using all 17 storms. The use of the sum of squares of the differences between the logarithms

of flows resulted in an inordinately large amount of weight being given to smaller storms because of the resulting low-flow volumes. The objective function was changed to the sum of squares and the analysis repeated.

Simulated storm runoff was generally much greater than observed prior to optimization. Following optimization, the results were variable. Runoff from each storm was reduced by an average of 93 percent, resulting in undersimulation of most storm runoff. All parameters increased in value.

The order of parameter sensitivity was KSAT, PSP, RGF, and DRN with the results being insensitive to DRN. Two-parameter optimizations were made using KSAT-RGF and PSP-RGF. As in the four-parameter optimization, parameter values were increased. The results of each of these analyses were similar and were as good as the four-parameter optimization. A one-parameter optimization using RGF did not provide as much reduction in the objective function as did the previous three.

The values of all parameters were increased as the result of optimization. Often, the final values were unrealistically large, especially KSAT. The model results indicate that infiltration is being underestimated. The underestimation may be due to inadequate parameter estimation, to inadequate characterization of the soils and clinker outcrops on the hydrologic response units, or to underestimation when point infiltration rates were extended to areal rates. Overestimation of areal average precipitation due to an inadequate gage network may also have contributed.

The effects of precipitation variability were evaluated. The average precipitation amount and the coefficient of variation were calculated for the three-precipitation-gage network and the five-precipitation-gage network. Often the coefficients of variation were very large, particularly for summer convective storms. Failure to account for the areal variability of precipitation can result in considerable error in simulated runoff.

A detailed test of the rainfall excess routing component of the model was deferred in view of the uncertainty in simulating infiltration. Trial runs were made for 16 storms and the optimized values of PSP and RGF, however. The results were variable. Simulated peak flows were less than observed in 12 of 16 storms. The error in time to peak was variable, although the least error was associated with larger peak flows. Errors in peak flow appeared to be associated with the coefficient of variation of total storm precipitation ( $r = 0.73$ ), whereas error in time to peak was correlated with relative infiltration ( $r = 0.60$ ).

## REFERENCES CITED

- Aggelides, S., and Youngs, E. G., 1978, The dependence of the parameters in the Green and Ampt infiltration equation on the initial water content in draining and wetting states: *Water Resources Research*, v. 14, no. 5, p. 857-862.
- Aron, Gert, and Borelli, John, 1973, Stream baseflow prediction by convolution of antecedent rainfall effects: *Water Resources Bulletin*, v. 9, no. 2, p. 360-365.
- Barnes, H. H., Jr., 1967, Roughness characteristics of natural channels: U.S. Geological Survey Water-Supply Paper 1849, 213 p.
- Bouwer, H., 1966, Rapid field measurement of air entry value and hydraulic conductivity of soil as significant parameters in flow system analysis: *Water Resources Research*, v. 2, no. 4, p. 729-738.
- Brakenseik, D. L., 1977, Estimating the effective capillary pressure in the Green and Ampt infiltration equation: *Water Resources Research*, v. 13, no. 3, p. 680-682.
- Branson, F. A., Gifford, G. F., Renard, K. G., and Hadley, R. F., 1981, *Rangeland hydrology*, 2d ed: Dubuque, Kenall/Hunt Publishing Co., 340 p.
- Brooks, R. H., and Corey, A. T., 1964, Hydraulic properties of porous media: Fort Collins, Colorado State University, Hydrology Paper No. 3, 27 p.
- Campbell, G. S., 1974, A simple method for determining unsaturated conductivity from moisture retention data: *Soil Science*, v. 117, no. 6, p. 311-313.
- Cary, J. W., Campbell, G. S., and Papendek, R. I., 1978, Is the soil frozen or not? An algorithm using weather records: *Water Resources Research*, v. 14, no. 6, p. 1117-1122.
- Cary, L. E., and Johnson, J. D., 1981, Selected hydrologic and climatologic data from the Prairie Dog Creek basin, southeastern Montana, water year 1979: U.S. Geological Survey Open-File Report 81-412, 73 p.
- Clapp, R. B., and Hornberger, G. M., 1978, Empirical equations for some soil hydraulic properties: *Water Resources Research*, v. 14, no. 4, p. 601-604.
- Dawdy, D. R., Lichty, R. W., and Bergan, J. M., 1972, A rainfall-runoff simulation model for estimation of flood peaks for small drainage basins: U.S. Geological Survey Professional Paper 506-B, p. B1-B28.
- Dawdy, D. R., Schaake, J. C., Jr., and Alley, W. M., 1978, User's guide for distributed routing rainfall-runoff model: U.S. Geological Survey Water-Resources Investigations 78-90, 146 p.
- DeJong, E., and MacDonald, K. B., 1975, The soil moisture regime under native grassland: *Geoderma*, v. 14, p. 207-221.

- Frank, E. C., and Lee, Richard, 1966, Potential solar beam irradiation on slopes: tables for 30° to 50° latitude: U.S. Forest Service, Rocky Mountain Forest and Range Experiment Station, Research Paper RM-18, 116 p.
- Garstka, W. U., 1964, Snow and snow survey, Section 10, in V. T. Chow, ed., Handbook of applied hydrology, p. 10-1 to 10-57.
- Glover, R. E., 1960, Well pumping and drainage formulas, Section A, of Studies of ground-water movement: U.S. Department of the Interior, Bureau of Reclamation, Technical Memorandum 657, 179 p.
- Glover, R. E., 1966, Use of mathematical models in drainage design: American Society of Agricultural Engineers Transactions, v. 9, no. 2, p. 210-212.
- Granger, R. J., Chanasyk, D. S., Male, D. H., and Norum, D. I., 1977, Thermal regime of a prairie snowcover: Soil Science Society of America Journal, v. 41, p. 839-842.
- Granger, R. J., and Male, D. H., 1978, Melting of a prairie snowpack: Journal of Applied Meteorology, v. 17, no. 2, p. 1833-1842.
- Gray, D. M., and Wigham, J. M., 1970, Peak flow-rainfall events, Section VIII, in D. M. Gray, Editor-in-Chief, Handbook on the principles of hydrology, p. 8.1 - 8.102.
- Hamon, W. R., 1961, Estimating potential evapotranspiration: Proceedings of the American Society of Civil Engineers, Journal of the Hydraulic Division, v. 87, no. HY3, p. 107-120.
- Hershfield, D. M., 1961, Rainfall frequency atlas of the United States: U.S. Department of Commerce, Weather Bureau Technical Paper No. 40, 113 p.
- Hewlett, J. D., and Nutter, W. L., 1970, The varying source area of streamflow from upland basins: Bozeman, Montana State University, American Society of Civil Engineers Proceedings of the Symposium of Interdisciplinary Aspects of Watershed Management, p. 65-83.
- Hillel, Daniel, 1980, Applications of soil physics: New York, Academic Press, 385 p.
- Hjelmfelt, A. T., Jr., Piest, R. P., and Saxton, K. E., 1975, Mathematical modeling of erosion on upland areas: International Association for Hydraulic Research, p. 40-49.
- Hoaglin, D. C., and Welsch, R. E., 1978, The hat matrix in regression and ANOVA: The American Statistician, v. 32, no. 1, p. 17-22.
- Jensen, M. E., and Haise, H. R., 1963, Estimating evapotranspiration from solar radiation: American Society of Civil Engineers, Journal of Irrigation and Drainage, v. 89, no. IR4, p. 15-41.
- Johnston, P. R., and Pilgrim, D. H., 1976, Parameter optimization for watershed models: Water Resources Research, v. 12, no. 3, p. 477-486.

- Kittredge, Joseph, 1948, Forest influences: New York, McGraw-Hill, 394 p.
- Leaf, C. F., and Brink, G. E., 1973a, Computer simulation of snowmelt within a Colorado subalpine watershed: U.S. Forest Service, Rocky Mountain Forest and Range Experiment Station Research Paper RM-99, 22 p.
- \_\_\_\_\_ 1973b, Hydrologic simulation model of Colorado subalpine forest: U.S. Forest Service, Rocky Mountain Forest and Range Experiment Station Research Paper RM-107, 23 p.
- Leavesley, G. H., 1973, A mountain watershed simulation model: Fort Collins, Colorado State University, Ph.D. dissertation, 174 p.
- Leavesley, G. H., Lichty, R. W., Troutman, B. M., and Saindon, L. G., 1981, A precipitation-runoff modeling system for evaluating the hydrologic impacts of energy resources development: Proceedings 49th Annual Western Snow Conference, p. 65-76.
- \_\_\_\_\_ 1984, Precipitation-runoff modeling system--User's manual: U.S. Geological Survey Water-Resources Investigations Report 83-4238, 207 p.
- Li, E. A., Shanholtz, V. O., and Carson, E. W., 1976, Estimating saturated hydraulic conductivity and capillary potential at the wetting front: Blacksburg, Department of Agricultural Engineering, Virginia Polytechnical Institute and State University, cited by Clapp, R. B., and Hornberger, G. M., 1978, Empirical equations for some soil hydraulic properties: Water Resources Research, v. 14, no. 4, p. 601-604.
- Male, D. H., and Granger, R. J., 1979, Energy and mass fluxes at the snow surface in a prairie environment, in Colbeck, S. C., and Ray, M., eds., Proceedings of Modeling of Snow Cover Runoff, Hanover, N.H., Sept. 26-28, 1978: U.S. Army, Corps of Engineers, CRREL, p. 101-124.
- McClymonds, N. E., 1982, Hydrology of the Prairie Dog Creek basin, Rosebud and Big Horn Counties, Montana: U.S. Geological Survey Water-Resources Investigations 81-37, 64 p.
- McCuen, R. H., Rawls, W. J., and Brakenseik, D. L., 1981, Statistical analysis of the Brooks-Corey and the Green-Ampt parameters across soil textures: Water Resources Research, v. 17, no. 4, p. 1005-1013.
- Mein, R. G., and Brown, B. M., 1978, Sensitivity of optimized parameters in watershed models: Water Resources Research, v. 14, no. 2, p. 299-303.
- Meshnick, J. C., Smith, J. H., Gray, L. G., Peterson, R. F., Gentz, D. H., and Smith, Ralph, 1977, Soil survey of Big Horn County area, Montana: U.S. Soil Conservation Service and U.S. Bureau of Indian Affairs, 223 p.
- Miller, D. H., 1962, Snow in the trees - Where does it go?: Proceedings 29th Annual Western Snow Conference, p. 21-27.
- Morel-Seytoux, H. J., and Khanji, J., 1974, Derivation of an equation of infiltration: Water Resources Research, v. 10, no. 4, p. 795-800.

- Naney, J. W., DeCoursey, D. G., Barnes, B. B., and Gander, G. A., 1978, Predicting baseflow using hydrogeologic parameters: Water Resources Bulletin, v. 14, no. 3, p. 640-649.
- Overton, D. E., and Meadows, M. E., 1976, Stormwater modeling: New York, Academic Press, 358 p.
- Philip, J. R., 1954, An infiltration equation with physical significance: Soil Science Society of America Proceedings, v. 77, p. 153-157.
- Rawls, W. J., Brakensiek, D. L., and Miller, Norman, 1983, Prediction of Green and Ampt parameters from soils data: American Society of Civil Engineers, Hydraulics Division, Journal of Hydraulic Engineering v. 109, no. 1 p. 62-70.
- Riley, J. P., Israelson, E. K., and Eggleston, K. O., 1973, Some approaches to snowmelt prediction: International Association of Hydrological Sciences Publication 107, p. 956-971.
- Rorabaugh, M. I., 1960, Use of water levels in estimating aquifer constants: International Association of Scientific Hydrology Publication 52, p. 314-323.
- 1964, Estimating changes in bank storage and ground-water contributions to streamflow: International Association of Scientific Hydrology Publication 63, p. 432-441.
- Rosenbrock, H. H., 1960, An automatic method of finding the greatest or least value of a function: The Computer Journal, v. 3, p. 175.
- Satterlund, D. R., 1972, Wildland watershed management: New York, The Ronald Press Co., 370 p.
- Satterlund, D. R., and Haupt, H. F., 1967, Snow catch by conifer crowns: Water Resources Research, v. 3, no. 4, p. 1035-1039.
- Smith, R. E., 1976, Field test of a distributed watershed erosion/sedimentation model: Proceedings of a National Conference of Soil Erosion, May 24-29, Purdue University, p. 201-209.
- Solomon, R. M., Ffolliott, P. F., Baker, M. B., and Thompson, J. R., 1976, Computer simulation of snowmelt: U.S. Forest Service, Rocky Mountain Forest and Range Experiment Station Research Paper RM-174, 8 p.
- U.S. Army, 1956, Snow hydrology; Summary report of the snow investigations: North Pacific Division, Corps of Engineers, 437 p.
- U.S. Department of Agriculture, 1978, Soil survey data for Rosebud County, Montana: Soil Conservation Service, Soil Survey Office, Forsyth, Mont., unpublished data.
- U.S. Department of the Interior, 1983, Resource and potential reclamation evaluation, Prairie Dog Creek study area: Bureau of Land Management and Bureau of Reclamation EMRIA report 21-78, 25 p.

- U.S. Geological Survey, 1975, WATSTORE user's guide, volume 1: U.S. Geological Survey Open-File Report 75-426.
- Walton, W. C., 1970, Groundwater resource evaluation: New York, McGraw-Hill Book Company, 664 p.
- Weeks, J. B., Leavesley, G. H., Welder, F. A., and Saulnier, G. J., Jr., 1974, Simulated effects of oil-shale development on the hydrology of Piceance Basin, Colorado: U.S. Geological Survey Professional Paper 908, 83 p.
- West, N. E., and Gifford, G. F., 1976, Rainfall interception by cool-desert shrubs: Journal of Range Management, v. 29, no. 2, p. 171-172.
- Zahner, Robert, 1967, Refinement in empirical functions for realistic soil moisture regimen under forest cover: International Symposium on Forest Hydrology, W. E. Sopper and H. W. Lull, eds., New York, Pergamon Press, p. 261-274.

## SUPPLEMENTAL INFORMATION

### Subroutine BASFL1

#### Introduction

Initial model runs using Prairie Dog Creek data indicated that the current base-flow subroutine (BASFLW) did not adequately account for conditions found in the Prairie Dog Creek basin. During the 1978 and 1979 water years, Prairie Dog Creek functioned almost as a perennial stream--flowing from after the onset of spring snowmelt until freezeup the following winter. During subsequent years, Prairie Dog Creek has flowed only in direct response to snowmelt runoff over frozen soils and in response to convective storms. A base-flow component must be capable of handling base flow that begins a considerable time after infiltration occurs.

A search of the literature revealed an approach to base flow first used by Glover (1960, 1966) in the 1950's. This approach was an adaptation of the theory of heat flow to the study of subsurface flow to parallel drains. It was used by Rorabaugh (1960, 1964) in estimating aquifer characteristics, and later in estimating base flow. With some relaxation of assumptions and coupling with a convolution integral, a base-flow model was obtained which has provided useful results in small basin studies in Pennsylvania (Aron and Borelli, 1973) and in Oklahoma (Naney and others, 1978).

#### Model development

The equation for discharge,  $q(t)$ , per unit volume placed in storage at time  $t=0$  is (Aron and Borelli, 1973; Naney and others, 1978):

$$q(t) = 2R^2 \sum_{n=1,3,5,\dots}^{\infty} \exp \left[ - \frac{\pi^2 n^2 R^2 t}{4} \right] \quad (1)$$

where

$$R = \frac{1}{L} \left[ \frac{T}{S_y} \right]^{1/2}$$

and

- L - distance from ground-water divide to channel, in feet
- T - transmissivity, in feet squared per day
- S<sub>y</sub> - specific yield, in percent

If the ground-water system being studied meets the assumptions underlying the derivation of equation 1 and if aquifer test data are available from which T and S<sub>y</sub> can be computed, then the equation can be used as it was by Naney and others (1978). In the absence of such information, the equation can still provide useful results when used in the parametric sense. In this case, the watershed's aquifer characteristics are represented by the parameter R (Aron and Borelli, 1973).

Increments to ground water, as in the watershed model being tested, are computed in the soil moisture accounting component using daily snowmelt and rainfall as input. The base-flow component must then be capable of incorporating multiple increments. A convolution integral (discrete form) is used to add multiple increments. The unit discharge on day t, computed using equation 1, becomes the unit response or kernel function in the convolution with the daily increment, I(τ), to ground water,

$$Q(t) = \sum_{\tau=1}^t I(\tau) \Delta \tau q(t-\tau-1) \quad (2)$$

In a daily model, Δτ = 1.

### Application

BASFL1 is a modification of BASFLW. All variables are initialized on the first day of model operation then bypassed thereafter. Because the unit-response function need only be calculated once for each ground-water reservoir, the calculation is also made in the initialization part of the subroutine. If there is any initial ground-water storage on the first day of operation, it is computed as residual base flow and stored in dimensioned variable YGW.

The number of terms in the infinite series in equation 1 required for convergence is a function of the parameter RCB (R in equation 1) and of time, t. This dependence is shown as a function of the product of RCB and time in figure 1a. Only the first term is required for values of the product greater than about 2. In the subroutine, the summation is truncated when succeeding terms agree to within 5 percent.

The number of terms (days) before the unit-response function decreases to a negligible value is a function of RCB (fig. 2a). The number of terms is computed up to a maximum of 150 in the subroutine.

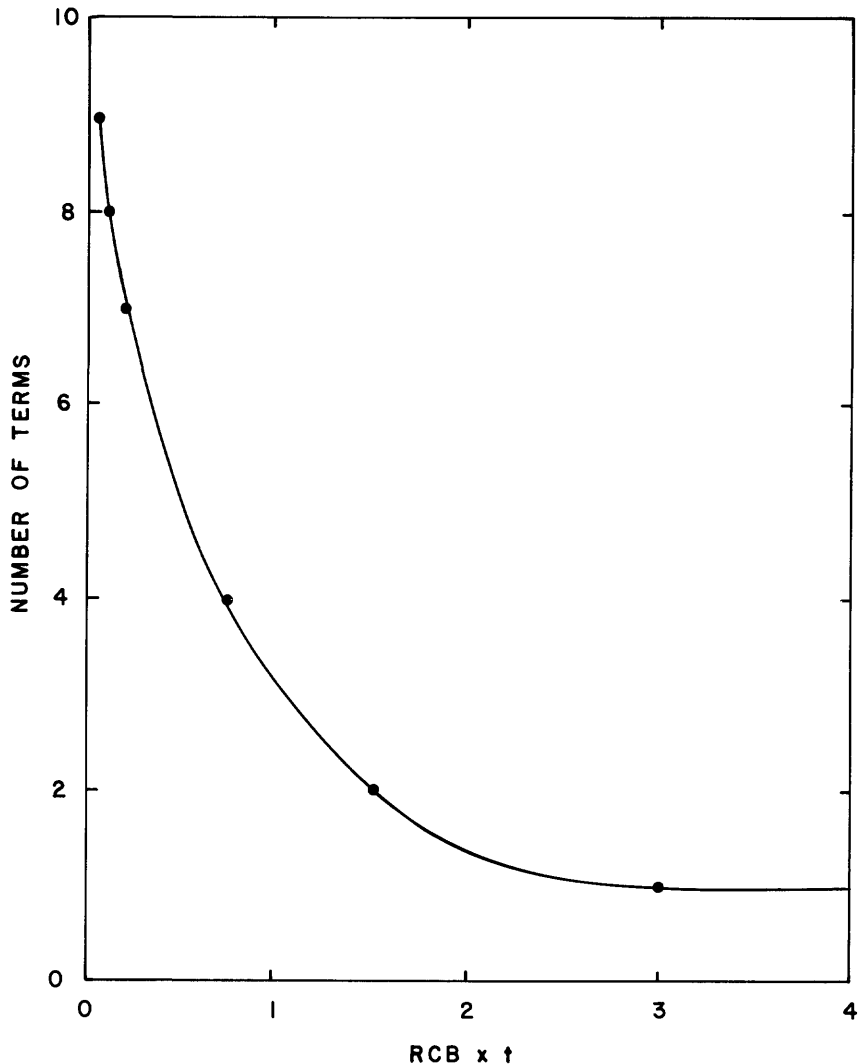


Figure 1a.--Number of terms of infinite series in equation 1 required for convergence to within 0.0001, as a function of RCB times t.

Although the lagtime (the number of days before an increment to ground water begins being discharged as base flow) can be externally specified, it is computed here as the inverse of  $(RCB)^2$ .

On the first and subsequent days, a check is made for residual base flow (KTS=1). If there is residual base flow, it is the current element of YGW, which is added to BASQ.

After the first day, a test is made for an increment to ground water (ZX). On the day of the first increment to ground water, the convolution algorithm is activated. The increment is weighted by each element in the unit-response function (QKER) and stored in XGW. IDAY, the day the increment occurred plus lagtime, is also computed. On each subsequent day an increment occurs, the increment is weighted by QKER and added to the appropriate element of XGW.

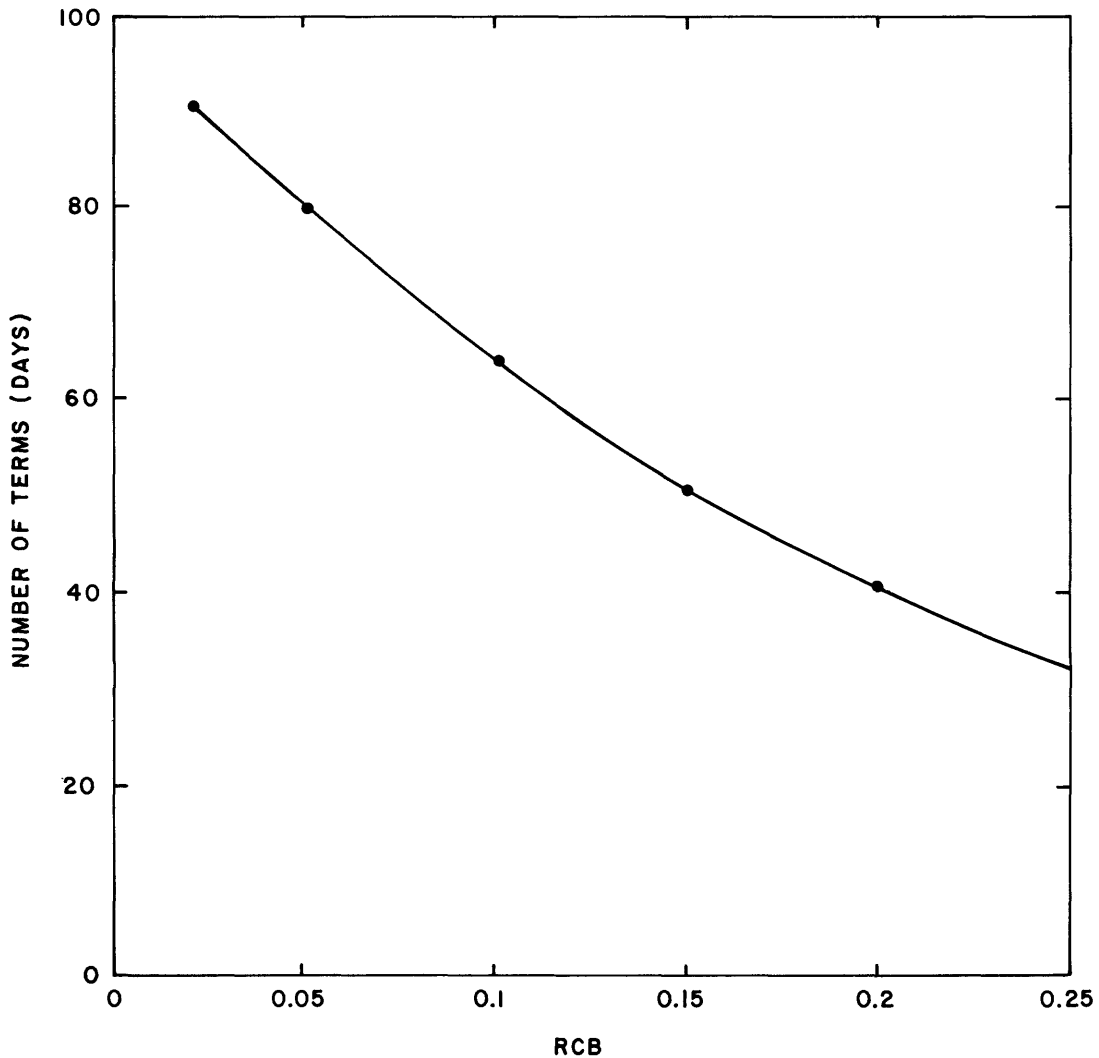


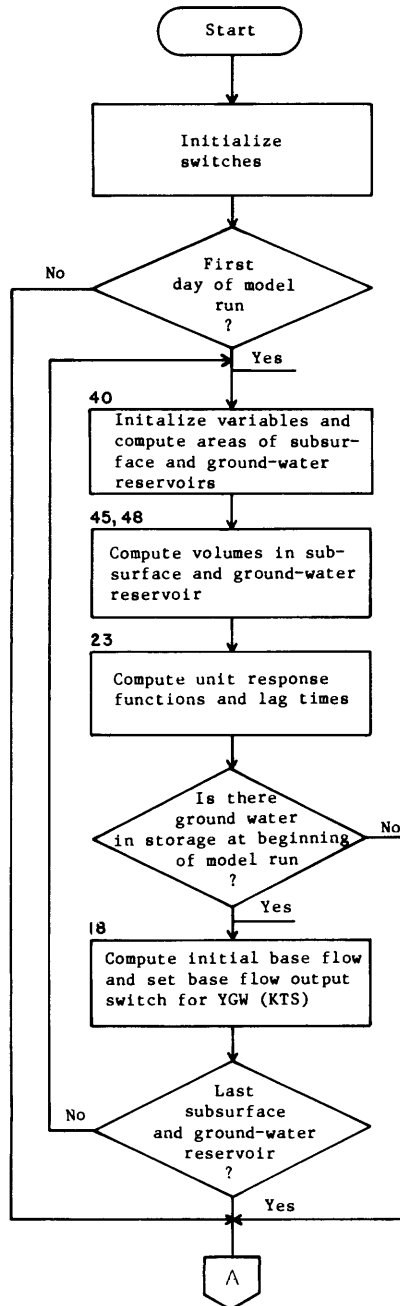
Figure 2a.--Number of terms (days) in the unit-response function versus RCB.

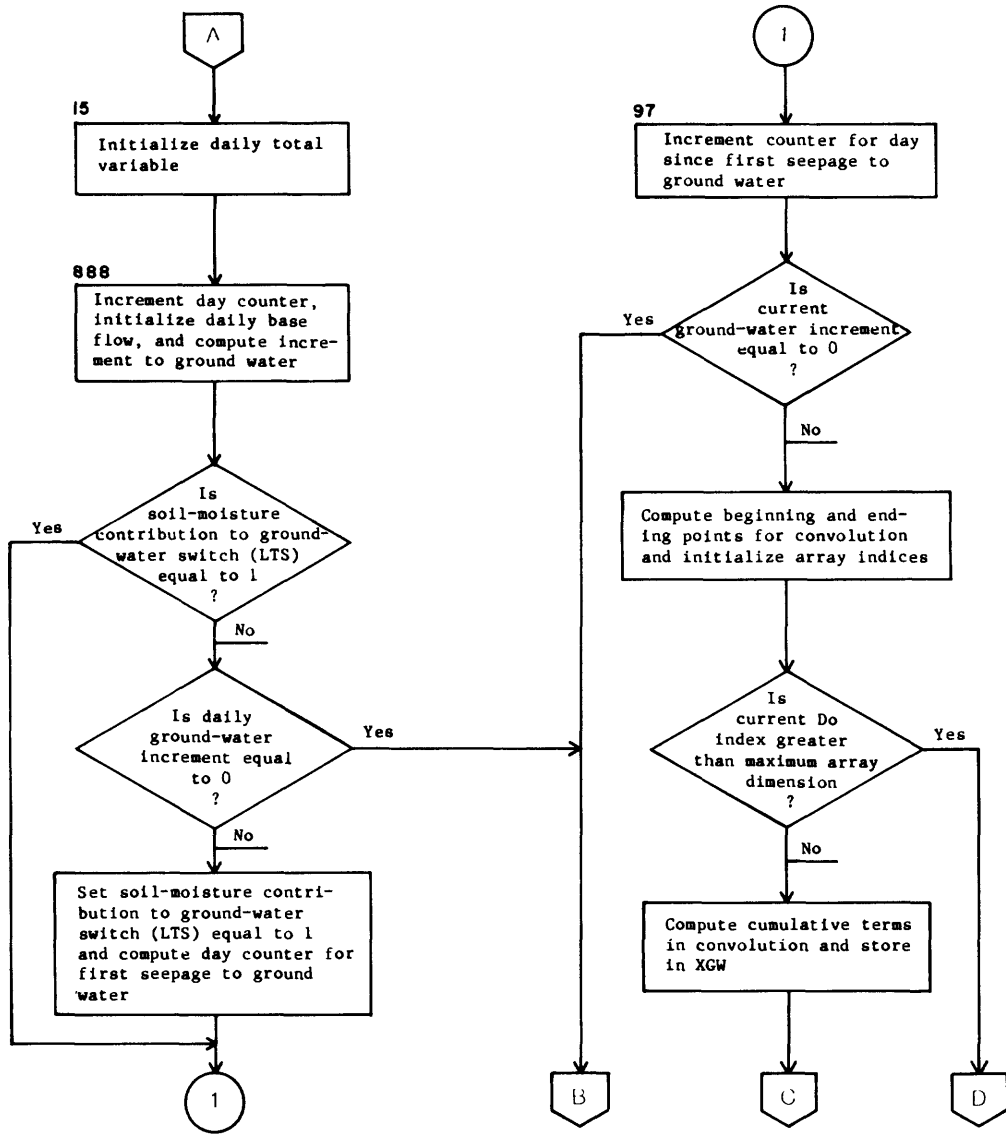
When the current day (II) equals IDAY, base flow begins (JTS=1). This process continues until the specified dimension of XGW is reached. By this time any residual base flow has ceased. Therefore, YGW is used as the storage variable for base flow in excess of the capacity of XGW. In the base-flow calculation, XGW and its associated counters and switch, JTS, are reinitialized when its last element has been reached. Similarly, YGW is reinitialized. The cycle of use of XGW and YGW is then begun again. This scheme was adopted to keep central memory requirements from becoming too large, yet permit model operation for any length of time.

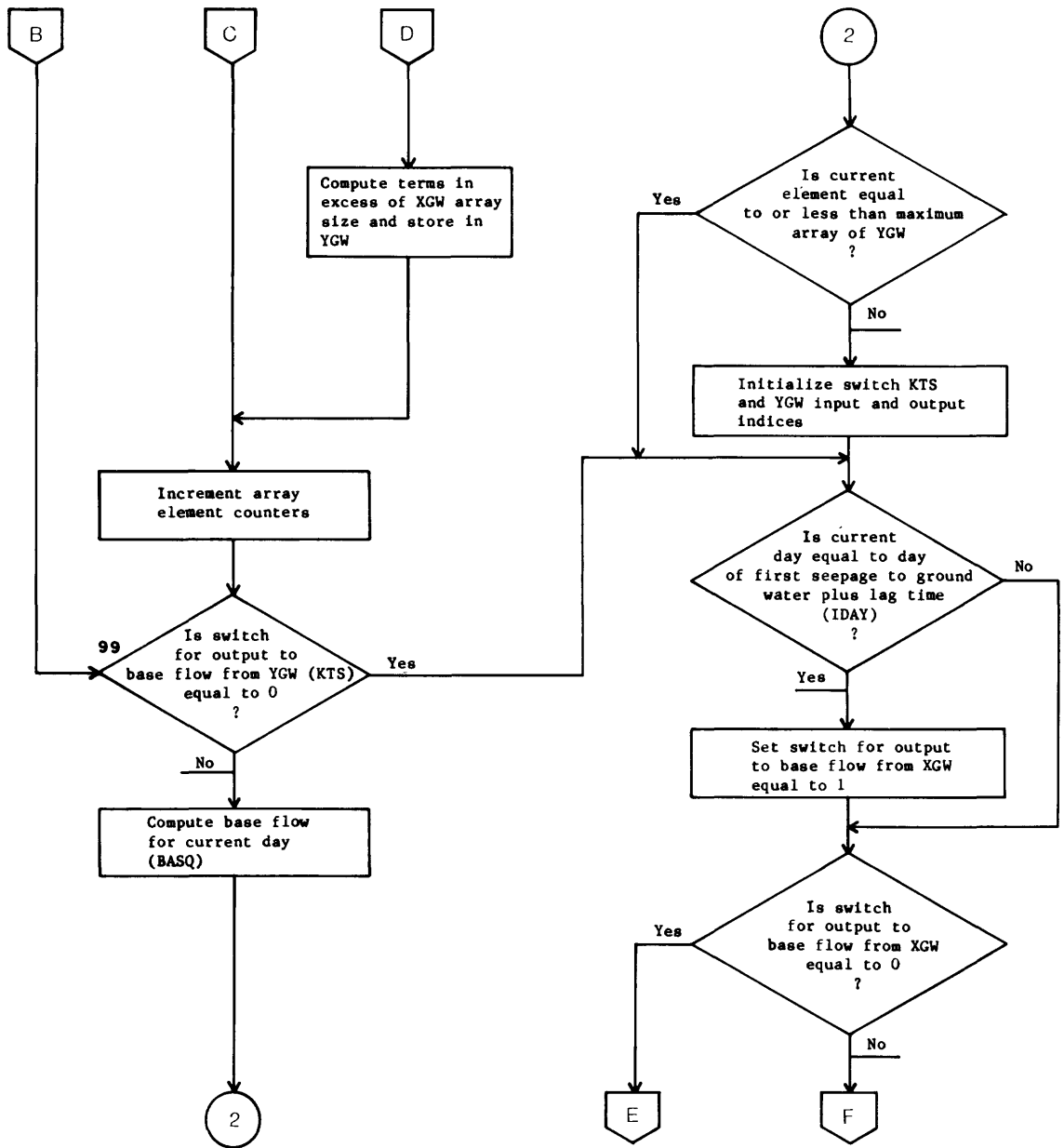
In this version of the base-flow subroutine, subsurface reservoir flow is computed in the same way it was in BASFLW. However, the scheme described above could also be used for this component of streamflow.

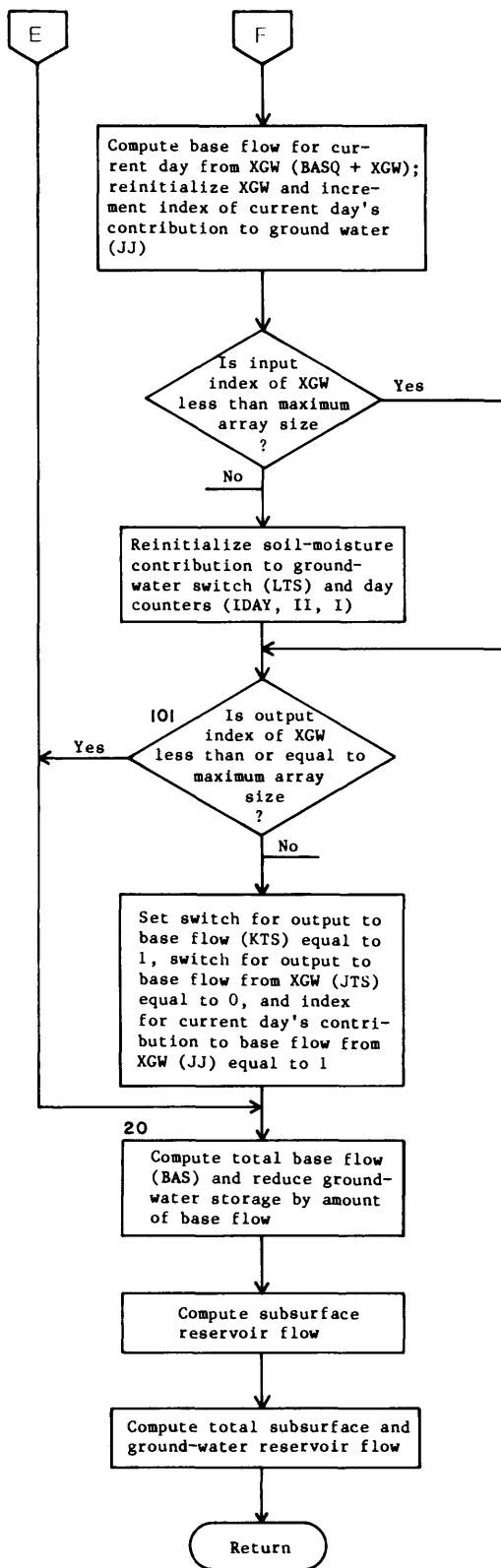
A flow chart of BASFL1 is presented as figure 3a.

Subroutine BASFLI









Dictionary of new and revised variables in BASFL1

I	Day counter for days since first increment to ground water
IDAY	Output index, day of first increment to ground water plus lag time
II	Day counter for days since beginning of model operation
IJJ	Index for current day's contribution to base flow from variable YGW
JJ	Index for current day's contribution to base flow from variable XGW
JIJ	Equals current value of IJJ
JTS	Switch for output to base flow from XGW
KK	Lag time (days) for the Jth ground-water reservoirs
KKJ	Index for the current element of the unit response function, QKER
KKM	Equals current value of KM
KM	Index for current day's contribution to base flow from variable YGW
KTS	Switch for output to base flow from YGW
LTS	Switch for beginning of soil moisture contribution to ground water (XGW)
MTS	Switch for beginning of soil moisture contribution to ground water (YGW)
MXTRM	Maximum number of terms in Jth unit response function
QKER	Unit response function for Jth ground-water reservoir
RCB	The parameter, R, in equation 1
TEMP	Variable used in the calculation of the unit response function
XGW	Variable used in the convolution calculations
XM	Equal to the previous day's ground-water reservoir contents
XTEMP	Variable used in the calculation of the unit response function
YGW	Variable initially used to store base flow occurring at the beginning of model operations, later used to store overflow when dimensions of XGW are exceeded
ZX	Current day's increment to ground water, equal to current day's ground-water storage minus previous day's storage